Etude de quelques questions mathématiques apparaissant en optique adaptative

Pierre Le Gall

Département de formation doctorale en mathématiques **École doctorale IAEM Lorraine**
UFR STMIA

Etude de quelques questions mathématiques apparaissant en optique adaptative

THÈSE

présentée et soutenue publiquement le 7 novembre 2006

pour l'obtention du

Doctorat de l'université Henri Poincaré – Nancy 1

(spécialité mathématiques)

par

Pierre Le Gall

Composition du jury

Président :	Jean-Michel Coron Professeur à l'Université de Paris XI
Rapporteurs :	Assia Benabdallah Maître de Conférences à l'Université de Provence Pierre Rouchon Professeur à l'Ecole Nationale Supérieure des Mines de Paris
Examinateurs :	Christophe Prieur, Chargé de Recherche au LAAS Marius Tucsnak Professeur à l'Université Nancy I
Directeur de thèse :	Lionel Rosier, Professeur à l'Université de Nancy I

Institut de Mathématiques Élie Cartan — UMR 7502

Mis en page avec la classe thloria.

Remerciements

En premier lieu je tiens à remercier mon directeur de thèse Monsieur Lionel Rosier pour l'intérêt qu'il a porté à mon travail.

Je suis reconnaissant à Madame Assia Benabdallah et Monsieur Pierre Rouchon qui ont accepté d'être les rapporteurs de cette thèse, ainsi que, tout particulièrement, à Monsieur Jean-Michel Coron qui m'a fait l'honneur d'être le président de mon jury.

Monsieur Christophe Prieur, avec lequel j'ai eu par ailleurs la chance de travailler au cours de ma thèse, et Monsieur Marius Tucsnak ont aussi aimablement accepté de prendre part à ce jury : Je les en remercie.

Pour les conditions de travail agréable au sein de l'Institut Élie Cartan je suis reconnaissant. Je tiens, plus localement, à remercier les membres du groupe Corida de l'équipe d'Équations aux Dérivées partielle et plus particuliérement Monsieur Antoine Henrot sans lequel cette thèse n'aurait pas été possible.

J'ai beaucoup apprécié le travail avec Madame Agnès Volpi dans le contexte de mes enseignements à l'ESSTIN : qu'elle en soit remerciée.

Enfin, je souhaite témoigner ma reconnaissance à ma famille et mes amis pour leur soutien indéfectible.

Je dédie cette thèse à SW.

Table des matières

Introduction générale

1 Présentation des problématiques

L'optique adaptative est une technique qui permet de corriger en temps réel les déformations évolutives et non-prédictibles d'un front d'onde grâce à un miroir déformable.

Par exemple, en astronomie, la turbulence atmosphérique dégrade la qualité de nos images. Si nous avons l'impression qu'une étoile scintille, ce n'est pas parce que l'étoile émet de la lumière d'une façon particulière mais parce que la turbulence atmosphérique déforme l'image que nous en avons (et plus particulièrement une caractéristique du rayonnement lumineux appelé le *front d'onde* ou la *phase*). En optique adaptative, on utilise alors un analyseur de front d'onde pour estimer la perturbation due à l'atmosphère, puis l'on déforme un miroir (grâce à un système de pistons) de façon à compenser exactement cette perturbation. Ainsi l'image après réflexion sur le miroir apparaît comme s'il n'y avait pas eu de dégradation.

Tout d'abord développée dans les années 70 pour des besoins militaires de focalisation de faisceaux laser, le domaine principal d'utilisation de l'optique adaptative est l'astronomie mais commence à s'étendre à bon nombre d'autres domaines (fusion, médical, télécommunications). On commence à l'utiliser en ophtalmologie afin de produire des images très précises de la rétine.

Lorsque l'optique adaptative est utilisée pour corriger des déformations lentes introduites non par l'atmosphère mais par l'instrument optique lui-même (effet du vent, de dilatation des matériaux, de la gravité, etc.) on parle alors plutôt d'*optique active*.

Le seul fait de pointer un télescope de 20cm de diamètre vers une étoile brillante permet de mettre en évidence de grands défauts dans l'image obtenue, en mesurant la tache de diffustion (*point spread function* en anglais, et notée par la suite PSF) du système atmosphère-télescope. Même si le télescope est dépourvu d'aberrations, le PSF mesuré lors d'une exposition de plusieurs secondes sera bien plus large que celui prédit par la simple diffraction. Une exposition très courte, de l'ordre d'une dizaine de millisecondes, présente elle des défauts d'une nature différente : les images ont une apparence tachetée. L'origine de ces défauts est en fait la turbulence atmosphérique. En l'absence de méthodes de compensation, la turbulence atmosphérique réduit de manière fondamentale la performance des systèmes d'imagerie qui doivent regarder à travers l'atmosphère.
La turbulence atmosphérique dégrade la qualité des systèmes optiques parce qu'elle correspond à un milieu non homogène : cette inhomogénéité se répercute au niveau de l'index de réfraction, et les ondes n'ont plus les mêmes chemins optiques. La lumière émise par une source de lumière distante, par exemple une étoile, dans un milieu homogène peut être modélisée de manière très satisfaisante par une onde plane. Dans le vide, cette onde reste plane, l'indice de réfraction étant homogène. En revanche, au niveau de l'atmosphère, les inhomogénéités vont déformer le front d'onde, d'où la nécessité de trouver des solutions compensant ces défauts. Les outils en verre classiques sont malheureusement à écarter, car le fait que les caractéristiques de l'atmosphère évoluent assez rapidement ajoutent une difficulté supplémentaire, et rendent le problème à la fois compliqué et excitant.
En pratique, on s'aperçoit que la turbulence atmosphérique est un facteur bien plus limitant que la conception ou la qualité du système optique. Même aux meilleurs sites d'observation, la résolution angulaire est limitée à environ 1 arcsec (environ 5μ rad) dans le domaine visible, quelle que soit la taille du télescope. Cela est à comparer à la résolution

théorique de $0,013$ arcsec obtenue pour un télescope de 8 mètres de diamètre. Le Hubble Space Telescope, placé au-dessus de l'atmosphère, permet lui d'atteindre une résolution de 0.05 arcsec. Les très grands télescopes (Very Large Telescopes, notés VLT) ont été conçus pour l'imagerie en astronomie. Malgré leur diamètre qui leur permet de capturer un nombre important de photons, leur résolution angulaire n'est pas meilleure que celle de télescopes de diamètres bien plus faibles.
Depuis les études très poussées entre 1950 et 1970 pour comprendre les effets de la turbulence atmosphérique sur les systèmes optiques, plusieurs solutions ont été proposées pour en atténuer les effets. On en distingue trois sortes : 1. Le *postprocessing*, qui correspond au traitement des données qui ont déjà été recueillies ; 2. des techniques d'optique adaptative, qui utilisent des moyens techniques pour mesurer et corriger les aberrations dues à la turbulence ; 3. des méthodes hybrides, qui combinent des éléments du post-traitement et de l'optique adaptative.

Cette thèse s'intéresse plus particulièrement aux méthodes liées à l'optique adaptative.

2 Historique

Isaac Newton était déjà conscient des effets négatifs de la turbulence atmosphérique, en particulier de l'impossibilité d'atteindre sans correction les limites imposées par la diffraction, quel que soit le télescope utilisé. On avait déjà remarqué que, contrairement aux planètes, les étoiles scintillent, et que la tache mesurée lors de l'observation d'une étoile était beaucoup plus large que lors des essais en laboratoire. C'est pourquoi Newton attribua ces effets à l'agitation des gaz dans l'atmosphère :

> "If the theory of making Telescopes could at length be fully brought into Practice, yet would there be certain Bounds beyond which Telescopes could not perform. For the air through which we look upon the Stars, is in perpetual Tremor ; as may be seen by the tremulous Motion of Shadows cast from high Towers, and by the twinkling of the fix'd stars."

Newton était également capable d'expliquer pourquoi les étoiles scintillent lorsqu'elles sont regardées à l'œil nu, et pas à travers un télescope :

> "But these Stars do not twinkle when viewed through Telescopes which have large apertures. For the Rays of Light which pass through divers parts of the aperture, tremble each of them apart, and by means of their various and sometimes contrary Tremors, fall at one and the same time upon different points at the bottom of the Eye, and their trembling Motions are too quick and confused to be perceived severally."

Les recommandations de Newton furent donc de construire des télescopes aussi larges que possible, et placés en altitude, afin de diminuer l'épaisseur d'atmosphère à traverser. Ces deux préoccupations restent deux des principes de base actuels lors de la mise en place d'un nouveau télescope.

> "The only Remedy is a most serene and quiet Air, such as may perhaps be found on the tops of the highest Mountains above the grosser Clouds."

Malgré tout, comprendre le phénomène ne permit pas d'améliorer grandement la qualité des mesures avant les années 1960. Les contemporains de Newton ne disposaient comme détecteur de lumière que leurs yeux. Au début du 19$^{\text{ème}}$ siècle, l'apparition de la photographie autorisa l'obtention d'images des astres ; mais la durée de l'exposition, bien supérieure aux durées intervenant dans les phénomènes liés à la turbulence, limita la qualité de ces clichés. Avec l'arrivée de nouveaux appareils photos dans les années 1950, la turbulence est comme *gelée*, et le facteur limitant devient la diffraction lors des prises de vue.

Les premiers travaux qui réussirent à vaincre, au moins partiellement, la turbulence s'appuyèrent sur le post-traitement d'un grand nombre de clichés, avec une exposition très courte, grâce à des outils comme la transformée de Fourier. Malheureusement, ces méthodes souffraient du fait que le bruit était bien plus important que le signal, et le nombre de prises de vue nécessaires à une qualité satisfaisante était énorme. Une autre méthode fut alors proposée, qui consistait à récupérer non seulement les images, mais aussi des informations sur le front d'onde grâce à un analyseur de front d'onde. Une déconvolution sur les données donnait alors l'image désirée On parle alors d'*optique active*.

L'idée que les aberrations induites par l'atmosphère pourraient être compensées par des procédés mécaniques fut présentée par Babcock dans **??**Bab48]. Cette conjecture suit directement la prise de conscience que les aberrations dues à la turbulence correspondent à des variations dans le chemin optique entre l'objet et le télescope. Si un moyen permettait d'ajuster ce chemin optique, la qualité de l'image s'en retrouverait améliorée. Désormais, de tels procédés existent, et sont appelés des *systèmes d'optique adaptative*. Un système d'optique adaptative analyse le front d'onde, détermine la correction à apporter au front d'onde, et effectue cette compensation, le tout en temps réel. Le principe est expliqué dans le schéma suivant :

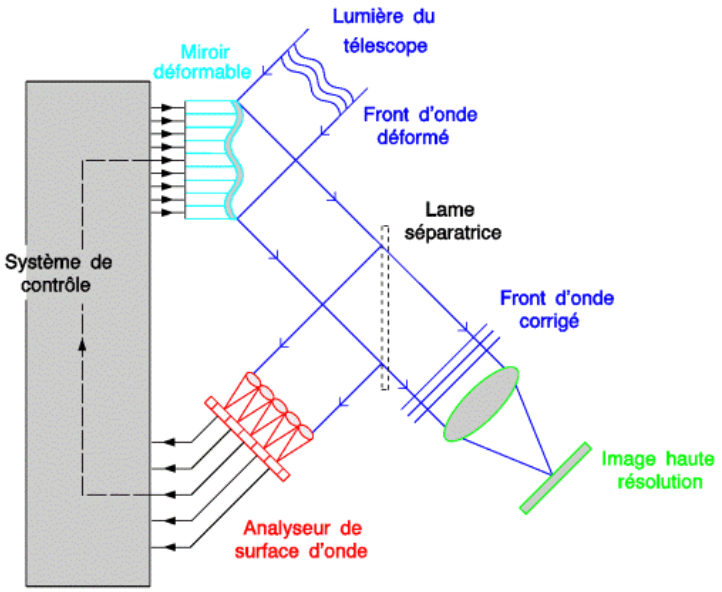

Pour se rendre compte de l'efficacité du procédé, il suffit de regarder les deux images suivante, correspondant à la galaxie NGC7569, observée avec et sans optique adaptative.

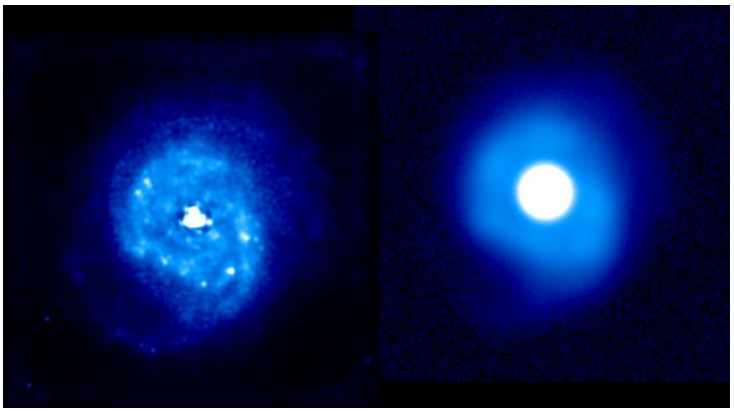

De nouvelles pistes sont actuellement explorées, permettant d'utiliser à la fois les techniques d'optique adaptative et d'optique active.

3 Plan de la thèse

Dans cette thèse nous nous intéressons à trois principaux problèmes liés aux systèmes d'optique adaptative :

- quel front d'onde faut-il corriger ? Cette idée est celle apparue avec l'optique active : avant de pouvoir éliminer les aberrations du front d'onde liées aux effets de la turbulence ou certains défauts du télescope, il est nécessaire de connaître le front d'onde incident. Celui-la se mesure sur une grille grâce à un analyseur de front d'onde, par exemple celui de Shack-Hartmann. Nous présenterons plusieurs méthodes permettant la reconstruction désirée à partir des mesures. En anticipant un peu sur la deuxième partie, un effort sera également fourni pour disposer d'informations sur le gradient du front d'onde.
- Babcock prévoyait que la compensation de la turbulence par des procédés mécaniques était possible, en modifiant le chemin optique des rayons incidents, grâce à un miroir déformable. Une fois le front d'onde incident connu, quelle forme du miroir assure la correction le front d'onde ? Une telle formule est-elle efficace lorsqu'on n'a accès qu'au front d'onde reconstruit ? Des équations paramétriques décrivant le miroir sont obtenues, et la correction obtenue est testée numériquement.
- Dans la deuxième partie, un modèle, issu des travaux de Lenczner et Prieur de miroir déformable est présenté : composé de trois couches, correspondant au miroir lui-même (couche flexible),et de deux couches équipées de piezoélectriques servant à respectivement de capteurs et d'actionneurs, ces miroirs sont appelés *miroirs bimorphes*. Une des caractéristiques importantes du modèle est le couplage de deux EDP de natures très différentes, la première faisant apparaître un opérateur elliptique du second ordre sans dérivée temporelle, et la deuxième étant une équation d'Euler-Bernoulli. Des résultats concernant le contrôle et la stabilisation de tels miroirs sont présentés.
- Dans la troisième partie, un modèle de miroir composé d'une poutre et de deux cellules piezoélectriques est étudié. distincts de miroir sont considérés, l'un mettant

en jeu deux EDP couplées, et l'autre une poutre avec deux cellules piezoélectriques. Divers théorèmes portant sur la stabilisation du système sont alors énoncés.

Première partie

Mesure et correction du front d'onde

1

Reconstruction du front d'onde

Introduction

La première partie de cette thèse est consacrée aux analyseurs de front d'onde, et à la reconstruction effective du front d'onde à partir des mesures expérimentales.

1.1 Analyseur de front d'onde

1.1.1 Principe de fonctionnement

L'analyseur de front d'onde permet la mesure de la phase du front d'onde, qui est ensuite utilisée dans la commande du miroir déformable, afin d'assurer la correction du front d'onde. Généralement, la valeur de la phase n'est pas mesurée directement. Au lieu de cela, on a accès au gradient ou au laplacien du front d'onde, autrement dit à la pente ou à la courbure du front d'onde, respectivement.

Dans la suite, l'analyseur retenu est celui de Shack-Hartmann pour mesurer les caractéristiques du front d'onde, en raison de sa fréquence d'utilisation dans les systèmes d'optique adaptative.

Un Shack-Hartmann est composé d'une matrice de micro-lentilles, placée devant un capteur sensible à la lumière. Ces deux composants sont situés dans des plans parallèles.

À l'arrivée d'un faisceau, chaque micro-lentille génère sur le capteur un point de focalisation, dont la position varie, en fonction de la déformation locale du front d'onde, autour de sa position de référence, correspondant à un front d'onde non déformé.

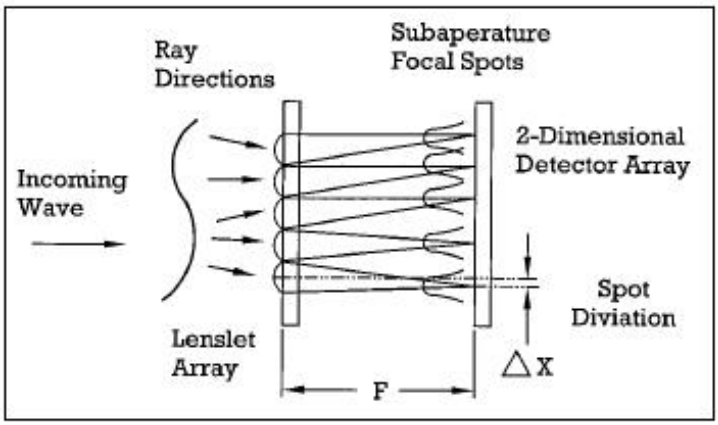

L'image donnée par le capteur est ainsi une matrice de taches dont le nombre correspond au nombre de micro-lentilles. La déviation de chaque tache par rapport à sa référence donnant la pente (ou dérivée) locale du front d'onde, l'ensemble des déviations donne directement le gradient moyen du front d'onde.

Si un front d'onde est plan ou sphérique (c'est-à-dire si il est issu d'une source lumineuse ponctuelle), les micro-lentilles génèrent une matrice de taches dont l'espacement est parfaitement régulier. Cet espacement est directement relié à la courbure du front d'onde (qui est directement reliée à la distance de la source) : plus celui-ci est courbé, plus les taches seront espacées.

1.1.2 Historique

En 1880, M. Hartmann, un astronome américain, eut l'idée de mettre une plaque trouée devant un télescope de type Cassegrain, et de capturer sur une plaque photo (dans un plan intra ou extra focale) le signal associé à une étoile. Une telle plaque trouée échantillonne le front d'onde mesuré. Le comportement du front d'onde est ainsi analysé par petite portions, les trous décomposant le front d'onde élémentaire en portions de front d'onde.

À l'époque de Hartmann, les mesures se faisaient au double-décimètre directement sur la plaque photo.

En 1970, M. Shack, un physicien américain, eu l'idée de remplacer la plaque de trou par des microlentilles. L'intérêt des microlentilles (de section carrée) est principalement de ne plus perdre de flux lumineux (taches plus lumineuses) et d'obtenir un « bras de levier » rendant la mesure plus précise !

En 1985, l'ONERA à participé au développemeny du détecteur de Shack-Hartmann dans le but de faire de l'image haute résolution (optique adaptative) ainsi que pour améliorer la focalisation des lasers de puissance à des fins militaires.

1.2 Reconstruction du front d'onde

A partir des mesures du capteur, on cherche à reconstruire le front d'onde.

Le problème est tout d'abord résolu en dimension 1. La résolution du problème particulièrement simple permet de mettre en relief des idées très utiles pour les dimensions supérieures.

Une méthode directe est alors avancée, assurant à la fois une reconstruction directe, rapide et de bonne qualité.

Ensuite, une amélioration du travail de Fernando Cordero[**?**] est introduite : au lieu d'approcher les intégrales par la méthode des trapèzes, la méthode de Simpson est utilisée. L'algorithme reste sensiblement le même, mais la rapidité de convergence de l'algorithme est accrue, et l'information sur le gradient du front d'onde est disponible.

Enfin, quelques simulations numériques démontrent également l'efficacité des méthodes spectrales, utilisant les bases de fonctions propres du laplacien.

1.3 Enoncé du problème et notations

Dans ce chapitre, nous nous intéressons à la reconstruction locale du front d'onde à partir des mesures du Shack-Hartmann. Cordero a déjà proposé une méthode dans [**?**]. La deuxième partie mettra en lumière la nécessité de disposer d'informations non seulement sur le front d'onde, mais également sur son gradient.

D'une manière générale, nous disposons d'un maillage du segment $[0,1]$ ou du carré $R = [0,1] \times [0,1]$, et de la mesure des moyennes des gradients sur chaque maille. A partir de ces données, nous reconstruisons la fonction aux nœuds ou aux centres des mailles selon les cas. Commençons par définir le maillage : il est régulier, et les mailles sont carrées en dimension 2. N est un entier strictement positif qui permet de caractériser la taille du maillage ; il y a N cellules en dimension 1, et N^2 en dimension 2. $h := 1/N$ est la longueur de la maille. Soit $x_i = ih$ et $y_j = jh$ pour tout j appartenant à $[0, N]$. La plupart du temps, i et j sont entiers, mais il est pratique de pouvoir les choisir demi-entiers. Les mailles sont définies respectivement en dimension 1 et 2 par :

$$R_i = [x_i, x_{i+1}], \quad i \in \{0, N-1\} \tag{1.1}$$

$$R_{i,j} = [x_i, x_{i+1}] \times [y_j, y_{j+1}], \quad (i,j) \in \{0, N-1\}^2. \tag{1.2}$$

Le front d'onde est la fonction réelle $\tilde{f}$ supposée *assez régulière* défini sur $[0,1]$ ou sur $[0,1]^2$. Les fonctions poids $W_{i,j}$ sont définies pour chaque lentille, et supposées elles-aussi *assez régulières*. Les mesures à notre disposition sont en dimension 1 :

$$p_i = \int_{R_i} W_i \tilde{f}' \tag{1.3}$$

et en dimension 2 :

$$p_{i,j} = \int\int_{R_{i,j}} \frac{W_{i,j} \partial \tilde{f}}{\partial x} \tag{1.4}$$

$$q_{i,j} = \int\int_{R_{i,j}} \frac{W_{i,j} \partial \tilde{f}}{\partial y}. \tag{1.5}$$

Etant donné que toutes les informations sont construites à partir du gradient, il est également supposé que N est pair et :

$$\tilde{f}(0) = 0 \tag{1.6}$$

$$\tilde{f}(\frac{1}{2}, \frac{1}{2}) = 0, \tag{1.7}$$

respectivement en dimensions 1 et 2.

1.4 Cas de la dimension $n = 1$

On se place dans le cas de la dimension $n = 1$. Le front d'onde $\tilde{f}$ est une fonction réelle au moins continue par morceaux sur $[0,1]$. Dans la suite, on suppose que toutes les

lentilles sont identiques, et qu'il existe W définie et au moins continue par morceaux sur $[0, 1]$ telle que :

$$W_i(x) = W\left(\frac{x}{h} - i + 1\right). \tag{1.8}$$

Pour W, nous envisageons deux possibilités : soit $W \equiv 1$, soit W est de classe $\mathcal{C}^1$, avec $W(0) = 0$ et telle que $W(1 - x) = W(x)$. Le premier cas est extrêmement simple en dimension $n = 1$, mais se complique en dimension $n = 2$.

1.4.1 Cas du poids constant

A partir de ces mesures, on cherche à retrouver la valeur de $\tilde{f}$ aux points x_i. Soit f_i la valeur reconstruite au point x_i.

Si l'on suppose de manière supplémentaire que $\tilde{f}$ est de classe $\mathcal{C}^1$, il vient immédiatement que pour tout i de $[-N, N - 1]$,

$$m_i = \tilde{f}(x_{i+1}) - \tilde{f}(x_i) \tag{1.9}$$

$$\tilde{f}(x_i) = \sum_{j=0}^{i} m_j \tag{1.10}$$

Théorème 1.1. *Etant données une fonction $\tilde{f}$ dans $\mathcal{C}^1([-1, 1])$ et les mesures $(m_i)_{-N \leq i \leq N-1}$, on a :*

$$f(x_i) = \sum_{j=0}^{i} m_j \tag{1.11}$$

On choisit alors naturellement :

$$f_i = \sum_{j=0}^{i} m_j \tag{1.12}$$

Ce qui est étonnant, c'est que nous connaissons $f(x_i)$ sans erreur. Dans la suite (correction du front d'onde), nous aurons besoin d'estimations de la dérivée du front d'onde. Nous disposons donc ici des formules classiques de dérivation numérique.

Si nous utilisons par exemple la formule centrée :

$$\tilde{f}'(x_i) = \frac{\tilde{f}(x_{i+1}) - \tilde{f}(x_i)}{2h} + \mathcal{O}(h^2) \tag{1.13}$$

On s'aperçoit en fait que l'on retrouve :

$$\tilde{f}'(x_i) \approx m_{i-1} + m_i \tag{1.14}$$

1.4.2 Cas du poids W

Dans la situation où W n'est plus constante, on ne peut pas intégrer $W_i\tilde{f}$. Une intégration par parties nous permet de trouver :

$$m_i = -\int_{x_i}^{x_{i+1}} W_i'\tilde{f}. \tag{1.15}$$

L'approche n'est pas la même que dans le cas précédent, on va ici obtenir des informations sur $\tilde{f}'$, et ensuite remonter à $\tilde{f}$ par une intégration numérique. On ne cherche plus les valeurs de $\tilde{f}$ aux points x_i, mais aux points correspondant au milieu des lentilles $x_{i+1/2}$.

La formule de Simpson nous permet d'écrire :

$$\int_a^b f(x)dx = \frac{b-a}{6}\left(f(a) + 4f\left(\frac{a+b}{2}\right) + f(b)\right) - \frac{(a-b)^5}{90}f^{(4)}(\xi), \tag{1.16}$$

d'où on retire pour m_i, étant donné que $W(0) = W(1) = 0$:

$$m_i = \frac{2h}{3}W(\frac{1}{2})\tilde{f}'(x_{i+1/2}) + \mathcal{O}(h^5) \tag{1.17}$$

Ensuite, l'utilisation de la méthode du point milieu au niveau de chaque cellule permet de trouver une approximation de $\tilde{f}(x_i)$ avec une erreur en $\mathcal{O}(h^2)$. La formule du point milieu nous permet d'écrire[1] :

$$\int_a^b f(x)dx = (b-a)f\left(\frac{a+b}{2}\right) - \frac{(a-b)^3}{12}f^{(2)}(\xi). \tag{1.18}$$

En utilisant le fait que

$$\tilde{f}(x_i) - \tilde{f}_(x_{i-1}) = \int_{x_{i-1}}^{x_i}\tilde{f}' \approx h\frac{3}{2W(\frac{1}{2})}m_i, \tag{1.19}$$

et le fait que $f(0) = 0$, on parvient à retrouver que

$$\tilde{f}(x_i) = \frac{3}{2W(\frac{1}{2})}\sum_{k=1}^{i} m_i + \mathcal{O}(h^2). \tag{1.20}$$

[1] à vérifier

1.5 Reconstruction directe en dimension 2

A partir de maintenant, on se place dans le cas de la dimension 2. Pour W, les deux cas suivants sont successivement envisagés : celui où $W \equiv 1$, et celui où W est une fonction plus générale, qui s'annule sur le bord de chaque lentille, et est telle que $W(1/2, 1/2) \neq 0$.

On va montrer que l'on peut reconstruire la valeur du front d'onde aux nœuds du maillage, avec une erreur en $\mathcal{O}(h^2)$. L'idée principale du raisonnement réside dans l'utilisation du lemme suivant :

Lemme 1.1. *Si $g : \mathbb{R} \to \mathbb{R}$ est de classe $\mathcal{C}^2$, on peut écrire que :*

$$g(\alpha) = \frac{1}{2h} \int_{\alpha-h}^{\alpha+h} g(x)dx + O(h^2) \tag{1.21}$$

Démonstration. Suppposons g comme dans le lemme. La formule de Taylor-Lagrange appliquée à g en α permet d'écrire pour tout x appartenant à $[\alpha - h, \alpha + h]$:

$$|g(x) - g(\alpha) - (x - \alpha)g'(\alpha)| \leq \frac{(\alpha - x)^2}{2} \sup_{t \in [\alpha-h, \alpha+h]} |g''(t)| \tag{1.22}$$

Une intégration sur $[\alpha - h, \alpha + h]$ nous garantit tout de suite l'existence de $M \geq 0$, indépendant de α tel que :

$$|\int_{\alpha-h}^{\alpha+h} g(x)dx - 2hg(\alpha)| \leq Mh^3. \tag{1.23}$$

Le résultat du lemme apparaît lorsque on isole $g(\alpha)$ et que l'on divise par $2h$. □

Le lemme précédent va nous permettre de reconstruire le front d'onde aux nœuds du maillage avec une erreur en $O(h^2)$. La reconstruction se fait en deux étapes, la reconstruction sur l'axe des abscisses, puis la reconstruction sur le reste du maillage

1.5.1 Etape 1 : Reconstruction sur l'axe des abscisses

Lemme 1.2. *On pose : Alors,*

$$\bar{f}(x_i, 0) = f_{i,0} + O(h^2). \tag{1.24}$$

Démonstration. Supposons que $i > 0$:

$$1 = 0 \tag{1.25}$$

□

Démonstration. Plaçons-nous dans les conditions du théorème, et considérons la somme, et réécrivons-là sous la forme d'une intégrale double :

$$\sum_{l=i_0}^{i-1} p_{i,j_0-1} + p_{i,j_0} = \int_{-h}^{h} \int_{i_0 h}^{ih} \frac{\partial \tilde{f}}{\partial x} dxdy. \tag{1.26}$$

Il est alors naturel d'effectuer l'intégration par rapport à x. Il vient :

$$\sum_{l=i_0}^{i-1} p_{i,j_0-1} + p_{i,j_0} = \int_{-h}^{h} \tilde{f}(ih, ydy - \int_{-h}^{h} \tilde{f}(ih, ydy, \tag{1.27}$$

et l'utilisation du lemme précédent nous permet de conclure :

$$\phi_{i,j_0} = \phi_{i_0,j_0} + \sum_{l=i_0}^{i-1} p_{i,j_0-1} + p_{i,j_0} + \mathcal{O}(h^2). \tag{1.28}$$

□

Remarquons maintenant que ce résultat permettant des évaluations selon l'axe des abscisses a un équivalent pour l'axe des ordonnées :

Lemme 1.3. *Soit M_{i_0,j_0} un noeud intérieur du carré $[0,1] \times [0,1]$, pour lequel ϕ_{i_0,j_0} peut déjà être évalué avec :*

$$\phi_{i_0,j_0} = \tilde{f}(i_0 h, j_0 h) + (O)(h^2) \tag{1.29}$$

On a alors, pour tout i et tout j de $[0, N] \cap \mathbb{N}$

$$\phi_{i,j_0} = \phi_{i_0,j_0} + \sum_{l=i_0}^{i-1} p_{i,j_0-1} + p_{i,j_0} + \mathcal{O}(h^2). \tag{1.30}$$

Les trois lemmes précédents sont les outils nécessaires au théorème suivant :

Théorème 1.2. *Soit $\tilde{f}$ une fonction de classe $\mathcal{C}^2$ sur le carré $[0,1] \times [0,1]$, telle que $\tilde{f}(0,0) = 0$. En supposant que $f_{0,0} = 0$, et en utilisant :*

$$f(i,j) = \sum_{l=0}^{i-1} p_{l,-1} + p_{l,0} + \sum_{l=0}^{j-1} q_{i-1,l} + q_{i,l}, \tag{1.31}$$

l'erreur commise est :

$$||f - \tilde{f}||_\infty = \mathcal{O}(h^2). \tag{1.32}$$

Démonstration. Etant donné que $\tilde{f}(0,0) = 0$, on choisit $f_{0,0}$. L'erreur commise est donc nulle, et donc est $\mathcal{O}(h^2)$. On est donc dans le cadre du lemme précédent, et on a :

$$f_{i,0} = \sum_{l=i_0}^{i-1} p_{i,j_0-1} + p_{i,j_0} + \mathcal{O}(h^2). \tag{1.33}$$

Ensuite, on applique le résultat du lemme aux points $(i,0)$ et (i,j).

$$f_{i,j} = f(i,0) + \sum_{l=0}^{i-1} p_{i,j_0-1} + p_{i,j_0} + \mathcal{O}(h^2) \tag{1.34}$$

$$= \sum_{l=0}^{i-1} p_{l,-1} + p_{l,0} + \sum_{l=0}^{j-1} q_{i-1,l} + q_{i,l} + \mathcal{O}(h^2). \tag{1.35}$$

□

Remarque 1.1. L'utilisation de formules de dérivation numérique classiques va nous permettre d'obtenir des estimations du gradient du front d'onde aux nœuds. Classiquement, cette opération fait perdre un ordre, et l'erreur sera en $\mathcal{O}(h)$.

Remarque 1.2. La méthode ne fait intervenir aucune résolution de système, seulement la multiplication d'une matrice par le vecteur des mesures : elle permettra donc de passer rapidement des mesures à une approximation du front d'onde. Cette caractéristique est très importante dans le cadre de l'optique adaptative, où l'on recherche un traitement en temps réel de l'information.

Remarque 1.3. La formule utilisée dans le lemme est du deuxième ordre, et correspond à l'ordre de l'erreur dans le théorème. On peut facilement, en considérant plus de cellules, améliorer l'ordre de la méthode. Par exemple :

$$g(0) = \frac{2}{3h}\int_{-h}^{h} g - \frac{1}{12h}\int_{-2h}^{2h} g + \mathcal{O}(h^2) \tag{1.36}$$

Remarque 1.4. Si l'on suppose qu'une erreur de mesure est commise au niveau de chaque lentille, et que ces erreurs suivent la même loi de probabilité mais ne sont pas corrélées, on peut choisir différents *chemins* pour rejoindre (i, j) depuis $(0, 0)$, la moyenne permettant de diminuer l'erreur due à la mesure, en appliquant le théorème central limite.

Remarque 1.5. L'un des autres avantages de cette approche réside dans le fait que cette méthode peut être très facilement utilisée pour des géométries très diverses. Ici, elle est présentée dans le cas d'un carré, mais elle fonctionnerait de la même manière dans le cas d'un maillage couvrant un disque.

1.6 Cas de W s'annulant au bord

La grande différence entre le cas précédent et celui-ci est l'impossibilité d'intégrer une première fois et ainsi de faire disparaître les dérivées partielles. La présence de W impose d'utiliser dès le départ une approximation de l'intégrale, dont le résultat est donné dans le lemme suivant :

Lemme 1.4. *Si $g : \mathbb{R}^2 \to \mathbb{R}$ appartient à $\mathcal{C}^2$, on peut écrire que :*

$$W(1/2, 1/2)g(1/2, 1/2) = \frac{9}{4}\int\int_{R_{ij}} W g dx dy + \mathcal{O}(h^5) \tag{1.37}$$

Démonstration. Il suffit pour trouver ce résultat d'appliquer deux fois la formule de Simpson.

$$\int\int W g dx dy = \frac{h}{6}\int \big(W(0, y)g(0, y) + 4W(1/2, y)g(1/2, y) + W(1, y)g(1, y) + \mathcal{O}(h^5)\big)\, dy \tag{1.38}$$

$$= \frac{4h^2}{9} W(1/2, 1/2)g(1/2, 1/2) + \mathcal{O}(h^5). \tag{1.39}$$

□

L'utilisation de ce lemme permet d'approximer le gradient au centre de chaque lentille. Ensuite, si l'on connaît le front d'onde en un milieu de cellule, il suffit de procéder à l'intégration numérique de ce gradient, grâce par exemple à la formule des trapèzes, appliqué entre deux centres de cellules contigues.

Lemme 1.5. *Soit M_{i_0,j_0} un centre de cellule, pour lequel ϕ_{i_0,j_0} peut être évalué avec :*

$$\phi_{i_0,j_0} = \tilde{f}((i_0+1/2)h,(j_0+1/2)h) + \mathcal{O}(h^5). \tag{1.40}$$

On a alors pour tout i et tout j de $[0,N]\cap\mathbb{N}$:

$$\phi_{i,j_0} = \phi_{i_0,j_0} + \frac{4}{9}W(1/2,1/2)\frac{h}{2}\left(p_{i_0,j_0}+p_{i,j_0}\right) + \frac{4}{9}W(1/2,1/2)h\sum_{l=i_0+1}^{i-1} p_{l,j_0} + \mathcal{O}(h^3). \tag{1.41}$$

Démonstration. Plaçons-nous dans les conditions du théorèmes, et considérons l'intégrale, que nous calculons numériquement avec la méthode des trapèzes :

$$\begin{aligned}
\phi_{i,j_0} - \phi_{i_0,j_0} &= \int_{(i_0+1/2)h}^{(i+1/2)h} \frac{\partial \tilde{f}}{\partial x}dx && (1.42)\\
&= \frac{h}{2}\left(\frac{\partial \tilde{f}((i_0+1/2)h,(j_0+1/2)h)}{\partial x} + \frac{\partial \tilde{f}((i+1/2)h,(j_0+1/2)h)}{\partial x}\right) && (1.43)\\
&+ h\sum_{l=i_0+1}^{i-1}\frac{\partial \tilde{f}((l+1/2)h,(j_0+1/2)h)}{\partial x} && (1.44)\\
&+ \mathcal{O}(h^2). && (1.45)
\end{aligned}$$

Le lemme précédent nous assure alors que :

$$\phi_{i,j_0} = \phi_{i_0,j_0} + \frac{4}{9}W(1/2,1/2)\frac{h}{2}\left(p_{i_0,j_0}+p_{i,j_0}\right) + \frac{4}{9}W(1/2,1/2)h\sum_{l=i_0+1}^{i-1} p_{l,j_0} + \mathcal{O}(h^3). \tag{1.46}$$

□

Remarquons maintenant que ce résultat permettant des évaluations selon l'axe des abscisses a un équivalent pour l'axe des ordonnées :

Lemme 1.6. *Soit M_{i_0,j_0} un centre de cellule, pour lequel ϕ_{i_0,j_0} peut être évalué avec :*

$$\phi_{i_0,j_0} = \tilde{f}((i_0+1/2)h,(j_0+1/2)h) + \mathcal{O}(h^5). \tag{1.47}$$

On a alors pour tout i et tout j de $[0,N]\cap\mathbb{N}$:

$$\phi_{i,j_0} = \phi_{i_0,j_0} + \frac{4}{9}W(1/2,1/2)\frac{h}{2}\left(p_{i_0,j_0}+p_{i,j_0}\right) + \frac{4}{9}W(1/2,1/2)h\sum_{l=i_0+1}^{i-1} p_{l,j_0} + \mathcal{O}(h^3). \tag{1.48}$$

Les trois lemmes précédents permettent d'aboutir au résultat suivant :

Théorème 1.3. *Soit $\tilde{f}$ une fonction de classe $\mathcal{C}^2$ sur le carré $[0,1]\times[0,1]$, telle que $\tilde{f}(1/2,1/2)=0$. En supposant que N est impair et que $f_{(N-1)/2,(N-1)/2}=0$:*

$$\phi_{i,j_0}=\phi_{i_0,j_0}+\frac{4}{9}W(1/2,1/2)\frac{h}{2}\left(p_{i_0,j_0}+p_{i,j_0}\right)+\frac{4}{9}W(1/2,1/2)h\sum_{l=i_0+1}^{i-1}p_{l,j_0}+\mathcal{O}(h^3). \quad (1.49)$$

l'erreur commise est :

$$\|f-\tilde{f}\|_\infty=\mathcal{O}(h^2). \quad (1.50)$$

Lemme 1.7. *La construction de la solution se fait en trois étapes : Le choix de $f_{(N-1)/2,(N-1)/2}=0$ permet d'avoir une erreur nulle en ce point $M_{(N-1)/2,(N-1)/2}$, donc en $\mathcal{O}(h^2)$. On passe ensuite de ce point au point $M_{i,(N-1)/2}$ grâce au lemme ? ? ? puis du point $M_{i,(N-1)/2}$ au point $M_{i,j}$ grâce au lemme ? ? ?.*

Les remarques formulées dans le cas $W\equiv 1$ restent généralement vraies.

1.7 Reconstruction indirecte

Cette partie s'intéresse plus particulièrement aux travaux de F. Cordero, et permettent d'améliorer grandement la précision de la méthode tout en conservant une facilité de traitement. Dans cette partie, W est supposée constante, et égale à 1.

Pour rappel, Cordero présente ce théorème :

Théorème 1.4 (Cordero)**.** *Soit $\bar{f} \in C^3(R)$ une fonction telle que $\bar{f}(\frac{1}{2}, \frac{1}{2}) = 0$. Si $(p_{i,j})$ et $(q_{i,j})$ sont les mesures associées à $\tilde{f}$, et $(f_{i,j})$ les valeurs reconstruites aux noeuds (x_i, y_j), on a :*

$$\|\tilde{f}(ih, jh) - f_{i,j}\|_\infty = \mathcal{O}(h|\log(h)|) \tag{1.51}$$

Le fait que l'erreur soit en $h\log(h)$ empêche l'obtention d'informations sur le gradient de $\bar{f}$. Une idée naturelle pour diminuer l'erreur est de remplacer la méthode des trapèzes utilisée pour approximer les mesures par la méthode de Simpson, en réunissant 4 cellules, pour avoir suffisamment de points, et recommencer le même traitement. Malheureusement, même si cette méthode est un peu meilleure, l'erreur étant en $\mathcal{O}(h)$, elle reste inefficace.

Le moyen de dépasser cet obstacle réside dans la recherche d'une équation de Poisson. Mais au lieu d'attendre un schéma sympathique, nous allons le faire apparaître en accordant des poids aux cellules.

Etant donné un noeud à l'intérieur du carré R, considérons les mesures :

$$P_{i,j} := p_{i,j-1} + p_{i,j} - p_{i-1,j-1} - p_{i-1,j} \tag{1.52}$$

et

$$Q_{i,j} := q_{i-1,j} + q_{i,j} - q_{i-1,j-1} - q_{i,j-1}. \tag{1.53}$$

Lemme 1.8. *Si $\tilde{f}$ appartient à $\mathcal{C}^2$, et si (x_i, y_j) est un point intérieur au carré, alors :*

$$P_{i,j} = \frac{h}{6}\left(\tilde{f}(x_{i-1}, y_{j-1} + 4\tilde{f}(x_{i-1}, y_j) + \tilde{f}(x_{i-1}, y_{j+1})\right) \tag{1.54}$$

$$+ \frac{h}{6}\left(-2\tilde{f}(x_i, y_{j-1}) - 8\tilde{f}(x_i, y_j) - 2\tilde{f}(x_i, y_{j+1})\right) \tag{1.55}$$

$$+ \frac{h}{6}\left(\tilde{f}(x_{i+1}, y_{j-1} + 4\tilde{f}(x_{i+1}, y_j) + \tilde{f}(x_{i+1}, y_{j+1})\right) + \mathcal{O}(h^5). \tag{1.56}$$

et

$$Q_{i,j} = \frac{h}{6}\left(\tilde{f}(x_{i-1}, y_{j-1} + 4\tilde{f}(x_i, y_{j-1}) + \tilde{f}(x_{i+1}, y_{j-1})\right) \tag{1.57}$$

$$+ \frac{h}{6}\left(-2\tilde{f}(x_{i-1}, y_j - 8\tilde{f}(x_i, y_j) - 2\tilde{f}(x_{i+1}, y_j)\right) \tag{1.58}$$

$$+ \frac{h}{6}\left(\tilde{f}(x_{i-1}, y_{j+1} + 4\tilde{f}(x_i, y_{j+1}) + \tilde{f}(x_{i+1}, y_{j+1})\right) + \mathcal{O}(h^5). \tag{1.59}$$

Démonstration. La preuve de ce lemme repose sur la méthode de Simpson : après avoir effectué l'intégration possible, il reste trois intégrales à calculer numériquement. La présence de trois points permet d'utiliser la méthode de Simpson, bien plus efficace que celle des trapèzes. □

L'addition de $P_{i,j}$ et $Q_{i,j}$ nous permet de discerner deux schémas d'approximation du laplacien. Appelons donc $\Delta_{i,j} := P_{i,j} + Q_{i,j}$.

Lemme 1.9. *Si $\tilde{f}$ appartient à $\mathcal{C}^2$, et si (x_i, y_j) est un point intérieur au carré, alors :*

$$\Delta_{i,j} = 2h^3 \Delta\tilde{f} + \mathcal{O}(h^5) \tag{1.60}$$

Démonstration. On part de :

$$\Delta_{i,j} = \frac{2h}{3}\left(\tilde{f}(x_{i-1,j-1} + f(x_{i,j-1} + f(x_{i+1,j-1})\right) \tag{1.61}$$
$$+ \frac{2h}{3}\left(\tilde{f}(x_{i-1,j} - 8f(x_{i,j} + f(x_{i+1,j})\right) \tag{1.62}$$
$$+ \frac{2h}{3}\left(\tilde{f}(x_{i-1,j+1} + f(x_{i,j+1} + f(x_{i+1,j+1})\right) + \mathcal{O}(h^5). \tag{1.63}$$

Après avoir réorganisé les termes, on trouve :

$$\Delta_{i,j} = \frac{2h}{3}\left(\tilde{f}(x_{i-1,j-1} + \tilde{f}(x_{i-1,j+1} + f(x_{i+1,j+1}) + f(x_{i+1,j-1})\right) \tag{1.64}$$
$$+ \frac{2h}{3}\left(\tilde{f}(x_{i,j-1} + \tilde{f}(x_{i-1,j} - 8f(x_{i,j} + f(x_{i+1,j} + f(x_{i,j+1})\right) \tag{1.65}$$
$$+ \mathcal{O}(h^5). \tag{1.66}$$

On reconnaît alors deux schémas à cinq points du laplacien :

$$\Delta_{i,j} = \frac{2h}{3} 2h^2 \Delta\tilde{f} + \frac{2h}{3} h^2 \Delta\tilde{f} + \mathcal{O}(h^5). \tag{1.67}$$

□

Le cas des points intérieurs a maintenant été traité. Regardons maintenant des cas sur le bord de R (sauf les sommets, qui sont négligés). Regroupons maintenant pour chaque point M du bord la somme des deux mesures des cellules auxquelles il appartient et appelons $D_{i,j}$ la combinaison choisie. Le calcul va maintenant faire apparaître des conditions de Neumann au bord.

Lemme 1.10. *Si $\tilde{f}$ appartient à $\mathcal{C}^2$, et si $M = (x_i, y_j)$ est un point sur la frontière du carré, alors :*

$$D_{i,j} = 6h^2 \frac{\partial\tilde{f}}{\partial n} + \mathcal{O}(h^5) \tag{1.68}$$

Démonstration. Pour la démonstration, on se place dans le cas où $y_j = 0$. Les autres cas sont analogues. On considère maintenant les cellules associées à la deuxième composante du gradient, pour $R_{i-1,0}$ et $R_{i,0}$. Après intégration, on a :

$$D_{i,j} = q_{i-1,0} + q_{i,0} = \int_{x_{i-1}}^{x_{i+1}} \left(\tilde{f}(x,h) - \tilde{f}(x,0)\right) dx. \tag{1.69}$$

La règle de Simpson permet alors de trouver :

$$D_{i,j} = \frac{h}{3}\Big(\tilde{f}(x_{i-1},h) + 4\tilde{f}(x_i,h) + \tilde{f}(x_{i+1},h)\Big) \tag{1.70}$$
$$- \frac{h}{3}\Big(\tilde{f}(x_{i-1},0) + 4\tilde{f}(x_i,0) + \tilde{f}(x_{i+1},0)\Big) \tag{1.71}$$
$$+ \mathcal{O}(h^5). \tag{1.72}$$

Il ne reste plus qu'à reconnaître la discrétisation de la dérivée normale. □

La dernière étape reste le théorème :

Théorème 1.5. *Soit $\tilde{f}$ une fonction de classe $\mathcal{C}^3$ sur le carré R. une fonction telle que $\tilde{f}(\frac{1}{2},\frac{1}{2}) = 0$. Si $(p_{i,j})$ et $(q_{i,j})$ sont les mesures associées à $\tilde{f}$, et $(f_{i,j})$ les valeurs reconstruites aux noeuds (x_i, y_j), on a :*

$$\|\tilde{f}(ih,jh) - f_{i,j}\|_\infty = \mathcal{O}(h^2) \tag{1.73}$$

Démonstration. Ce résultat vient immédiatement des résultats sur les méthodes de différences finies, étant donné qu'on s'est ramené à une équation de Poisson. □

Remarque 1.6. La méthode étant du deuxième ordre, on peut évaluer numériquement le gradient, en commettant ici une erreur en $\mathcal{O}(h)$.

Remarque 1.7. Il est en théorie possible d'améliorer encore la qualité de la reconstruction, en faisant par exemple un schéma à neuf points. Cependant, afin de ne pas perdre de précision en effectuant l'intégration numérique, il sera nécessaire de prendre une méthode à cinq points, et le nombre de cellules mises en jeu pour faire apparaître le laplacien en un point s'élèvera à 64.

2

Correction du front d'onde

Introduction

Après avoir établi les caractéristiques du front d'onde et pris conscience de ses perturbations, il est temps de les faire disparaître, ou au moins de les atténuer. Les perturbations sont générées par la traversée des zones turbulentes de l'atmosphère : le passage dans un milieu non homogène crée des différences dans le chemin optique des rayons lumineux. Il suffit pour rendre le front plan de compenser pour chaque rayon, l'avance prise sur les autres, et de faire en sorte que tous arrivent parallèles et en même temps.

L'outil le plus classique et le plus performant pour corriger un front d'onde est le miroir déformable. Dans ce chapitre, nous cherchons la forme adéquate à donner au miroir pour assurer à chaque rayon lumineux le même chemin optique. La correction sera alors parfaite et le front d'onde réfléchi plan.

Le chapitre dédié à la correction du front d'onde se divise en trois parties.

Nous commencerons par nous intéresser au problème en dimension 2, et en profiter pour avoir un aperçu d'un système complet d'optique adaptative. Ce travail a été publié dans un proceedings à l'occasion de l'IFAC World Congress, qui a eu lieu à Prague en juillet 2005.

Ensuite viendra la généralisation de l'étude à la dimension n. Quelle que soit la dimension, il est possible de corriger n'importe quel front d'onde incident, sous toutefois certaines hypothèses de régularité. Les résultats valident également le choix souvent pris de donner une forme au miroir qui *copie* celle du front d'onde.

Enfin, nous montrerons que le couplage de l'analyseur de Shack-Hartmann et du miroir déformable permet de réduire considérablement l'ampleur des perturbations.

2.1 IFAC 2005

EXACT WAVEFRONT CORRECTION IN ADAPTIVE OPTICS.

Pierre Le Gall * **Lionel Rosier** *

* *Institut Elie Cartan, Université Nancy 1, B.P. 239, Vandœuvre-lès-Nancy Cedex, France*

Abstract: In this work we consider an adaptive optical system in which a deformable mirror is controlled to compensate for random wavefront disturbances. For most systems of this type, the shape of the mirror is taken as a linear function of the wavefront error, leading to satisfactory results in *linear* regimes. Here, the geometric shape of the mirror leading to a *perfect* correction of the wavefront is derived. Next, a control is designed to reach that geometric shape when the deformable mirror is a membrane mirror with electrostatic actuators. Numerical simulations illustrating the improvements supplied by the geometric approach are also reported here.

Keywords: Adaptive optics, exact wavefront correction, membrane mirror.

1. INTRODUCTION

Adaptive Optics (AO) is the technology developed for 25 years for correcting random optical wavefront distortions in real time (see e.g. (Roggeman and Welsh, 1996); (Hardy, 1998); (Tyson, 1998); (Roddier, 1999); (Plemmons and Pauca, 2000); (Luke *et al.*, 2002); (Zakynthinaki and Saridakis, 2003)). Wavefront disturbances typically appear when optical rays cross the Earth's atmosphere, since the refraction index depends on the air density, and the air density fails to be uniform in a turbulent environment.

An adaptive optics system is composed of a wavefront sensor and of a deformable mirror which is controlled in real time to compensate for random wavefront disturbances. The correction of the wavefront is said to be *perfect* (or *exact*) when the wavefront obtained after the reflection on the deformable mirror is planar. For most systems encountered in AO, the shape of the mirror is taken as a linear function of the wavefront error, leading to satisfactory results in *linear* regimes. Obviously, a perfect correction of the wavefront cannot be obtained this way, in general. In this work we investigate the possibility of achieving a perfect correction of any incident wavefront. That issue proves to be of great importance in nonlinear regimes where linear compensation does not work well.

The mathematical issue whether any incident wavefront may be corrected through the reflection on a convenient mirror is not obvious at all. The first reason is that computations based upon the Snell-Descartes first law reveal that a loss of derivative occurs, and that the Nash-Moser fixed-point theorem cannot be applied. The second reason is that the solution may fail to exist in certain circumstances: if the incident wavefront is a sphere, then we cannot find any corrector mirror passing through the center of the sphere.

Here, following a different approach we succeed in deriving a parametric representation of a deformable mirror achieving a perfect correction of any given incident wavefront. The formulas are provided in any dimension and for any incident angle. Next, a control is designed to compensate

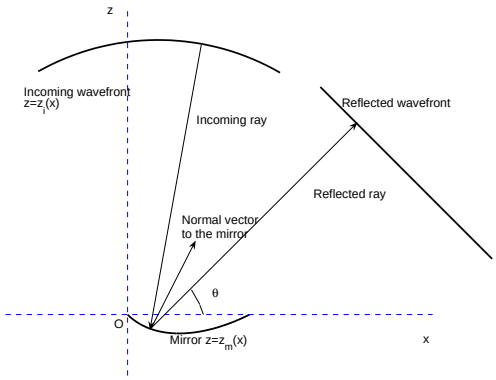

Fig. 1. Adaptive Optics device

for slowly time-varying wavefront disturbances when the deformable mirror is a membrane mirror with electrostatic actuators. Numerical simulations illustrating the improvements supplied by the geometric approach are provided.

The paper is organized as follows. In Section 2 we provide the parametric equations of the corrector mirror in the n-dimensional framework (Theorem 1), and we sketch the derivation of such formulas in dimension 2. These formulas are given when the incident wavefront is a hypersurface. Their generalization to parametrically defined incident wavefronts is also supplied in dimensions 2 and 3. Section 3 is devoted to the determination of the incident wavefront when the measured wavefront is the reflected one (closed-loop configuration). Numerical simulations are displayed in Section 4. In Section 5 we investigate the tracking problem for a membrane mirror. Section 6 is a brief conclusion.

2. OPEN LOOP

2.1 The n-dimensional problem

Let $\mathbb{R}^n$ be the Euclidean n-dimensional space, whose generic point is denoted by $(x,z) = (x_1,...,x_{n-1},z)$. Let $\{\boldsymbol{e}_i\}_{1\le i\le n}$ denote the canonical basis of $\mathbb{R}^n$. The incoming wavefront (resp., the deformable mirror) is assumed to be defined by the equation $z = z_i(x) = z_i(x_1,...,x_{n-1})$ (resp., $z = z_m(x)$), where $z_i : [0,1]^{n-1} \to \mathbb{R}$ and $z_m : [0,1]^{n-1} \to \mathbb{R}$ are given functions of class C^1. The undeformed mirror is assumed to lie on the hyperplane $z = 0$, so that a planar incident wavefront of the form $\cos(\theta)x_1 - \sin(\theta)z = const$ gives rise to a planar reflected wavefront of the form $\cos(\theta)x_1 + \sin(\theta)z = const$. The wave vector associated with the reflected wavefront is defined as $\boldsymbol{f} = \cos(\theta)\boldsymbol{e}_1 + \sin(\theta)\boldsymbol{e}_n$, where $\theta \in [0, \frac{\pi}{2}]$ is some given angle. (See Figure 1.)

The following function is introduced for notational convenience

$$\Delta := \left(1 + \sum_{j=1}^{n} \left(\frac{\partial z_i}{\partial x_j}\right)^2\right)^{\frac{1}{2}}.$$

The following theorem provides a parametric representation of the mirror achieving a perfect correction of any given incoming wavefront.

Theorem 1. Assume that the function z_i is of class C^2. Then for any number C, the following parametric equations

$$X_j = x_j + \frac{\cos(\theta)x_1 + \sin(\theta)z_i(x) + C}{\Delta - \cos(\theta)\frac{\partial z_i}{\partial x_1} + \sin(\theta)} \cdot \frac{\partial z_i}{\partial x_j}, \quad j = 1,\dots,n-1 \tag{1}$$

$$Z = z_i(x) - \frac{\cos(\theta)x_1 + \sin(\theta)z_i(x) + C}{\Delta - \cos(\theta)\frac{\partial z_i}{\partial x_1} + \sin(\theta)} \tag{2}$$

with $(x_1,\dots,x_{n-1}) \in [0,1]^{n-1}$, define a mirror shape leading to a perfect correction of the incoming wavefront $z = z_i(x)$.

The proof of Theorem 1 presents two steps.

- In a first step, assuming that the problem has indeed a solution, we derive the formulas (1)-(2) in using the fact that (i) all the reflected rays share the same wave vector (namely, $\boldsymbol{f}$) and (ii) the planar reflected wavefront is an equiphase surface (i.e., the time needed to reach the reflected wavefront from the incident wavefront does not depend of the ray under consideration.) Notice that the Snell-Descartes first law is not explicitly used in the computations.
- In a second step, we check that the reflected wavefront computed in applying the Snell-Descartes first law is indeed *planar* when the shape of the mirror is given by (1)-(2).

The full details of the proof will appear elsewhere. The derivation of (1)-(2) when $n = 2$ is sketched in the next section. Let us do some comments.

(1) The shape of the deformable mirror that enables a perfect correction of an arbitrary incoming wavefront is given as a parametrized surface. When the map $x \mapsto X = (X_1,...,X_{n-1})$ is invertible, then the mirror may be defined by some equation $Z = z_m(X_1,...,X_{n-1})$.

(2) A loss of regularity occurs: if z_i is of class C^r, then the functions $X_1(x),...,X_{n-1}(x),Z(x)$ are expected to be of class C^{r-1} only, due to the presence of the derivatives $\partial z_i/\partial x_j$ in (1)-(2). Notice that the formulas (1)-(2) may be used when z_i is merely of class C^1, although the Snell-Descartes first law cannot

be applied to check whether the reflected wavefront is still planar. Indeed, to apply the Snell-Descartes reflection law, the existence of a normal vector to the mirror surface is required at each point of the mirror. That property is guaranteed if the functions $X_i(x)$ $(1 \leq i \leq n-1)$ and $Z(x)$ are of class C^1, but these functions are only continuous when z_i is of class C^1. Notice that a loss of regularity (expressed in a statistical framework) has also been pointed in (Le Roux, 2003).

(3) The shape of the mirror which works fine turns out not to be unique. Actually, we found a one-parameter family of solutions (C being the parameter). Geometrically, giving a value to C amounts to choosing the location where some incident ray and the mirror intersect. Notice that the different shapes of the mirror do not correspond to simple translations of one of them: the shape of the mirror change with C. On the other hand, the surface defined by (1)-(2) may reduce to a point for certain value of C (see below for some example).

2.2 The 2D problem

Here, we consider the simplest case where $n = 2$, hence $x = x_1$. We aim to derive the parametric form of the mirror shape thanks to which a perfect correction of the incident wavefront may be carried out. An incident ray issued from $(x, z_i(x))$ admits as (tangent) wave vector the vector $\boldsymbol{n} = \frac{1}{\Delta}(z_i'(x), -1)$. The intersection point of the ray with the mirror is given by

$$\begin{cases} X = x + \dfrac{t}{\Delta} z_i'(x) \\ Z = z_i(x) - \dfrac{t}{\Delta} \end{cases} \tag{3}$$

where $\Delta(x) = \sqrt{1 + |z_i'(x)|^2}$ and t denotes the time needed to reach the mirror. (The speed of light, whose value does not matter here, is chosen to be one.) The key point is that the wave vector of the reflected ray is $\boldsymbol{f} = (\cos(\theta), \sin(\theta))$, which amounts to saying that the reflected wavefront takes the form $g(x) := \cos(\theta)x + \sin(\theta)z = const.$ Therefore, for T large enough, the function

$$\begin{aligned} g(x) = &\cos(\theta)(X + (T-t)\cos(\theta)) \\ &+ \sin(\theta)(Z + (T-t)\sin(\theta)) \\ = &(x + \frac{t}{\Delta} z_i'(x))\cos(\theta) \\ &+ (z_i(x) - \frac{t}{\Delta})\sin(\theta) + (T-t) \end{aligned}$$

has to be constant with respect to x. Expressing t as a function of x and plugging it in (3), we arrive to

$$\begin{cases} X = x + \dfrac{\cos(\theta)x + \sin(\theta)z_i(x) + C}{\Delta - \cos(\theta)z_i'(x) + \sin(\theta)} z_i'(x) \\ Z = z_i(x) - \dfrac{\cos(\theta)x + \sin(\theta)z_i(x) + C}{\Delta - \cos(\theta)z_i'(x) + \sin(\theta)}, \quad x \in [0,1]. \end{cases}$$

Let us now assume that the incident wavefront is only slightly disturbed (i.e. $z_i(x) = x + K + \delta(x)$ with $|\delta(x)| << 1$, K being some constant), and that $\theta = \pi/4$. Then taking the second order Taylor expansion of X and Z one obtains for $C = -K/\sqrt{2}$

$$\begin{cases} X = 2x + \dfrac{\delta}{2} + x\delta' - \dfrac{1}{8}x\delta'^2 + \dfrac{\delta\delta'}{2} + o(\delta'^2 + |\delta\delta'|), \\ Z = K + \dfrac{1}{2}\delta + \dfrac{1}{8}x\delta'^2 + o(\delta'^2). \end{cases}$$

It is then easy to derive the second order approximation of Z as a function of X: $Z = K + \frac{1}{2}\delta(X/2) - \frac{1}{16}\delta'(X/2)^2 - \frac{1}{8}\delta(X/2)\delta'(X/2)$. In particular, we obtain at the first order in δ

$$Z = K + \frac{1}{2}\delta(X/2).$$

Thus, at the first order the shapes of the mirror and of the wavefront must overlap (up to a translation and a dilatation). This is the rule used in most classical systems.

To illustrate the comments (2) and (3) of the previous section, let us assume that $\theta = \pi/4$ and that the incoming wavefront is spherical, e.g. $z_i(x) = \sqrt{1-x^2}$, $x \in [-1, 0]$. According to Theorem 1, the shape of the mirror which achieves a perfect correction of the wavefront is given by

$$\begin{cases} X = \dfrac{x}{1 + (x/\sqrt{2}) + (\sqrt{1-x^2}/\sqrt{2})}(1 - C) \\ Z = \dfrac{\sqrt{1-x^2}}{1 + (x/\sqrt{2}) + (\sqrt{1-x^2}/\sqrt{2})}(1 - C), \end{cases}$$

C being any real constant. It follows that the mirror is a part of the parabola $(X - Z)^2 = \frac{2}{C-1}(X + Z) - 2$, as illustrated in Figure 2. The well-known property that a parabolic mirror transforms a planar wavefront into a spherical one (and vice-versa) is recovered. Notice that the parabola reduces to the origin when $C = 1$, and that the parabolas associated with different values of C fail to be isometric.

The result in Theorem 1 may be extended to the case where the incoming wavefront is defined in a parametric way. This extension proves to be useful when the wavefront measure is performed *after* the reflection on the deformable mirror; indeed, in that case the incident wavefront is defined by parametric equations (see below). Assume the incoming wavefront to be defined as $(x, z) = (x_i(s), z_i(s))$, where x_i and z_i are given functions

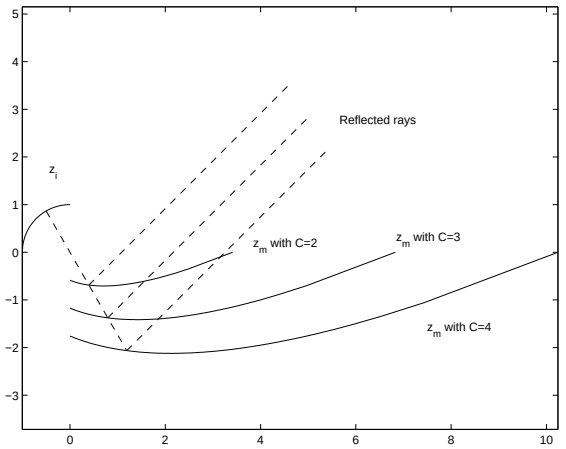

Fig. 2. Correction of a spherical wavefront

belonging to $C^1(I,\mathbb{R})$ ($I \subset \mathbb{R}$ is some interval) and set

$$\tilde{\Delta} = \left(x_i'^2 + z_i'^2\right)^{\frac{1}{2}}.$$

Then the following result holds true.

Proposition 1. Assume that the functions x_i and z_i are of class C^2. Then for any number C, the following parametric equations

$$X = x_i + \frac{\cos(\theta)x_i + \sin(\theta)z_i + C}{\tilde{\Delta} - \cos(\theta)z_i' + \sin(\theta)x_i'} \cdot z_i' \qquad (4)$$

$$Z = z_i - \frac{\cos(\theta)x_i + \sin(\theta)z_i + C}{\tilde{\Delta} - \cos(\theta)z_i' + \sin(\theta)x_i'} \cdot x_i' \qquad (5)$$

define a mirror shape leading to a perfect correction of the incoming wavefront $x = x_i(s), z = z_i(s)$.

The proof follows the same line as for Theorem 1.

2.3 The 3D Problem

Clearly, the case $n = 3$ corresponds to the most interesting one from a physical viewpoint. An application of Theorem 1 provides the following parametric representation of the mirror

$$X_1 = x_1 + \frac{\cos(\theta)x_1 + \sin(\theta)z_i(x_1,x_2) + C}{\Delta - \cos(\theta)\frac{\partial z_i}{\partial x_1} + \sin(\theta)} \frac{\partial z_i}{\partial x_1}$$

$$X_2 = x_2 + \frac{\cos(\theta)x_1 + \sin(\theta)z_i(x_1,x_2) + C}{\Delta - \cos(\theta)\frac{\partial z_i}{\partial x_1} + \sin(\theta)} \frac{\partial z_i}{\partial x_2}$$

$$Z = z_i(x_1,x_2) - \frac{\cos(\theta)x_1 + \sin(\theta)z_i(x_1,x_2) + C}{\Delta - \cos(\theta)\frac{\partial z_i}{\partial x_1} + \sin(\theta)},$$

where (x_1, x_2) ranges over $[0,1]^2$.

In order to extend above formulas to the case where the incident wavefront is defined by parametric equations we need to introduce a few notations. Let the incident wavefront be defined as $(x,z) = (x_{i1}(s,t), x_{i2}(s,t), z_i(s,t))$, where x_{i1}, x_{i2} and z_i are given functions belonging to $C^1(I^2,\mathbb{R})$ (I is again some real interval). Let $\boldsymbol{n} = (n_1, n_2, n_3)$ denote the wave vector of any incident ray. We readily find

$$\begin{cases} n_1 = \dfrac{\partial x_{i2}}{\partial t}\dfrac{\partial z_i}{\partial s} - \dfrac{\partial x_{i2}}{\partial s}\dfrac{\partial z_i}{\partial t} \\ n_2 = \dfrac{\partial x_{i1}}{\partial s}\dfrac{\partial z_i}{\partial t} - \dfrac{\partial x_{i1}}{\partial t}\dfrac{\partial z_i}{\partial s} \\ n_3 = \dfrac{\partial x_{i1}}{\partial t}\dfrac{\partial x_{i2}}{\partial s} - \dfrac{\partial x_{i1}}{\partial s}\dfrac{\partial x_{i2}}{\partial t}. \end{cases}$$

Set

$$\tilde{\Delta} = ||\boldsymbol{n}|| = (|n_1|^2 + |n_2|^2 + |n_3|^2)^{\frac{1}{2}}.$$

The extension of Proposition 1 to the 3D case is as follows.

Proposition 2. Assume that the functions x_{i1}, x_{i2} and z_i are of class C^2. Then for any number C, the following parametric equations

$$X_1 = x_{i1} + \frac{\cos(\theta)x_{i1} + \sin(\theta)z_i + C}{\tilde{\Delta} - \cos(\theta)n_1 - \sin(\theta)n_3} n_1$$

$$X_2 = x_{i2} + \frac{\cos(\theta)x_{i1} + \sin(\theta)z_i + C}{\tilde{\Delta} - \cos(\theta)n_1 - \sin(\theta)n_3} n_2$$

$$Z = z_i - \frac{\cos(\theta)x_{i1} + \sin(\theta)z_i + C}{\tilde{\Delta} - \cos(\theta)n_1 - \sin(\theta)n_3} n_3,$$

define a mirror shape leading to a perfect correction of the incoming wavefront $x_1 = x_{i1}(s,t), x_2 = x_{i2}(s,t), z = z_i(s,t)$.

3. 2D CLOSED LOOP CONFIGURATION

Here we focus on the so-called *closed loop configuration* for which the wavefront sensors are located on the optical path after the reflection.

To define the shape of the corrector mirror, we first have to derive the form of the incident wavefront from the measure of the reflected wavefront. Then we may use (1)-(2) to get the parametric equations defining the mirror.

For the sake of simplicity, we restrict ourselves to the two-dimensional case. Thanks to the reversibility of Snell-Descartes laws, the incoming wavefront may be seen as the reflected wavefront associated with the measured wavefront (which is the authentic reflected wavefront). Assume that the mirror is given by the equation $z = z_m(x)$ and that the reflected wavefront is described by the system of parametric equations $x = x_r(s), z = z_r(s)$. Let us set

$$\Delta_r := \sqrt{{x_r'}^2 + {z_r'}^2},$$
$$\Delta_m := \sqrt{1 + {z_m'}^2}.$$

If $t(s)$ is the time elapsed from the reflection (i.e., the length of the optical path between the mirror and the reflected wavefront), then the incoming wavefront is defined by

$$x_i(s) = x_r(s) + \frac{t(s)}{\Delta_r} z_r'(s) - (T - t(s))\, n_{i1} \quad (6)$$
$$z_i(s) = z_r(s) - \frac{t(s)}{\Delta_r} x_r'(s) - (T - t(s))\, n_{i2} \quad (7)$$

where $T > 0$ is a given duration and

$$\begin{aligned} \boldsymbol{n_i} &= (n_{i1}, n_{i2}) \\ &= \frac{2(x_r' + z_m' z_r')}{\Delta_m^2 \Delta_r}(z_m', -1) + \frac{1}{\Delta_r}(-z_r', x_r') \end{aligned}$$

stands for the incident wave vector. Notice that to compute $t(s)$ we need to find the intersection of a ray with the mirror. This task cannot be done in an analytical way in general.

Combining (6)-(7) to (4)-(5), we obtain a parametric representation of the mirror.

4. NUMERICAL SIMULATIONS

In order to numerically compute the reflection of the wavefront on a mirror, we need to determine the intersection points of the incoming rays with the mirror together with the normal vectors to the mirror surface at these points. Using parametric representations of both the mirror surface and the rays, the intersection points are found by solving a 1D nonlinear equation by means of a variant of the secant method.

One of the burning issues is how to obtain an "efficient" shape of the mirror from the parametric representation. It turns out that only a part of the mirror may be used in practice for the wavefront correction. Indeed, a parametrized surface is generally the graph of a function only locally. An incident ray may intersect the mirror several times, and the first intersection point may be on the wrong side of the mirror. One way to overcome this problem is to impose that Z be an increasing (or slightly decreasing) function of X, so that any incident ray meets the mirror only one time. On the other hand, the parametrized surface may go beyond the zone which may be reached by the incident rays. The parameter C arising in (1)-(2) and the range of the variable x have to be chosen in such a way that the deformed mirror remains as close as possible of the undeformed mirror.

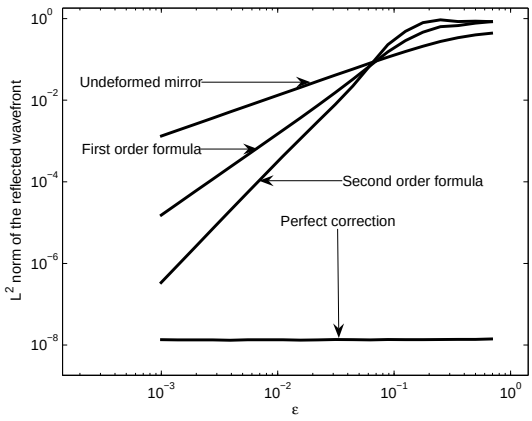

Fig. 3. Residual error versus ϵ

A sample of tests when $n = 2$ have been carried out with a planar mirror (no correction), and with mirrors defined respectively by first-order, second-order and parametric formulas.

The incident wavefront, depending on a small parameter $\varepsilon \in [0, 1]$, is defined as

$$z_i(x) = 2 + \varepsilon \sin(\pi x), \;\; x \in [0, 1]$$

The *residual error* is

$$e_r = \left(\int_0^1 |z_r(x) - z_p(x)|^2 \, dx \right)^{\frac{1}{2}}$$

where $z = z_r(x)$ (resp., $z = z_p(x)$) is the equation defining the reflected wavefront (resp., the planar wavefront).

The residual error associated to each type of correction is plotted in Figure 3. As expected, using a deformable mirror designed with a first-order or second order formula allows to correct in a convenient way the incoming wavefront in a *linear* regime ($\varepsilon < 10^{-2}$). The error is proportional to ε^2 with a mirror defined by the first-order formula. A dramatic improvement of the correction of the wavefront in a nonlinear regime ($\varepsilon \sim 10^{-1}$) is achieved with a deformable mirror designed along the parametric equations (1)-(2).

5. MEMBRANE MIRROR

In this section, we assume that the deformable mirror is a clamped *membrane mirror* (see e.g. (Welsh and Gardner, 1989)); (Tyson, 1998); (Hardy, 1998); (Fernández and Artal, 2003)). Then its dynamics is governed by the wave equation (written here in its normalized form)

$$y_{tt} - \Delta y = v \qquad \text{in } \Omega \times]0, T[$$

supplemented with the initial conditions $y(0) = y^0$, $y_t(0) = y^1$ and the boundary conditions $y = 0$ on $\Sigma := \partial\Omega \times]0, T[$. Here, Ω is an open set in $\mathbb{R}^2$ and v stands for the control input. We stress that

in AO, the control input is usually assumed to be applied *everywhere*. The following result deals with the tracking problem for the wave equation.

Theorem 2. Let $(y^0, y^1) \in H_0^1(\Omega) \times L^2(\Omega)$ and let $\bar{y} \in H^2_{loc}(\mathbb{R}^+, L^2(\Omega)) \cap L^2_{loc}(\mathbb{R}^+, H^2(\Omega) \cap H_0^1(\Omega))$ be a given trajectory. Pick any number $k > 0$ and set

$$\varepsilon(t,x) := y - \bar{y}$$
$$v(t,x) := \bar{y}_{tt} - \Delta\bar{y} - k\,\varepsilon_t.$$

Then $\varepsilon(t) \to 0$ strongly in $H_0^1(\Omega)$ as $t \to +\infty$.

Proof. Clearly, ε fulfills

$$\begin{aligned} \varepsilon_{tt} - \Delta\varepsilon = -k\varepsilon_t \qquad & \text{in } \Omega \times (0,T) \\ \varepsilon = 0 \qquad & \text{on } \Sigma. \end{aligned}$$

The proof is completed by applying a classical result (see e.g. (Lions, 1988)) on the internal stabilization of the wave equation. □

Assume now that the incident wavefront z_i is a smooth function of both t and x. Applying Theorem 1, we may associate to it a nominal mirror shape $\bar{y}$ achieving a perfect correction of the incident wavefront. Then it follows from Theorem 2 that a control input may be designed in such a way that the difference between the nominal mirror shape and the actual mirror shape tends to 0. As a consequence, we obtain that the residual error tends also to zero.

Remarks.

(1) Actually, the nominal trajectory $\bar{y}$ has to belong to $H_0^1(\Omega)$ (hence, $y = 0$ on $\partial\Omega$). That condition is fulfilled by taking the projection on $H_0^1(\Omega)$ of the mirror shape provided by Theorem 1. The error with respect to the exact mirror shape may be minimized by a convenient choice of the parameter C.

(2) In practice, a flat mirror (the so-called *tilt* correction mirror, see (Roggeman and Welsh, 1996); (Tyson, 1998)) is used to compensate for low frequency wavefront disturbances. With such a device at hand, the mirror shape to be reached is actually almost flat at the boundary.

(3) In a closed loop framework, the incident wavefront depends also on y. Then the nominal trajectory is a function of z_r and y.

6. CONCLUSION

A parametric representation of a mirror achieving a perfect correction of a given incident wavefront has been given here. When the deformable mirror is a membrane mirror, a control input allowing to compensate for a slowly time-varying wavefront disturbance has been proposed. Such control deserves to be numerically studied, in the open loop or in the closed loop configurations. The tracking problem may also be investigated when the deformable mirror is a bimorph mirror ((Tyson, 1998), (Lenczner and Prieur, 2004)). It will be the purpose of further works in a near future.

REFERENCES

Fernández, Enrique J. and Pablo Artal (2003). Membrane deformable mirror for adaptive optics: performance limits in visual optics. *Opt. Express* **11**(9), 1056–1069.

Hardy, John W. (1998). *Adaptive Optics for Astronomical Telescopes*. Oxford Series in Optical and Imaging Science. Oxford University Press. New York.

Le Roux, Brice (2003). Commande optimale en optique adaptative classique et multiconjuguée. *Ph.D. Thesis*.

Lenczner, Michel and Christophe Prieur (2004). Modélisation d'une plaque fine. *preprint*.

Lions, Jacques-Louis (1988). *Contrôlabilité exacte et stabilisation de systèmes distribués, Vol. 1.* Masson. Paris.

Luke, D. Russell, James V. Burke and Richard G. Lyon (2002). Optical wavefront reconstruction: theory and numerical methods. *SIAM Rev.* **44**(2), 169–224 (electronic).

Plemmons, Robert J. and Victor P. Pauca (2000). Some computational problems arising in adaptive optics imaging systems. *J. Comput. Appl. Math.* **123**(1-2), 467–487. Numerical analysis 2000, Vol. III. Linear algebra.

Roddier, François (1999). *Adaptive Optics in Astronomy*. Cambridge University Press.

Roggeman, Michael C. and Byron Welsh (1996). *Imaging Through Turbulence*. CRC Press.

Tyson, Robert K. (1998). *Principles of Adaptive Optics*. Academic Press. San Diego. 2nd ed.

Welsh, Byron M. and Chester S. Gardner (1989). Performance analysis of adaptive-optics systems using laser guide stars and slope sensors. *J. Opt. Soc. Am. A* **6**(12), 1913–1923.

Zakynthinaki, M. S. and Y. G. Saridakis (2003). Stochastic optimization for adaptive real-time wavefront correction. *Numer. Algorithms* **33**(1-4), 509–520. International Conference on Numerical Algorithms, Vol. I (Marrakesh, 2001).

2.2 Miroir en dimension n

Ce chapitre est consacré à la correction d'un front d'onde dans un espace de dimension n, avec n un entier naturel non nul. Après avoir rappelé les notations utilisées dans le chapitre précédent, la formule permettant une correction parfaite du miroir est présentée. Enfin, quelques liens sont établis entre les résultats et les pratiques actuelles en optique adaptative.

Soit $\mathbb{R}^n$ l'espace euclidien de dimension n, et désignons par $(x, z) = (x_1, \ldots, x_{n-1}, z)$ un point générique. Soit $\{\mathbf{e}_i\}_{1\leq i\leq n}$ la base canonique de $\mathbb{R}^n$. Le front d'onde incident à l'instant $t = 0$ et le miroir déformable sont respectivement définis par les équations :

$$z = z_i(x) = z_i(x_1, \ldots, x_{n-1}) \tag{2.1}$$

$$z = z_m(x), \tag{2.2}$$

où z_i et z_m sont des fonctions appartenant à $\mathcal{C}^1([0, 1]^{n-1}, \mathbb{R})$. Le miroir non déformé est supposé contenu dans l'hyperplan $z = 0$.

Le milieu est supposé homogène et isotrope, la lumière se déplace avec une vitesse constante, que l'on prendra égale à 1. Si le gradient du front d'onde est $\tilde{n}_i = (\nabla z_i, -1)$, on note $n_i = \tilde{n}_i/\|\tilde{n}_i\|$, qui correspond à la direction des rayons lumineux. Les fronts d'onde correspondant à des surfaces équipotentielles, on déduit le front d'onde à l'instant t à partir de celui à l'instant 0 par la formule suivante, tant qu'aucune réflexion n'a eu lieu :

$$\begin{pmatrix} X(x,t) \\ Z(x,t) \end{pmatrix} = \begin{pmatrix} x \\ z_i(x) \end{pmatrix} + tn_i \tag{2.3}$$

Une application directe de la première formule de variation nous permet de dire que les droites normales au front d'onde en $(x, z_i(x))$ le sont également en $(X(x,t), Z(x,t))$.

Lorqu'un rayon lumineux rencontre la surface du miroir, il y a *réflexion*. Le point de rencontre du rayon incident et de la surface réfléchissante est appelé *point d'incidence*. Le plan contenant le rayon incident et la normale au miroir au point d'incidence est dit *plan d'incidence*. La loi de la réflexion, ou première loi de Snell-Descartes s'énonce ainsi :

– le rayon réfléchi est dans le plan d'incidence.
– les angles incident et réfléchi sont égaux.

En notant n_m et le vecteur normal normé au point d'incidence, et n_r le vecteur d'onde réfléchi, on a :

$$n_r = n_i - 2(n_i \cdot n_m)n_m \tag{2.4}$$

Notre objectif est de corriger le front d'onde incident, en donnant une forme adaptée au miroir. Un front d'onde réfléchi corrigé correspond ici à un front d'onde plan après réflexion. Le théorème suivant donne une représentation paramétrique du miroir assurant la correction parfaite du front d'onde incident.

Théorème 2.1. *Supposons que la fonction z_i est de classe C^2. Alors pour tout réel C et tout vecteur normé e, les équations paramétriques suivantes :*

$$x(t) = x + t\frac{\|\nabla z_m\|}{\sqrt{1 + \|z_m\|^2}} \tag{2.5}$$

$$z(t) = z - t\frac{\|\nabla z_m\|}{\sqrt{1 + \|z_m\|^2}} \tag{2.6}$$

avec $(x_1, \ldots, x_n) \in [-1, 1]^{n-1}$ *définissent la forme d'un miroir permettant une correction parfaite du front d'onde* $z = z_i(x)$.

Démonstration. Pour les besoins de la preuve, notons $\tilde{t}$ le temps nécessaire au rayon lumineux pour atteindre le miroir.

La démonstration se fait en deux étapes : dans la première, on considère que le rayon réfléchi part dans la direction souhaitée e sans prendre en compte les lois de la réflexion. Cela nous fournit des équations paramétrées décrivant le miroir. Dans un second temps, il faut vérifier que les lois de Snell-Descartes sont bien vérifiées.

Supposons qu'après réflexion, le front d'onde soit parfaitement corrigé, et donc que $n_r = e$ pour tous les rayons réfléchis. Après réflexion, le rayon lumineux atteint pour tout temps $t > \tilde{t}$ le point :

$$\begin{pmatrix} X \\ Z \end{pmatrix} = \begin{pmatrix} x \\ z_i \end{pmatrix} + \tilde{t} n_i + (t - \tilde{t}) e. \tag{2.7}$$

Le front d'onde réfléchi est plan ssi il existe un réel k tel que pour tout x :

$$\begin{pmatrix} X \\ Z \end{pmatrix} \cdot e = k \tag{2.8}$$

On parvient alors à déterminer le temps mis par le rayon lumineux pour atteindre le miroir :

$$\tilde{t} = \frac{k - t - \begin{pmatrix} x \\ z_i \end{pmatrix} \cdot e}{n - i \cdot e - 1} \tag{2.9}$$

et la forme que doit avoir le miroir :

$$\begin{pmatrix} X_m(x) \\ Z_m(x) \end{pmatrix} = \begin{pmatrix} x \\ z_i(x) \end{pmatrix} + \frac{k - t - \begin{pmatrix} x \\ z_i \end{pmatrix} \cdot e}{n_i \cdot e - 1} n_i. \tag{2.10}$$

Notons $C = k - t$

Maintenant qu'une condition nécessaire a été trouvée sur la forme du miroir, il est temps de vérifier qu'elle est suffisante, c'est-à-dire que la loi de la réflexion est vérifiée : il suffit pour cela de vérifier que

$$(e - n_i) \cdot = \begin{pmatrix} X'_m(x) \\ Z'_m(x) \end{pmatrix} = 0 \tag{2.11}$$

Comme

$$\begin{pmatrix} X'_m(x) \\ Z'_m(x) \end{pmatrix} = \begin{pmatrix} 1 \\ z'_i(x) \end{pmatrix} + \frac{\left(-\begin{pmatrix} 1 \\ z'_i \end{pmatrix} \cdot e\right)(n_i \cdot e - 1) - \left(C - \begin{pmatrix} x \\ z_i \end{pmatrix} \cdot e\right)(n'_i \cdot e)}{(n_i \cdot e)^2} \frac{k - t - \begin{pmatrix} x \\ z_i \end{pmatrix} \cdot e}{n_i \cdot e - 1} n'_i,$$

qui donne 0 après simplifications. □

2.3 Approximations

Depuis l'apparition de l'optique adaptative, différentes méthodes ont été mises en place pour choisir la forme à donner au miroir : certaines approches ne demandent même pas la reconstruction du front d'onde, le système étant considéré comme une boîte noire, et la sortie correspondant aux mesures du capteur de Shack-Hartmann. La forme du miroir est supposée convenable lorsque les tâches se superposent au schéma. D'autres approches comprennent la reconstruction du front d'onde, et en déduisent alors *simplement* les équations à donner au miroir. En fait, elles correspondent à un développement au premier ordre des équations paramétrées présentées ci-dessus.

Supposons maintenant que le front d'onde incident est peu perturbé (i.e. $z_i(x) = K + \delta(x)$, où $|\delta(x)| << 1$ et K est une constante donnée,) et que $n_r = (0, \dots, 0, 1)$.

Proposition 2.1. *Soit δ une fonction de classe $\mathcal{C}^2$, avec $z_i(x) = K + \delta(x)$, où $|\delta(x)| << 1$ et K est une constante donnée. Alors pour $C = K$, l'équation suivante correspond à un développement au premier ordre des équations du miroir :*

$$Z = K + \frac{1}{2}\delta(X) \tag{2.12}$$

Démonstration. Avec le choix des fonctions et constantes précédentes, on trouve que :

$$\begin{pmatrix} X_m(x) \\ Z_m(x) \end{pmatrix} = \begin{pmatrix} x \\ K + \delta \end{pmatrix} + \frac{-\delta}{-\frac{1}{\sqrt{1+\|\nabla\delta\|^2-1}}} \begin{pmatrix} \nabla\delta \\ -1 \end{pmatrix} \tag{2.13}$$

□

Pour d'autres choix de e, on peut en fait montrer que, au premier ordre, la forme du miroir et celle du front d'onde se superposent (à une translation et une dilatation près). De manière générale, les remarques présentées dans l'article précédent restent vraies :

Remarque 2.1. La forme du miroir déformé permettant une correction parfaite du miroir d'un front d'onde quelconque est donné par des équations paramétriques. Dans le cas où l'application $x \mapsto X_m$ est inversible, l'équation du miroir peut être présentée sous la forme :

$$Z = z_m(X_m) \tag{2.14}$$

Remarque 2.2. Une perte de régularité est obervée : si z_i est de classe $\mathcal{C}^r$, les fonctions X_m et Z_m sont de classe $\mathcal{C}^{r-1}$, à cause de la présence de ∇z_i.

Remarque 2.3. Le miroir qui permet de corriger le front d'onde n'est en fait pas unique : il existe une famille à un paramètre, C, qui permet d'obtenir le résultat souhaité. Choisir C revient à choisir le temps mis par le front d'onde pour atteindre le miroir. Il est essentiel de remarquer que les différents miroirs ne se déduisent l'un des autres par une simple translation. Des cas dégénérés de miroirs réduits à un point peuvent apparaître.

Deuxième partie

Contrôle des Miroirs Bimorphes

Introduction

ON THE CONTROL OF A BIMORPH MIRROR

Pierre Le Gall * **Christophe Prieur** ** **Lionel Rosier** *

* *Institut Elie Cartan, Université Henri Poincaré Nancy 1, B.P. 239, 54506 Vandœuvre-lès-Nancy Cedex, France*
** *LAAS-CNRS, 7 avenue du colonel Roche, 31077 Toulouse, France*

Abstract: We consider a large bimorph mirror which is composed of three layers: a purely elastic layer, a layer equipped with a distribution of sensor piezoelectric inclusions, and a layer equipped with a distribution of actuator piezoelectric inclusions. Such a device is modelized by a system of two coupled PDE, the first one involving a second-order operator without time derivative, and the second one being a plate equation. The controllability properties are investigated for both the 1D model and the 2D model, and an output feedback law is proposed for the stabilization of the 1D model.

Keywords: Bimorph mirror, beam equation, plate equation, controllability, output feedback stabilization.

1. INTRODUCTION

The general problem under study in this paper is the control and the stabilization of a bimorph mirror. Such a structure is an active multi-layered flexible plate (see Figure 1):

- a layer is assumed to be a purely flexible plate (this is the mirror);
- another layer is equipped with a distribution of piezoelectric inclusions, which are used as *actuators*;
- the last layer is also equipped with a distribution of piezoelectric inclusions, which are used as *sensors.*

Such a device is used in Adaptive Optics with large ground-based telescopes. Recall that the main goal of Adaptive Optics is to compensate in real time for random wavefront disturbances.

This kind of flexible structure has been investigated in (Lenczner and Prieur, 2006). A PDE-type model has been obtained by making the characteristic dimension of the heterogeneities tend to zero in elastic plates including small inclusions. Two-scale convergence for homogenization as in (Allaire, 1992) was used. The goal of the present paper is to investigate the controllability and the stabilization properties of that model.

There exists a wide literature for the controllability and the stabilization of flexible plates equipped with piezoelectric inclusions. See e.g. (Tucsnak, 1996; Crépeau and Prieur, to appear) where controllability results for the Bernoulli Euler equation are obtained by using the Hilbert Uniqueness Method and Diophantine approximations. Stabilization results for the beam equation are given in (Ammari and Tucsnak, 2000;

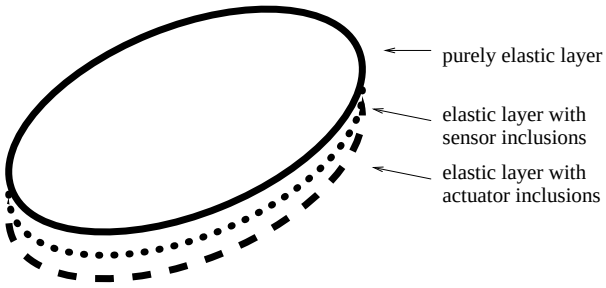

Fig. 1. An active bimorph mirror

Ammari *et al.*, 2001), (Liu and Zheng, 1999) and (Le Gall *et al.*, 2006).

An important feature of the model considered here is that there are two coupled PDE of very different nature: the first one is defined by a second-order operator without any time derivative, and the second one is a Euler-Bernoulli equation.

The model under consideration will be investigated in 1D and in 2D.

1D MODEL (BEAM)

$$\begin{cases} -\partial_x^2 u = -s\partial_x\varphi + a\partial_x^2\varphi, \\ \partial_t^2 w + \partial_x^4 w + w = \partial_x^2\varphi, \\ w(0,t) = w(L,t) = \partial_x w(0,t) = \partial_x w(L,t) = 0, \\ u(0,t) = u(L,t) = 0. \end{cases}$$

In above system, $x \in (0,L)$ is the spatial coordinate and t is time, w stands for the transverse deflection of the beam, u is the scalar longitudinal displacement, and φ is the voltage applied to the inclusions of the actuator layer. We shall assume that $a > 0$ and that s is any real number.

2D MODEL (PLATE)

$$-(\lambda+\mu)\partial_1 \mathrm{div}\, U - \mu\Delta u_1 = -s_\beta\partial_\beta\varphi + a_{\gamma\delta}\partial^2_{\gamma\delta}\varphi, \quad (1)$$

$$-(\lambda+\mu)\partial_2 \mathrm{div}\, U - \mu\Delta u_2 = -t_\beta\partial_\beta\varphi + b_{\gamma\delta}\partial^2_{\gamma\delta}\varphi, \quad (2)$$

$$\partial_t^2 w + \Delta^2 w + w = g_{\alpha\beta}\partial^2_{\alpha\beta}\varphi, \quad (3)$$

$$w = \frac{\partial w}{\partial n} = 0 \quad \text{on } \partial\Omega, \quad (4)$$

$$u_1 = u_2 = 0 \quad \text{on } \Omega. \quad (5)$$

In above system, $x = (x_1, x_2) \in \Omega$, where $\Omega \subset \mathbb{R}^2$ is a Lipschitzian bounded open set, $\partial_1\varphi = \partial\varphi/\partial x_1$, $\partial_2\varphi = \partial\varphi/\partial x_2$, $U = (u_1, u_2)$ stands for the 2D-longitudinal displacement, $\mathrm{div}\, U = \partial_1 u_1 + \partial_2 u_2$, and Einstein's convention of summation for repeated indices has been adopted. As usual, $\lambda > 0$ and $\mu > 0$ stand for the Lame coefficients. We shall assume that the 2×2 matrices $A = (a_{\gamma\delta})$, $B = (b_{\gamma\delta})$, and $G = (g_{\alpha\beta})$ are positive definite.

The paper is organized as follows. In Section 2, we prove the controllability of our model by treating separately the 1D model and the 2D model. In Section 3 we investigate the stabilization of the 1D model by identifying a compatibility condition.

2. CONTROLLABILITY PROPERTIES

2.1 Toy problem

We first investigate the possibility of achieving the exact controllability in finite time. The main feature of the control problem under study is the fact that we have to control the solution u (resp $U = (u_1, u_2)$) of an elliptic equation, in addition of the solution w of the beam (resp. plate) equation. In a certain sense, u or U may be viewed as an "output" depending only on the input φ. The consideration of the following "toy problem" is quite illuminating. Consider three matrices $A \in \mathbb{R}^{n\times n}$, $B \in \mathbb{R}^{n\times m}$ and $C \in \mathbb{R}^{k\times m}$ and the following controlled linear system in finite dimension:

$$\begin{cases} \dot{x} = Ax + Bu, \\ y = Cu. \end{cases} \quad (6)$$

We shall say that (x,y) is *controllable in time T* if for all pairs (x^0, y^0), (x^T, y^T) in $\mathbb{R}^n \times \mathbb{R}^k$ one may find a control input $u \in C([0,T];\mathbb{R}^m)$ and a solution $(x(t), y(t))$ of (6) connecting (x^0, y^0) to (x^T, y^T). Then the following result holds.

Proposition 1. (x,y) is controllable in time T for any $T > 0$ if and only if the pair of matrices (A,B) is controllable and the matrix C is onto.

Proof. The sense $\Rightarrow$ is obvious. Conversely, assume that the pair (A,B) is controllable and that the matrix C is onto (i.e., the map $u \in \mathbb{R}^m \mapsto Cu \in \mathbb{R}^k$ is onto). Let two pairs (x^0, y^0) and (x^T, y^T) be given in $\mathbb{R}^n \times \mathbb{R}^k$. In a first step we construct a trajectory $(\bar{x}, \bar{y})$ associated with a control $\bar{u}$ such that $\bar{y}(0) = y^0$ and $\bar{y}(T) = y^T$. To do this we pick some vectors u^0 and u^T such that $y^0 = Cu^0$ and $y^T = Cu^T$, and we set $\bar{u}(t) := (1 - t/T)u^0 + (t/T)u^T$. Let $\bar{x}$ denote the solution of $\dot{\bar{x}} = A\bar{x} + B\bar{u}$, $\bar{x}(0) = 0$, and let $\bar{y}(t) = C\bar{u}(t)$. Performing the change of variables $\hat{x} = x - \bar{x}$, $\hat{u} = u - \bar{u}$, and $\hat{y} = y - \bar{y}$, we notice that the pair $(\hat{x}, \hat{y})$ has to satisfy the system

$$\begin{cases} \dot{\hat{x}} = A\hat{x} + B\hat{u}, \\ \hat{y} = C\hat{u}, \end{cases}$$

the constraints being now $C\hat{u}(0) = C\hat{u}(T) = 0$, $\hat{x}(0) = x_0 - \bar{x}(0)$, and $\hat{x}(T) = x_T - \bar{x}(T)$. The pair (A,B) being controllable, it is well known that we may find a control input $u \in C_0^\infty(0,T)$ steering $\hat{x}$ from $x_0 - \bar{x}(0)$ to $x_T - \bar{x}(T)$. ∎

Roughly speaking, to design the control we first construct a "static" control allowing to connect y^0 to y^T, and next we add to it a dynamical correction allowing to connect x^0 to x^T. The point is that this correction may be chosen with the additional constraint that it vanishes at both extremities of $[0,T]$. We shall see in the next section that this method works as well for the control of the bimorph mirror.

2.2 Controllability of the 1D system.

Let us introduce the spaces $V = H^2(0,L) \cap H_0^1(0,L)$, $\tilde{V} = H_0^2(0,L)$, $H = L^2(0,L)$ and the operator $\mathcal{A}(w,v) = (v, -w^{(4)} - w)$ with domain $\mathcal{D}(\mathcal{A}) = (H^4(0,L) \cap H_0^2(0,L)) \times H_0^2(0,L) \subset \tilde{V} \times H$. Then we have the following result.

Theorem 1. Each pair $((w^0,w^1),u^0)$, $((w^{0,T},w^{1,T}),u^T)$ of triplets of functions in $\mathcal{D}(\mathcal{A}) \times V$ may be connected by a trajectory associated with a control function $\varphi \in C([0,T];H^2(0,L))$.

Proof: As the system is time-reversible, we may assume without loss of generality that $w^{0,T} = w^{1,T} = u^T = 0$. Pick any triplet $((w^0,w^1),u^0)$ in $\mathcal{D}(\mathcal{A}) \times V$. As $a \neq 0$, there exists a unique solution $\varphi^0 \in V$ to the elliptic problem

$$\begin{cases} a\partial_x^2\varphi^0 - s\partial_x\varphi^0 = -\partial_x^2 u^0, \\ \varphi^0(0) = \varphi^0(L) = 0. \end{cases}$$

Let us set $\overline{\varphi}(t) = (1-t/T)\varphi^0$ and let $(\overline{w},\overline{u})$ be the corresponding solution of the system

$$\begin{cases} -\partial_x^2\overline{u} = -s\partial_x\overline{\varphi} + a\partial_x^2\overline{\varphi}, \\ \partial_t^2\overline{w} + \partial_x^4\overline{w} + \overline{w} = \partial_x^2\overline{\varphi}, \\ \overline{w}(0,t) = \overline{w}(L,t) = \partial_x\overline{w}(0,t) = \partial_x\overline{w}(L,t) = 0, \\ \overline{u}(0,t) = \overline{u}(L,t) = 0, \\ \overline{w}(x,0) = \partial_t\overline{w}(x,0) = 0. \end{cases}$$

Notice that $\overline{u}(x,0) = u^0(x)$ and $\overline{u}(x,T) = 0$, for $\overline{\varphi}(0) = \varphi^0$ and $\overline{\varphi}(T) = 0$. As $\partial_x^2\overline{\varphi} \in C^1([0,T];H)$, we infer from a classical result in semigroup theory (see e.g. (Cazenave and Haraux, 1998)) that $(\overline{w},\partial_t\overline{w}) \in C([0,T];\mathcal{D}(\mathcal{A})) \cap C^1([0,T],\tilde{V} \times H)$. Next, we perform a change of unknown functions. We set $\hat{w} = w - \overline{w}$, $\hat{u} = u - \overline{u}$, and $\hat{\varphi} = \varphi - \overline{\varphi}$. Then the pair $(\hat{w},\hat{u})$ solves

$$\begin{cases} -\partial_x^2\hat{u} = -s\partial_x\hat{\varphi} + a\partial_x^2\hat{\varphi}, \\ \partial_t^2\hat{w} + \partial_x^4\hat{w} + \hat{w} = \partial_x^2\hat{\varphi}, \\ \hat{w}(0,t) = \hat{w}(L,t) = \partial_x\hat{w}(0,t) = \partial_x\hat{w}(L,t) = 0, \\ \hat{u}(0,t) = \hat{u}(L,t) = 0, \\ \hat{w}(x,0) = w^0(x),\ \partial_t\hat{w}(x,0) = w^1(x). \end{cases}$$

and $\hat{\varphi}$ has to be designed in such a way that $\hat{u}(.,0) = 0$ and $(\hat{w}(.,T),\partial_t\hat{w}(.,T),\hat{u}(.,T)) = (-\overline{w}(.,T),-\partial_t\overline{w}(.,T),0)$. In particular, the condition $\hat{\varphi}(.,0) = \hat{\varphi}(.,T) = 0$ is required. A classical result (Lions, 1988) on the controllability of the plate equation gives the existence of some control input $\hat{\varphi}$, which is compactly supported in time, and such that the corresponding trajectory fulfills all the above conditions. Alternatively, using the fact that the control is applied on the *whole* domain, we may design an *explicit* control input by specifying some trajectory $(\hat{w},\hat{w}_t)$ in the class $C([0,H];\mathcal{D}(\mathcal{A})) \cap C^1([0,T];\tilde{V} \times H)$ and fulfilling the above conditions. Next, $\hat{\varphi}(t)$ may be defined for each $t \in [0,T]$ as the solution of the elliptic problem

$$\begin{cases} \partial_x^2\hat{\varphi} = \partial_t^2\hat{w} + \partial_x^4\hat{w} + \hat{w}, \\ \hat{\varphi}(0,t) = \hat{\varphi}(L,t) = 0. \end{cases}$$

To complete the proof of Theorem 1, we need the following result:

Proposition 2. Let v^0, v^1, v^2 be three functions in $H^4(0,L) \cap H_0^2(0,L)$, $H_0^2(0,L)$ and $L^2(0,L)$, respectively. There there exists a function $v \in C([0,T];H^4(0,L)) \cap C^1([0,T];H_0^2(0,L)) \cap C^2([0,T];L^2(0,L))$ fulfilling $v(0) = v^0$, $v'(0) = v^1$, $v''(0) = v^2$ and $v(T) = v'(T) = v''(T) = 0$.

Proof of Proposition 2. Let $(\psi_k)_{k\geq 1}$ denote an orthonormal basis of $L^2(0,L)$ constituted of eigenfunctions for the operator $Aw = w^{(4)}$ with the boundary conditions $w(0) = w(L) = w'(0) = w'(L) = 0$. The eigenvalue associated with the function ψ_k is denoted by λ_k. Pick any function $h \in C^4(\mathbb{R}^+)$ such that $h(0) = h^{(3)}(0) = 1$, $h'(0) = h''(0) = h^{(4)}(0) = 0$, and any function $g \in C^4(\mathbb{R}^+)$ such that $g(t) = 1$ for $t \leq T/4$ and $g(t) = 0$ for $t \geq T/2$. If the functions v^0, v^1 and v^2 are decomposed along the ψ_k's as

$$v^0 = \sum_{k\geq 1} a_k\psi_k,\ v^1 = \sum_{k\geq 1} b_k\psi_k,\ v^2 = \sum_{k\geq 1} c_k\psi_k$$

then $\sum_{k\geq 1}\left(k^8|a_k|^2 + k^4|b_k|^2 + |c_k|^2\right) < \infty$. The function v is then defined as

$$v(x,t) := g(t)\sum_{k\geq 1}\left(a_k h(\sqrt{\lambda_k}t) + \frac{b_k}{\sqrt{\lambda_k}}h''(\sqrt{\lambda_k}t) + \frac{c_k}{\lambda_k}h'(\sqrt{\lambda_k}t)\right)\psi_k(x).$$

As $\lambda_k \sim Ck^4$ as $k \to \infty$, one readily obtains that $v \in C([0,T];H^4(0,L)) \cap C^1([0,T];H_0^2(0,L)) \cap C^2([0,T];L^2(0,L))$. The properties $v(0) = v^0$, $v'(0) = v^1$, $v''(0) = v^2$ and $v(T) = v'(T) = v''(T) = 0$ are obvious. ■

The proof of Theorem 1 is completed by applying Proposition 2 to $v^0 = w^0$, $v^1 = w^1$, and $v^2 = -\partial_x^4 w^0 - w^0$ on the interval $[0,T/2]$, and next to $v^0 = -\overline{w}(T)$, $v^1 = \overline{w}_t(T)$ and $v^2 = -\partial_x^4\overline{w}(T) - \overline{w}(T)$ on the interval $[T/2,T]$ by reversing the time. ■

Remark 1. To simplify the exposition, we have imposed Dirichlet boundary conditions ($\varphi(0,t) = \varphi(L,t) = 0$) to the control input φ, but Neumann boundary conditions (i.e. $\partial_x\varphi(0,t) = \partial_x\varphi(L,t) = 0$ together with e.g. $\int_0^L \varphi(x,t)\,dx = 0$) may be taken instead.

2.3 Controllability of the 2D system.

Notice first that for any trajectory $(w(t),U(t))$ of (1)-(5) associated with the control input $\varphi(t)$, $t \in [0,T]$,

the control φ has to be at each instant t a solution of the following system of elliptic PDE

$$-s_\beta \partial_\beta \varphi + a_{\gamma\delta}\partial^2_{\gamma\delta}\varphi = f_1, \quad (7)$$

$$-t_\beta \partial_\beta \varphi + b_{\gamma\delta}\partial^2_{\gamma\delta}\varphi = f_2, \quad (8)$$

where $f_i := -(\lambda+\mu)\partial_i \mathrm{div}\, U - \mu\Delta u_i$ for $i = 1,2$. Obviously, for φ to exist the functions f_1 and f_2 have to satisfy a *compatibility condition*, namely

$$(-t_\beta\partial_\beta + b_{\gamma\delta}\partial^2_{\gamma\delta})\, f_1 = (-s_\beta\partial_\beta + a_{\gamma\delta}\partial^2_{\gamma\delta})\, f_2. \quad (9)$$

If, moreover, $-t_\beta\partial_\beta + b_{\gamma\delta}\partial^2_{\gamma\delta} = \lambda(-s_\beta\partial_\beta + a_{\gamma\delta}\partial^2_{\gamma\delta})$, then $f_2 = \lambda f_1$.

It is not clear, however, that these conditions are sufficient to guarantee the existence of a solution of (7)-(8). We shall adopt the following

Definition 1. A quadruplet $(w^0, w^1, u_1, u_2) \in (H^4(\Omega)\cap H^2_0(\Omega)) \times H^2_0(\Omega) \times (H^2(\Omega)\cap H^1_0(\Omega))^2$ will be said to be *compatible* if the system (7)-(8) possesses a solution $\varphi \in H^2(\Omega)$, the functions f_1, f_2 being defined as $f_i := -(\lambda+\mu)\partial_i \mathrm{div}\,(u_1,u_2) - \mu\Delta u_i$ for $i = 1,2$.

Then the following result holds true.

Theorem 2. Each pair (w^0, w^1, u_1, u_2), $(w^{0,T}, w^{1,T}, u_1^T, u_2^T)$ of compatible quadruplets may be connected by a trajectory associated with a control function $\varphi \in C([0,T]; H^2(\Omega))$.

Proof. The proof follows the same pattern as for Theorem 1. Once again, we may assume that the terminal quadruplet is $(0,0,0,0)$.

Step 1: Control of the static equations.

As the quadruplet (w^0, w^1, u_1, u_2) is assumed to be compatible, there exists a function $\varphi^0 \in H^2(\Omega)$ solving (7)-(8). We set $\overline{\varphi}(t) := (1-t/T)\varphi^0$. Next, $\overline{w}$ is defined as the solution of the plate equation (3) (with $\overline{\varphi}$ substituted to φ) with the boundary conditions (4) and issuing from $(0,0)$, and $\overline{U} = (\overline{u_1}, \overline{u_2})$ is the solution of the elliptic problem (1), (2) and (5).

Step 2: Control of the plate equation.

We perform the change of unknown functions $\hat{w} = w - \overline{w}$, $\hat{u}_i = u_i - \overline{u_i}$ $(i = 1,2)$, and $\hat{\varphi} = \varphi - \overline{\varphi}$. Then $\hat{u}_1, \hat{u}_2, \hat{w}$ and $\hat{\varphi}$ have to fulfill (1)-(5). The constraints at time 0 and T are respectively $(\hat{w}(0), \hat{w}_t(0), \hat{u}_1(0), \hat{u}_2(0)) = (w^0, w^1, 0, 0)$ and $(\hat{w}(T), \hat{w}_t(T), \hat{u}_1(T), \hat{u}_2(T)) = (-\overline{w}(T), -\overline{w}_t(T), 0, 0)$. To conclude, we apply the following result whose proof is virtually the same as for Proposition 2.

Proposition 3. Let v^0, v^1, v^2 be three functions in $H^4(\Omega)\cap H^2_0(\Omega)$, $H^2_0(\Omega)$, and $L^2(\Omega)$, respectively. Then there exists a function $v \in C([0,T]; H^4(\Omega)) \cap C^1([0,T]; H^2_0(\Omega)) \cap C^2([0,T]; L^2(\Omega))$ fulfilling $v(0) = v^0$, $v'(0) = v^1$, $v''(0) = v^2$ and $v(T) = v'(T) = v''(T) = 0$.

The proof of Theorem 2 is complete. ■

3. OUTPUT STABILIZATION OF AN ADAPTIVE MIRROR

We consider the system

$$-\partial_x^2 u = -s\partial_x\varphi + a\partial_x^2\varphi \quad (10)$$

$$\partial_t^2 w + \partial_x^4 w + w = \partial_x^2\varphi \quad (11)$$

$$I = \partial_t(\partial_x^2 w + c\partial_x u) \quad (12)$$

I is the distributed current field measured through the layer equipped with sensor piezoelectric patches.

We are interested in the output stabilization of above system, the control φ being expressed as a function of the output I. In Adaptive Optics, this corresponds to the problem of the stabilization at the rest position of a large mirror equipped with piezoelectric sensors and actuators. This problem should be seen as a first step towards the tracking problem, for which a control input is designed so that the state of the mirror converges to a given trajectory.

We consider the following initial conditions:

$$w(x,0) = w^0(x),\ \partial_t w(x,0) = w^1(x). \quad (13)$$

We will prescribe the boundary conditions later.

To stabilize (10)-(12), it is natural to try to impose the following additional feedback condition

$$\partial_x^2\varphi = k\partial_t w + k'\partial_t\partial_x^2 w, \quad (14)$$

k and k' being two real numbers whose range will be specified later.

The feedback condition (14) is consistent with the output feedback condition (namely $\varphi = \Lambda(I)$ for some operator Λ) provided that some "compatibility condition" is fulfilled by any solution of (10)-(12) and (14).

3.1 The compatibility condition

To state this compatibility condition in a simple way, we consider first periodic boundary conditions on u, w and φ and we assume that $L = \pi$. Then we may rewrite (10)-(12) and (14) in using Fourier series. Indeed, we have

$$u(x,t)=\sum_{n\in\mathbb{Z}}\alpha_n(t)e^{inx},$$
$$w(x,t)=\sum_{n\in\mathbb{Z}}\beta_n(t)e^{inx},$$
$$I(x,t)=\sum_{n\in\mathbb{Z}}\gamma_n(t)e^{inx},$$

where (α_n), (β_n) and (γ_n) are three sequences of functions of time which are of class C^2. To express that φ depends only on I, we introduce also a sequence (λ_n) of complex numbers such that

$$\varphi(x,t)=\sum_{n\in\mathbb{Z}}\lambda_n\gamma_n(t)e^{inx}.$$

Let us rewrite (10)-(12) and (14) in terms of these sequences. Easily computations yields

$$\alpha_n=-\frac{is\lambda_n\gamma_n}{n}-a\lambda_n\gamma_n \tag{15}$$
$$\ddot{\beta}_n+\beta_n(n^4+1)=(k-n^2k')\dot{\beta}_n \tag{16}$$
$$\gamma_n=-n^2\dot{\beta}_n+inc\dot{\alpha}_n \tag{17}$$
$$-n^2\lambda_n\gamma_n=(k-n^2k')\dot{\beta}_n \tag{18}$$

The expression of $\beta_n(t)$ may be deduced from (16). Equations (15) and (18) allow us to compute α_n. The condition (17) can be restated as follows (with (15)):

$$c\dot{\gamma}_n\lambda_n(s-ian)-n^2\dot{\beta}_n-\gamma_n=0. \tag{19}$$

Note that (18) implies that

$$\frac{\dot{\beta}_n}{\gamma_n}(t)\equiv\frac{\dot{\beta}_n}{\gamma_n}(t=0). \tag{20}$$

This is a compatibility condition which has to be fulfilled for (14) to hold.

However, we note that when $c=0$, (19) implies

$$\gamma_n=-n^2\dot{\beta}_n.$$

In this case, the compatibility condition (20) is always satisfied. Thus we will assume thereafter that $c=0$, so that the compatibility condition holds.

3.2 Stability when $c=0$

Assuming $c=0$, (19) implies

$$\gamma_n=-n^2\dot{\beta}_n$$

and (18) yields

$$\lambda_n=\frac{k-n^2k'}{n^4},$$

which corresponds to the following output feedback law

$$\begin{aligned}\partial_x^2\varphi&=k\partial_t w+k'\partial_t\partial_x^2 w\\&=k\Lambda(I)+k'I,\end{aligned}$$

where $\Lambda=(\partial_x^2)^{-1}$ with periodic boundary conditions.

Let us go back to the framework of the clamped beam, and let Λ denote now the operator $(\partial_x^2)^{-1}$ with Dirichlet boundary conditions. The control input φ, which has to fulfill (14), is defined by

$$\varphi=\Lambda(k\Lambda(I)+k'I)=\Lambda(k\partial_t w+k'\partial_t\partial_x^2 w).$$

Then the model under study becomes

$$-\partial_x^2 u=-s\partial_x\varphi+a\partial_x^2\varphi \tag{21}$$
$$\partial_t^2 w+\partial_x^4 w+w=k\partial_t w+k'\partial_t\partial_x^2 w, \tag{22}$$
$$I=\partial_t\partial_x^2 w \tag{23}$$
$$\varphi=\Lambda(k\Lambda(I)+k'I), \tag{24}$$

with the initial conditions

$$w(x,0)=w^0(x),\ \partial_t w(x,0)=w^1(x), \tag{25}$$

and the boundary conditions

$$w(0,t)=\partial_x w(0,t)=w(L,t)=\partial_x w(L,t)=0, \tag{26}$$
$$u(0,t)=u(L,t)=0. \tag{27}$$

These boundary conditions mean physically that the beam is clamped at both extremities.

Let us introduce the following energy functional

$$E(w)=\frac{1}{2}\int_0^L(|\partial_x^2 w|^2+|\partial_t w|^2+|w|^2)dx.$$

Formal computations along the solutions of (22) yield

$$\frac{d}{dt}E(w)=\int_0^L k|\partial_t w|^2-k'|\partial_t\partial_x w|^2dx.$$

Let the spaces V and H be as in Section 2.2. Using Fourier series in the $sin(k\pi x/L)$'s, we may extend Λ as a continuous operator from $H^{-2}(0,L)$ into H. (21) and (27) may then be written as

$$u=s\Lambda(\partial_x\varphi)-a\varphi.$$

The following result is the last main result of the paper.

Theorem 3. Assume that $k<0$ and $k'>0$. Then for any $(w^0,w^1)\in V\times H$, there exists a unique solution (u,w) of (21)-(27) such that $u\in C^0(\mathbb{R}^+;H)$ and $w\in C^0(\mathbb{R}^+;V)\cap C^1(\mathbb{R}^+;H)$.

Moreover we have that

$$||u||_{L^2(0,L)}+E(w)\to 0$$

as $t\to+\infty$.

Proof. Let us introduce the operator $\tilde{A}(w,v)=(v,-w^{(4)}-w+kv+k'v'')$ with domain $\mathcal{D}(\tilde{A})=(H^4(0,L)\cap H_0^2(0,L))\times H_0^2(0,L)\subset V\times H$. The space $V\times H$ is endowed with the following scalar product

$$\langle\begin{pmatrix}w\\v\end{pmatrix},\begin{pmatrix}\tilde{w}\\\tilde{v}\end{pmatrix}\rangle=\int_0^L(w''\tilde{w}''+w\tilde{w})\,dx+\int_0^L v\tilde{v}\,dx. \tag{28}$$

We have, for all $(w,v)\in\mathcal{D}(\tilde{A})$,

$$\langle\tilde{A}\begin{pmatrix}w\\v\end{pmatrix},\begin{pmatrix}w\\v\end{pmatrix}\rangle=k\int_0^L v^2\,dx-k'\int_0^L(v')^2\,dx \tag{29}$$

and thus $\tilde{A}$ is a dissipative operator as soon as $k < 0$ and $k' > 0$. It may be seen that $\tilde{A}$ generates a continuous semigroup $(\tilde{S}(t))_{t\geq 0}$ of contractions in $V \times H$.

Let us now turn to the strong stability. To prove the strong stability, it is clearly sufficient to show that

$$\lim_{t\to\infty} \tilde{S}(t) \begin{pmatrix} w^0 \\ w^1 \end{pmatrix} = 0 \quad \forall \begin{pmatrix} w^0 \\ w^1 \end{pmatrix} \in \mathcal{D}(\tilde{A}).$$

Since the imbedding $\mathcal{D}(\tilde{A}) \subset V \times H$ is compact, the set

$$\text{orb} \begin{pmatrix} w^0 \\ w^1 \end{pmatrix} = \bigcup_{t\geq 0} \tilde{S}(t) \begin{pmatrix} w^0 \\ w^1 \end{pmatrix}$$

is precompact in $V \times H$ for any $\begin{pmatrix} w^0 \\ w^1 \end{pmatrix}$ in $\mathcal{D}(\tilde{A})$. In this case the ω-limit set of $\begin{pmatrix} w^0 \\ w^1 \end{pmatrix}$ defined by

$$\omega \begin{pmatrix} w^0 \\ w^1 \end{pmatrix} = \Big\{ W \in V \times H,\ \exists (t_n),\ t_n \to +\infty,\ S(t_n) \begin{pmatrix} w^0 \\ w^1 \end{pmatrix} \to W \text{ as } n \to \infty \Big\}$$

is nonempty for any $\begin{pmatrix} w^0 \\ w^1 \end{pmatrix}$ in $\mathcal{D}(\tilde{A})$. Moreover, according to LaSalle's invariance principle, if

$$W \in \omega \begin{pmatrix} w^0 \\ w^1 \end{pmatrix}$$

then, for all $t \geq 0$,

$$\|W\| = \|S(t)W\|$$

where $\|\cdot\|$ is the norm associated with (28). Pick any $W = (\bar{w}^0, \bar{w}^1)^T \in \omega(w^0, w^1)^T$, and set $(\bar{w}(t), \bar{v}(t))^T = S(t)(\bar{w}^0, \bar{w}^1)^T$. Using (29), we obtain that $\bar{v}(t) = 0$ for all $t \geq 0$. The function $\bar{w}$ then solves $\partial_x^4 \bar{w} + \bar{w} = 0$ together with the boundary conditions (26), hence $\bar{w} \equiv 0$. Therefore $\bar{w}^0 = \bar{w}^1 = 0$. Thus, when $t \to \infty$, $(w, \partial_t w) \to (0,0)$ in $V \times H$, hence $I \to 0$ in $H^{-2}(0,L)$ and $\varphi \to 0$ and $u \to 0$ in $L^2(0,L)$. ■

Remark 2. When $c = 0$, $k < 0$ and $k' > 0$, the result in Theorem 3 still holds for the 2D model with $V = H_0^2(\Omega)$ and $H = L^2(\Omega)$.

REFERENCES

Allaire, G. (1992). Homogenization and two-scale convergence. *SIAM J. Math. Anal.* **23**(6), 1482–1518.

Ammari, Kais and Marius Tucsnak (2000). Stabilization of Bernoulli-Euler beams by means of a pointwise feedback force. *SIAM J. Control Optim.* **39**(4), 1160–1181 (electronic).

Ammari, Kais, Antoine Henrot and Marius Tucsnak (2001). Asymptotic behaviour of the solutions and optimal location of the actuator for the pointwise stabilization of a string. *Asymptot. Anal.* **28**(3-4), 215–240.

Cazenave, Thierry and Alain Haraux (1998). *An introduction to semilinear evolution equations*. Vol. 13 of *Oxford Lecture Series in Mathematics and its Applications*. The Clarendon Press Oxford University Press. New York. Translated from the 1990 French original by Yvan Martel and revised by the authors.

Crépeau, Emmanuelle and Christophe Prieur (to appear). Control of a clamped-free beam by a piezoelectric actuator. *ESAIM Control Optim. Calc. Var.*

Le Gall, P., C. Prieur and L. Rosier (2006). Stabilization of a clamped-free beam with collocated piezoelectric sensor/actuator. In: *IFAC Control Applications of Optimisation (CAO'06)*. Cachan, France.

Lenczner, M. and C. Prieur (2006). Asymptotic model of an active mirror. In: *IFAC Control Applications of Optimisation (CAO'06)*. Cachan, France.

Lions, J.-L. (1988). *Contrôlabilité exacte, perturbations et stabilisation de systèmes distribués. Tome 1*. Vol. 8 of *Recherches en Mathématiques Appliquées [Research in Applied Mathematics]*. Masson. Paris. Contrôlabilité exacte. [Exact controllability], With appendices by E. Zuazua, C. Bardos, G. Lebeau and J. Rauch.

Liu, Zhuangyi and Songmu Zheng (1999). *Semigroups associated with dissipative systems.* Vol. 398 of *Research Notes in Mathematics*. Chapman & Hall/CRC.

Tucsnak, Marius (1996). Regularity and exact controllability for a beam with piezoelectric actuator. *SIAM J. Control Optim.* **34**(3), 922–930.

Troisième partie

Stabilisation de poutre

Procédés de compensation des fronts d'onde

Les deux grands facteurs qui dégradent la qualité des images sont les distortions de phases et d'amplitude. Cependant, les effets des fluctuations de phase sont prédominants. Les procédés d'optique adaptative correspondent à des systèmes où ces fluctuations sont compensées par des correcteurs de phase. Cela correspond à modifier le chemin optique des différents rayon, en jouant sur le chemin géométrique - en utilisant un miroir déformable, par exemple- ou en sur l'indice de réfraction du milieu -en utilisant des matériaux électro-optiques bi-réfringents. Jusqu'à aujourd'hui, l'utilisation des miroirs est privilégiée, car particulièrement adaptée à l'optique adaptative rencontrée en astronomie[2].

Depuis le début des années 70, divers miroirs déformables ont été mis au point, utilisant des effets divers pour déformer le miroir, comme l'électromagnétisme ou les effets hydrauliques. Nénamoins, dans la grande majorité des miroirs déformables opérationnels, ce sont des actionneurs ferro-électriques (piezo-électriques ou electrostrictives) qui sont à l'origine des déformations du miroir.

Les deux grands avantages de ce type de miroirs sont la densité d'actionneurs que l'on peut atteindre, ainsi que l'interaction électromécanique relativement forte entre les actionneurs et le miroir, mais aussi la faible dissipation de puissance, la rapidité de réponse, la grande précision et la grande stabilité. Ces actionneurs ont trouvé leur emploi à la fois dans des miroirs segmentés et des miroirs continus.

Dans les deux articles qui suivent, nous nous intéressons au modèle d'une poutre (Bernoulli-Euler), libre à une extrêmité et encastrée à l'autre, à laquelle sont attachés un actionneur piezoélectrique et un capteur, et nous expliquons comment placer la cellule piezoélectrique afin d'assurer la stabilisation du système.

[2]Rajouter ici pourquoi ?

Alors que l'idée du miroir bimorphe est relativement ancienne, il faut attendre 1994 pour voir un système d'optique adaptative équipé d'un tel système, à l'Université de Hawaii. Depuis, le laboratoire commun au Canada, à la France et à Hawaii a décidé lui aussi l'utilisation d'un tel procédé.

Un miroir bimorphe correspond à deux gaufrettes[3] superposées, et polarisées de manière opposée, parallèlement à leur axe. Les électrodes sont déposées entre les deux gaufrettes. Lorsqu'une tension est appliquée à une électrode, on observe localement une courbure de l'ensemble, résultant d'une contraction de l'un éléments et de la dilatation de l'autre. Pour obtenir un miroir, on recouvre l'une des surfaces d'une couche fine de verre poli.

L'un des grands avantages de ce type de miroir apparaît lors de l'association avec un analyseur de front d'onde, qui mesure non pas la pentes mais la courbure du front d'onde, la forme du miroir se déduisant alors très simplement des mesures.

Une façon de modéliser le miroir fait apparaître deux EDP couplées, dont une EDP du second degré sans dérivée temporelle, et une équation des plaques. La contrôlabilité en dimension 1 et 2 est démontrée dans les pages suivantes, et un rétrocontrôle permettant la stabilisation est proposé. Le proceedings a été publié lors du Congrès IFAC à Cachan d'avril 2006.

[3] autre mot ?

STABILIZATION OF A CLAMPED-FREE BEAM WITH COLLOCATED PIEZOELECTRIC SENSOR/ACTUATOR

Pierre Le Gall [*] **Christophe Prieur** [**] **Lionel Rosier** [*]

[*] *Institut Elie Cartan, Université Henri Poincaré Nancy 1, B.P. 239, 54506 Vandœuvre-lès-Nancy Cedex, France*
[**] *LAAS-CNRS, 7 avenue du colonel Roche, 31077 Toulouse, France*

Abstract: We consider a Bernoulli-Euler beam, which is clamped at one boundary and free at the other, and to which are attached a piezoelectric actuator and a collocated sensor. We provide an output feedback law and characterize the sensor/actuator location for which the strong stabilization holds.

Keywords: Bernoulli-Euler beam equation, collocated piezoelectric sensor/actuator, strong stabilization.

1. INTRODUCTION

There exists now an important literature devoted to the controllability and stabilizability of flexible structures. We focus in this paper on the use of piezoelectric devices to control flexible structures, as it has been modeled in (Destuynder *et al.*, 1992; Destuynder, 1999) with second order infinite dimensional models.

The controllability of a PDE is often considered as a first step towards the stabilization of the system. Classical controllability results for the beam (or plate) equation may be found in (Komornik, 1994). See also (Rebarber, 1989), where the eigenvalue specification problem is studied for the Bernoulli-Euler beam (with the same boundary condition but with different control than in our paper), and (Fliess *et al.*, 1997), where flatness technics are used for approximate controllability problems.

The main purpose of our paper is to study the strong stabilization of a clamped-free beam, i.e. a beam clamped at one end and free at the other end. There exist technological and industrial motivations to study the stabilization of a beam equipped with piezoelectric actuators/sensors with such boundary conditions (see (Leleu, 2002)).

A very important work related to our study is (Crépeau and Prieur, to appear), where the exact controllability of a clamped-free beam equipped with a piezoelectric actuator is studied in detail. Another important work related to our study is (Ammari and Tucsnak, 2000), where an unbounded feedback is designed for the Bernoulli-Euler beam equation with *different* boundary conditions.

Here, we consider the control problem modelling the vibrations of a Bernoulli-Euler beam that is subject to the action of an attached piezoelectric actuator. If we assume that the beam is clamped at one boundary and free at the other we obtain the system:

$$\begin{aligned} &w_{tt}(x,t) + w_{xxxx}(x,t) = h(t)\frac{d}{dx}[\delta_\eta(x) - \delta_\xi(x)], \\ &w(0,t) = w_x(0,t) = w_{xx}(\pi,t) = w_{xxx}(\pi,t), \\ &w(x,0) = w^0(x),\ w_t(x,0) = w^1(x) \end{aligned}$$

In the above equations, $x \in (0,\pi)$ is the spatial coordinate, t is time, w stands for the transverse deflection of the beam, $w_t = \partial w/\partial t$, etc., η and ξ stand for the ends of the actuator ($0 \le \eta < \xi \le \pi$), δ_y is the Dirac mass at the point y, and h stands for the control input (see Figure 1).

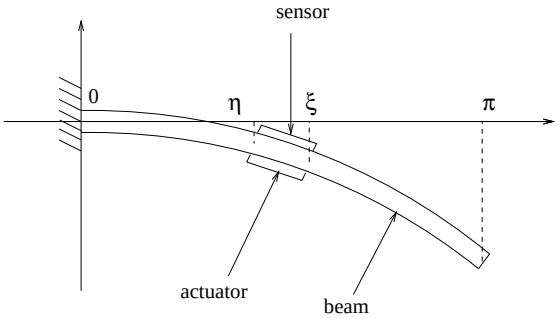

Fig. 1. A beam equipped with two piezoelectric devices.

We are interested in the stabilization of the above system, the control h being expressed as a function of the output $w_x(\eta) - w_x(\xi)$. This corresponds to the situation where the output comes from a piezoelectric sensor located on the same interval (η, ξ) as the actuator. Formal computations on the variations of the energy

$$E(w) = \int_0^\pi (|w_{xx}|^2 + |w_t|^2)\, dx$$

lead to take

$$h := k(w_{xt}(\eta) - w_{xt}(\xi))$$

where k is some number whose range will be specified later. Summing up, we will investigate the stability property of the system

$$w_{tt}(x,t) + w_{xxxx}(x,t) = k(w_{xt}(\eta) - w_{xt}(\xi))\frac{d}{dx}[\delta_\eta(x) - \delta_\xi(x)], \quad (1)$$

$$w(0,t) = w_x(0,t) = w_{xx}(\pi,t) = w_{xxx}(\pi,t) = 0, \quad (2)$$

$$w(x,0) = w^0(x),\ w_t(x,0) = w^1(x). \quad (3)$$

2. WELL-POSEDNESS OF (1)-(3)

The well-posedness of (1)-(3) in the standard energy space is obtained in this section as a direct application of the classical semi-group theory. To specify the operator, we have to see for which function w the r.h.s. of (1) belongs to $L^2(0,\pi)$. Let us introduce some notations. If w is any function in $H^1(0,\eta) \cap H^1(\eta,\xi) \cap H^1(\xi,\pi)$, we define $\{w_x\} \in L^2(0,\pi)$ by

$$\{w_x\}(x) := \begin{cases} w_x^{\mathcal{D}'(0,\eta)}(x) & \text{if } x \in (0,\eta), \\ w_x^{\mathcal{D}'(\eta,\xi)}(x) & \text{if } x \in (\eta,\xi), \\ w_x^{\mathcal{D}'(\xi,\pi)}(x) & \text{if } x \in (\xi,\pi). \end{cases}$$

We set also $[w]_\eta := w(\eta^+) - w(\eta^-)$, and $[w]_\xi := w(\xi^+) - w(\xi^-)$. Then it follows that

$$w_x = \{w_x\} + [w]_\eta \delta_\eta + [w]_\xi \delta_\xi \quad \text{in } \mathcal{D}'(0,\pi).$$

Assume now that $w \in H^2(0,\pi)$ and that $v \in H^2(0,\pi)$, and define $u \in \mathcal{D}'(0,\pi)$ by $u := -w_{xxxx} + k(v_x(\eta) - v_x(\xi))\frac{d}{dx}(\delta_\eta - \delta_\xi)$. If $u \in L^2(0,\pi)$, then the restriction of u to each of the intervals $(0,\eta)$, (η,ξ) and (ξ,π) has also to be a square integrable function. The same conclusion holds for w_{xxxx}, hence $w \in H^4(0,\eta) \cap H^4(\eta,\xi) \cap H^4(\xi,\pi)$. We may then compute w_{xxx}, w_{xxxx} and u. We obtain

$$w_{xxx} = \{w_{xxx}\} + [w_{xx}]_\eta \delta_\eta + [w_{xx}]_\xi \delta_\xi,$$

$$w_{xxxx} = \{w_{xxxx}\} + [w_{xxx}]_\eta \delta_\eta + [w_{xxx}]_\xi \delta_\xi + [w_{xx}]_\eta \frac{d}{dx}\delta_\eta + [w_{xx}]_\xi \frac{d}{dx}\delta_\xi,$$

and

$$\begin{aligned} u = &-\{w_{xxxx}\} \\ &-[w_{xxx}]_\eta \delta_\eta - [w_{xxx}]_\xi \delta_\xi \\ &-[w_{xx}]_\eta \frac{d}{dx}\delta_\eta - [w_{xx}]_\xi \frac{d}{dx}\delta_\xi \\ &+k(v_x(\eta) - v_x(\xi))\frac{d}{dx}(\delta_\eta - \delta_\xi). \end{aligned}$$

Then $u \in L^2(0,\pi)$ provided that all the coefficients in front of the Dirac masses vanish, i.e.

$$[w_{xx}]_\eta = k(v_x(\eta) - v_x(\xi)) = -[w_{xx}]_\xi$$

and

$$[w_{xxx}]_\eta = [w_{xxx}]_\xi = 0.$$

We are now in a position to define the operator associated with (1)-(3).

Let $V = \{w \in H^2(0,\pi) \,|\, w(0) = w'(0) = 0\}$, $(w_1, w_2)_V = \int_0^\pi w_1'' \overline{w_2''} dx$, and $H = L^2(0,\pi)$, $(v_1, v_2)_H = \int_0^\pi v_1 \overline{v_2} dx$. Then $\mathcal{H} = V \times H$ endowed with the usual product norm is a (complex) Hilbert space. If we introduce $v := w_t$ and define the operator A with domain

$$\begin{aligned} \mathcal{D}(A) = \{\, &z = (w,v) \,|\, (w,v) \in H^2(0,\pi)^2, \\ &w \in H^4(0,\eta) \cap H^4(\eta,\xi) \cap H^4(\xi,\pi), \\ &w(0) = w_x(0) = w_{xx}(\pi) = w_{xxx}(\pi) = 0, \\ &v(0) = v_x(0) = 0, \\ &[w_{xx}]_\eta = k(v_x(\eta) - v_x(\xi)) = -[w_{xx}]_\xi, \\ &[w_{xxx}]_\eta = [w_{xxx}]_\xi = 0 \Big\} \end{aligned}$$

and defined by

$$\begin{aligned} Az &= \left(v, -w_{xxxx} + k(v_x(\eta) - v_x(\xi))\frac{d}{dx}(\delta_\eta - \delta_\xi)\right) \\ &= (v, -\{w_{xxxx}\}), \end{aligned}$$

then the closed-loop system (1)-(3) may be seen as the initial value problem for the abstract first-order evolution equation in $\mathcal{H}$

$$\begin{cases} \dfrac{dz}{dt} = Az,\ t > 0 \\ z(0) = (w^0, w^1). \end{cases}$$

The first main result in this paper is the following one.

Theorem 1. If $k \geq 0$, then $\mathcal{A}$ generates a C_0-semigroup $(S(t))_{t \geq 0}$ of contractions on $\mathcal{H}$.

Proof: Obviously, $\mathcal{D}(A)$ is dense in $\mathcal{H}$. According to a classical result (see e.g. (Liu and Zheng, 1999, Thm 1.2.4)), the theorem is proved if we show that A is dissipative and that $0 \in \rho(A)$, the resolvent set of A. Let us begin with the dissipativity property.

Lemma 1. For any $z = (w, v) \in \mathcal{D}(A)$ we have that

$$(Az, z)_{\mathcal{H}} = 2i \,\mathrm{Im}\Big(\int_0^\pi v_{xx}\overline{w_{xx}}\,dx\Big) - k|v_x(\eta) - v_x(\xi)|^2.$$

In particular, $\mathrm{Re}\,(Az, z)_{\mathcal{H}} = -k|v_x(\eta) - v_x(\xi)|^2 \le 0$, i.e. A is dissipative.

Proof of Lemma 1: Pick any pair of functions $(w, v) \in \mathcal{H}$. Then

$$(A(w, v), (w, v))_{\mathcal{H}} = \int_0^\pi v_{xx}\overline{w_{xx}}\,dx - \int_0^\pi \{w_{xxxx}\}\overline{v}\,dx.$$

After some integrations by parts on the intervals $(0, \eta)$, (η, ξ), (ξ, π), we obtain that

$$\begin{aligned}
&-\int_0^\pi \{w_{xxxx}\}\overline{v} \\
&= -\int_0^\eta \{w_{xxxx}\}\overline{v} - \int_\eta^\xi \{w_{xxxx}\}\overline{v} - \int_\xi^\pi \{w_{xxxx}\}\overline{v} \\
&= -\int_0^\pi w_{xx}\overline{v_{xx}}\,dx + [w_{xx}\overline{v_x}]_{x=0}^{\eta} + [w_{xx}\overline{v_x}]_{x=\eta}^{\xi} \\
&\quad + [w_{xx}\overline{v_x}]_{x=\xi}^{\pi} \\
&= -\int_0^\pi w_{xx}\overline{v_{xx}}\,dx - [w_{xx}]_\eta\overline{v_x(\eta)} - [w_{xx}]_\xi\overline{v_x(\xi)}.
\end{aligned}$$

Hence

$$\begin{aligned}
&(A(w, v), (w, v))_{\mathcal{H}} \\
&= \int_0^\pi (v_{xx}\overline{w_{xx}} - w_{xx}\overline{v_{xx}})\,dx \\
&\quad - [w_{xx}]_\eta\overline{v_x(\eta)} - [w_{xx}]_\xi\overline{v_x(\xi)} \\
&= 2i \,\mathrm{Im}\Big(\int_0^\pi v_{xx}\overline{w_{xx}}\,dx\Big) - k|v_x(\eta) - v_x(\xi)|^2.
\end{aligned}$$

This completes the proof of Lemma 1. ∎

We now proceed to the study of A^{-1}. The following result holds true.

Proposition 1. $0 \in \rho(A)$.

Proof: We have to prove that the operator $A : \mathcal{D}(A) \to \mathcal{H}$ is one-to-one and onto, and that its inverse $A^{-1} : \mathcal{H} \to \mathcal{H}$ is continuous. Let a pair $(f, g) \in \mathcal{H}$ be given, and let us investigate the equation $A(w, v) = (f, g)$, where (w, v) has to be found in $\mathcal{D}(A)$. We have to solve the system

$$\begin{cases} v = f \\ -\{w_{xxxx}\} = g \end{cases}$$

supplemented by adequate boundary conditions. To eliminate g, we introduce the (unique) solution $\tilde{w} \in H^4(0, \pi)$ of the following elliptic problem

$$\begin{cases} -\tilde{w}_{xxxx} = g \\ \tilde{w}(0) = \tilde{w}_x(0) = \tilde{w}_{xx}(\pi) = \tilde{w}_{xxx}(\pi) = 0. \end{cases}$$

Setting $w = \tilde{w} + \hat{w}$ and $K := k(v_x(\eta) - v_x(\xi)) = k(f_x(\eta) - f_x(\xi))$, we have to solve

$$\{\hat{w}_{xxxx}\} = 0 \tag{4}$$

$$\hat{w}(0) = \hat{w}_x(0) = \hat{w}_{xx}(\pi) = \hat{w}_{xxx}(\pi) = 0 \tag{5}$$

$$[\hat{w}_{xx}]_\eta = K = -[\hat{w}_{xx}]_\xi \tag{6}$$

$$[\hat{w}_{xxx}]_\eta = [\hat{w}_{xxx}]_\xi = 0 \tag{7}$$

where $\hat{w}$ is to be found in $H^2(0, \pi) \cap H^4(0, \xi) \cap H^4(\xi, \eta) \cap H^4(\eta, \pi)$. In particular,

$$[\hat{w}]_\eta = [\hat{w}]_\xi = [\hat{w}_x]_\eta = [\hat{w}_x]_\xi = 0. \tag{8}$$

We infer from (4) and (5) that there exist some constants $a_2, a_3, b_0, b_1, b_2, b_3, c_0$ and c_1 such that

$$\hat{w}(x) = \begin{cases} a_2x^2 + a_3x^3 & \text{if } 0 < x < \eta, \\ b_0 + b_1x + b_2x^2 + b_3x^3 & \text{if } \eta < x < \xi, \\ c_0 + c_1(x - \pi) & \text{if } \xi < x < \pi. \end{cases}$$

It follows from (7) that $a_3 = b_3 = 0$. (6) gives $2b_2 - 2a_2 = K = 2b_2$, hence $a_2 = 0$ and $b_2 = K/2$. Finally, it is easily seen that b_0, b_1, c_0 and c_1 are uniquely determined by the following system of linear equations (coming from (8))

$$\begin{cases} b_0 + b_1\eta + \dfrac{K}{2}\eta^2 = 0 \\ b_1 + K\eta = 0 \\ b_0 + b_1\xi + \dfrac{K}{2}\xi^2 = c_0 + c_1(\xi - \pi) \\ b_1 + K\xi = c_1 \end{cases}$$

This proves the existence and uniqueness of $\hat{w}$, and the existence and uniqueness of a pair $(w, v) \in \mathcal{D}(A)$ such that $A(w, v) = (f, g)$. To see that $0 \in \rho(A)$, it remains to prove that the map $A^{-1} : \mathcal{H} \to \mathcal{H}$ is continuous. Let $(w, v) = A^{-1}(f, g)$. Then $||v||_H = ||f||_H$, $||\tilde{w}||_{H^4(0,\pi)} \le Const\,||g||_H$, $||\hat{w}||_V \le Const\,|K| \le Const\,||f||_V$. Therefore

$$||(w, v)||_{\mathcal{H}} \le Const\,||(f, g)||_{\mathcal{H}}.$$

This completes the proof of Proposition 1 and of Theorem 1. ∎

Proposition 2. The operator $A^{-1} : \mathcal{H} \to \mathcal{H}$ is compact.

Proof: Since

$$||A^{-1}(f, g)||_{\mathcal{D}(A)} = ||A^{-1}(f, g)||_{\mathcal{H}} + ||(f, g)||_{\mathcal{H}},$$

we see that A^{-1} is continuous from $\mathcal{H}$ into $\mathcal{D}(A)$, hence it is sufficient to prove that the embedding $\mathcal{D}(A) \to \mathcal{H}$ is compact. Let $\big((w^n, v^n)\big)_{n\ge 0}$ be any bounded sequence in $\mathcal{D}(A)$. We have to prove that a subsequence $\big((w^{n'}, v^{n'})\big)$ converges (strongly) in $\mathcal{H}$. As $||v^n||_{H^2(0,\pi)} \le Const$, there exists a subsequence $(v^{n'})$ and some function $v \in H = L^2(0, \pi)$ such that

$v^{n'} \to v$ in H. On the other hand, $||w^n||_{H^2(0,\pi)} + ||\{w^n_{xxxx}\}||_{L^2(0,\pi)} \leq Const$, so

$$||w^n||_{H^4(0,\eta)} + ||w^n||_{H^4(\eta,\xi)} + ||w^n||_{H^4(\xi,\pi)} \leq Const.$$

Extracting a subsequence once again, we infer that there exists a function $w \in V$ such that $w^{n'} \rightharpoonup w$ in V, and $w^{n'} \rightharpoonup w$ in $H^4(0,\eta)$, in $H^4(\eta,\xi)$ and in $H^4(\xi,\pi)$. It follows that $w^{n'} \to w$ in $H^2(0,\eta)$, in $H^2(\eta,\xi)$ and in $H^2(\xi,\pi)$. We conclude that $w^{n'} \to w$ in V. ■

3. STRONG STABILITY

3.1 Free evolution

In this section we recall some useful facts about the *free* evolution of (1)-(3) (i.e., when $k = 0$). Thus we consider the homogeneous Cauchy problem

$$\phi_{tt} + \phi_{xxxx} = 0, \tag{9}$$
$$\phi(0,t) = \phi_x(0,t) = \phi_{xx}(\pi,t) = \phi_{xxx}(\pi,t) = 0, \tag{10}$$
$$\phi(.,0) = \phi^0,\ \phi_t(.,0) = \phi^1. \tag{11}$$

Let $\mathcal{A} : \mathcal{D}(\mathcal{A}) \to L^2(0,\pi)$ be the operator with domain

$$\mathcal{D}(\mathcal{A}) := \{\phi \in H^4(0,\pi);\ \phi(0) = \phi_x(0) = \\ = \phi_{xx}(\pi) = \phi_{xxx}(\pi) = 0\}$$

and defined by $\mathcal{A}\phi = \phi_{xxxx}$. Obviously, $\mathcal{A}^{-1}$ is a compact symmetric operator on $\mathcal{H}$, hence there exists a countable orthonormal basis of $\mathcal{H}$ consisting of eigenvectors of $\mathcal{A}^{-1}$. The following result (Crépeau and Prieur, to appear, Lemma 2.1) provides useful results about the eigenvectors of $\mathcal{A}$.

Proposition 3. The $L^2(0,\pi)$-normalized eigenfunctions of $\mathcal{A}$ are the functions $(\psi_k)_{k\geq 1}$, defined by

$$\psi_k(x) = \gamma_k\big(\cos(\alpha_k x) - \cosh(\alpha_k x) \\ + \mu_k(\sinh(\alpha_k x) - \sin(\alpha_k x))\big), \tag{12}$$

where α_k is the k-th positive root of

$$1 + \cos(\alpha_k\pi)\cosh(\alpha_k\pi) = 0, \tag{13}$$

and

$$\mu_k = \frac{\cos(\alpha_k\pi) + \cosh(\alpha_k\pi)}{\sin(\alpha_k\pi) + \sinh(\alpha_k\pi)},$$

$$\gamma_k = \frac{1}{\sqrt{\pi}},$$

and the eigenvalue associated with ψ_k is $\lambda_k = \alpha_k^4$. Moreover, we have as $k \to +\infty$

$$\alpha_k = k - \frac{1}{2} + (-1)^{k+1}\frac{2e^{\frac{\pi}{2}}}{\pi}e^{-\pi k} + o(e^{-\pi k}), \tag{14}$$
$$\mu_k = 1 + 2(-1)^k e^{-\alpha_k\pi} + o(e^{-\alpha_k\pi}), \tag{15}$$

and

$$-\sinh(\alpha_k\rho) + \mu_k\cosh(\alpha_k\rho) = \\ \begin{cases} e^{-\alpha_k\rho} + o(e^{-\alpha_k\rho}) & \text{if } 0 < \rho < \dfrac{\pi}{2}, \\ (-1)^k e^{-\alpha_k(\pi-\rho)} + o(e^{-\alpha_k(\pi-\rho)}) & \text{if } \dfrac{\pi}{2} < \rho < \pi. \end{cases} \tag{16}$$

It is easily seen that if $\phi^0 = \sum_{k\geq 1}\phi^0_k\psi_k$, and $\phi^1 = \sum_{k\geq 1}\phi^1_k\psi_k$, then the solution $\phi = \phi(x,t)$ of (9)-(11) reads

$$\phi(x,t) = \sum_{k=1}^{+\infty}\left(\phi^0_k\cos(\alpha_k^2 t) + \frac{\phi^1_k}{\alpha_k^2}\sin(\alpha_k^2 t)\right)\psi_k(x). \tag{17}$$

Let $L := \xi - \eta$ denote the length of the actuator/sensor. For any $k \geq 1$ and any $L \in (0,\pi]$, let

$$\mathcal{S}_k(L) := \\ \{\eta \in [0,\pi - L]\,|\,\psi_k'(\eta) - \psi_k'(\eta + L) = 0\}, \tag{18}$$

and set

$$\mathcal{S}(L) := \cup_{k\geq 1}\mathcal{S}_k(L).$$

Definition 1. We say that (1)-(2) is *strongly stable* in $\mathcal{H}$, if for any $(w^0,w^1) \in \mathcal{H}$ we have that

$$E(w(t),w_t(t)) = ||(w(t),w_t(t))||^2_{\mathcal{H}} \to 0$$

as $t \to +\infty$.

The following theorem provides a characterization of the location of the actuator/sensor for which the strong stability holds. Its proof rests on LaSalle principle (see also (Ammari and Tucsnak, 2000) for strong stability results obtained this way).

Theorem 2. The system (1)-(2) is strongly stable in $\mathcal{H}$ if and only if $k > 0$ and $\eta \notin \mathcal{S}(L)$.

Proof: First of all, it follows from Lemma 1 that for any $(w^0,w^1) \in \mathcal{D}(A)$ and for any $t \geq 0$,

$$E(w(T),v(T)) - E(w^0,w^1) \\ = -k\int_0^T |v_x(\eta,t) - v_x(\xi,t)|^2\,dt. \tag{19}$$

Thus, the condition $k > 0$ is needed for the energy to decrease. Moreover, the relation (19) shows that the trace $v_x(\eta,.) - v_x(\xi,.)$ exists in $L^2(0,T)$ for any $T > 0$ and any $(w^0,w^1) \in \mathcal{H}$. Furthermore, a density argument shows that (19) still holds true for $(w^0,w^1) \in \mathcal{H}$. Since the embedding $\mathcal{D}(A) \subset \mathcal{H}$ is compact, we obtain that the set $\mathrm{orb}(w^0,w^1) := \{(w(t),v(t))|\ t \geq 0\}\}$ is precompact in $\mathcal{H}$ for any $(w^0,w^1) \in \mathcal{D}(A)$. Therefore, the $\omega-$limit set of (w^0,w^1), defined as

$$\omega(w^0,w^1) = \{z \in \mathcal{H}| \\ \exists(t_n) \to \infty,\ \lim_{n\to\infty} S(t_n)(w^0,w^1) = z\},$$

is nonempty. On the other hand, according to LaSalle's invariance principle (see (Cazenave and Haraux, 1998)),

for any $(\phi^0,\phi^1)\in\omega(w^0,w^1)$, we have that $S(t)(\phi^0,\phi^1)=(\phi(t),\phi_t(t))\in\omega(w^0,w^1)$ and $E(\phi(t),\phi_t(t))=E(\phi^0,\phi^1)$. The above relation and (19) imply that ϕ is a solution of (9)-(11) and fulfills

$$\phi_{xt}(\eta,t)-\phi_{xt}(\xi,t)=0\qquad\forall t\geq 0.$$

Derivating w.r.t. x and t in (17), we obtain

$$0\equiv\phi_{xt}(\eta,t)-\phi_{xt}(\xi,t)=-\sum_{k=1}^{+\infty}\big(\alpha_k^2\phi_k^0\sin(\alpha_k^2t)-\phi_k^1\cos(\alpha_k^2t)\big)\big(\psi_k'(\eta)-\psi_k'(\xi)\big).$$

Since $\alpha_{k+1}^2-\alpha_k^2\to\infty$, we infer from a generalization of Ingham's inequality that for any $T>0$

$$0=\int_0^T|\phi_{xt}(\eta,t)-\phi_{xt}(\xi,t)|^2dt\geq C_T\sum_{k=1}^{+\infty}\big(|\alpha_k^2\phi_k^0|^2+|\phi_k^1|^2\big)|\psi_k'(\eta)-\psi_k'(\xi)|^2.$$

Therefore, if $\eta\notin\mathcal{S}(L)$, then $\phi_k^0=\phi_k^1=0$ for all $k\geq 1$ and $S(t)(w^0,w^1)\to(\phi^0,\phi^1)=(0,0)$ in $\mathcal{H}$. Conversely, if $\eta\in\mathcal{S}_k(L)$ for some $k\geq 1$, then any state of the form $(\phi^0,\phi^1)=(\phi_k^0\psi_k,\phi_k^1\psi_k)$ gives rise to a solution of (1)-(3) (or (9)-(11)) whose energy does not tend to 0. The proof of Theorem 2 is achieved. ■

Remark 1. (1) In sharp contrast to (Tucsnak, 1996) and (Crépeau and Prieur, to appear), the length of the actuator/sensor may take here *any* real value. Furthermore, the position of the left endpoint for which the strong stability holds is given explicitly, and the theory of Diophantine approximation is not involved here.

(2) When $\eta\in\mathcal{S}(L)$, then there is also a strong stability in the quotient space $\mathcal{H}/\mathrm{Span}\{(\psi_k,0),(0,\psi_k)\}$ if $\mathcal{S}_{k'}(L)\cap\mathcal{S}_k(L)=\emptyset$ for any $k'\neq k$.

As the set $\mathcal{S}(L)$ plays a crucial role in the stability results, we collect some of its properties in the following proposition.

Proposition 4. For any $L\in(0,\pi)$ the set $\mathcal{S}(L)$ of critical values of η is countable and dense in $[0,\pi-L]$.

To prove that $\mathcal{S}(L)$ is countable, it is sufficient to prove that each set $\mathcal{S}_k(L)$ is finite. But $\mathcal{S}_k(L)=f_k^{-1}(0)\cap[0,\pi-L]$, where $f_k(\eta):=\psi_k'(\eta)-\psi_k'(\eta+L)$. As the function f_k is analytic, we infer that it has only a finite number of zeros in the interval $[0,\pi-L]$ (i.e., $\mathcal{S}_k(L)$ is finite) if it is not identically null. To check the last property, we need first to establish the following

CLAIM 1. $\mu_k\neq 1\quad\forall k\geq 1$.

Argue by contradiction. If the claim is false, then there exists some $k\geq 1$ with

$$\mu_k=\frac{\cos(\alpha_k\pi)+\cosh(\alpha_k\pi)}{\sin(\alpha_k\pi)+\sinh(\alpha_k\pi)}=1. \tag{20}$$

Let $x=\cos(\alpha_k\pi)$. Using (13) and (20), we arrive to the equation

$$x-x^{-1}=\pm\sqrt{1-x^2}+\sqrt{x^{-2}-1}$$

whose solutions are easily found to be ±1. Now, the equation (13) has no solution if $\cos(\alpha_k\pi)=\pm1$. The claim is proved. □

Derivating in (12) we obtain

$$\begin{aligned}\psi_k'(x)&=\gamma_k\big(-\alpha_k\sin(\alpha_kx)-\alpha_k\sinh(\alpha_kx)\\&\qquad+\mu_k(\alpha_k\cosh(\alpha_kx)-\alpha_k\cos(\alpha_kx))\big)\\&\sim\gamma_k\alpha_k(\mu_k\cosh(\alpha_kx)-\sinh(\alpha_kx))\\&\sim\gamma_k\alpha_k(\mu_k-1)e^{\alpha_kx}/2\end{aligned}$$

as $x\to+\infty$. Therefore, $f_k(\eta)\sim-\gamma_k\alpha_k(\mu_k-1)e^{\alpha_k(\eta+L)}/2$ as $\eta\to+\infty$, which shows that $f_k\not\equiv 0$. The proof that $\mathcal{S}(L)$ is countable is achieved.

Let us now check that $\mathcal{S}(L)$ is dense in $[0,\pi-L]$. The idea is that $f_k(\eta)$ oscillates like the function $\sin(\alpha_k(\eta+\frac{L}{2})-\frac{\pi}{4})$, so that the set $\mathcal{S}_k(L)$ is constituted of $O(k)$ points "almost equidistributed" in $[0,\pi-L]$. In a less formal way, using (20) and (16), we have that

$$\begin{aligned}f_k(\eta)&=\psi_k'(\eta)-\psi_k'(\eta+L)\\&=\gamma_k\alpha_k\big(\sin(\alpha_k(\eta+L))-\sin(\alpha_k\eta)\\&\qquad+\mu_k(\cos(\alpha_k(\eta+L))-\cos(\alpha_k\eta))\\&\qquad-\sinh(\alpha_k\eta)+\mu_k\cosh(\alpha_k\eta)\\&\qquad+\sinh(\alpha_k(\eta+L))-\mu_k\cosh(\alpha_k(\eta+L))\big)\\&=\gamma_k\alpha_k\big(2\cos(\alpha_k(\eta+\frac{L}{2}))\sin(\alpha_k\frac{L}{2})\\&\qquad-2\mu_k\sin(\alpha_k(\eta+\frac{L}{2}))\sin(\alpha_k\frac{L}{2})+o(e^{-\delta\alpha_k})\big)\\&=2\sqrt{2}\gamma_k\alpha_k\big(\sin(\frac{\pi}{4}-\alpha_k(\eta+\frac{L}{2}))\sin(\alpha_k\frac{L}{2})\\&\qquad+o(e^{-\delta\alpha_k})\big)\end{aligned}$$

for some positive constant $\delta\in(0,\pi/2)$, provided that η and $\eta+L$ are both different from $\frac{\pi}{2}$. The following claim is needed.

CLAIM 2. $\forall L\in(0,\pi],\ \forall k_0\geq 1,\ \exists k\geq k_0$ such that $|\sin(\alpha_k\frac{L}{2})|\geq e^{-\delta\alpha_k}$.

If the claim is false, then there exists an integer $k_0\geq 1$ such that

$$|\sin(\alpha_k\frac{L}{2})e^{\delta\alpha_k}|<1\quad\forall k\geq k_0.$$

As $|\sin(\alpha_k\frac{L}{2})-\sin((k-\frac{1}{2})\frac{L}{2})|\leq Ce^{-\pi k}$ by (14), we infer that

$$|\sin((k-\frac{1}{2})\frac{L}{2})e^{\delta\alpha_k}|\leq C'\quad\forall k\geq k_0, \tag{21}$$

where C and C' denote some positive constants. If $L\in\pi\mathbb{Q}$, then the sequence $\big(\sin((k-\frac{1}{2})\frac{L}{2})\big)_{k\geq0}$ is periodic (not constant). If $L\notin\pi\mathbb{Q}$, then the same sequence is dense in $[-1,1]$. In both cases, (21) cannot hold. Claim 2 is proved. □

With Claim 2 we conclude that for a sequence $k' \to \infty$, $f_{k'}$ vanishes between any pair of successive extrema of $\sin(\frac{\pi}{4} - \alpha_{k'}(\eta + \frac{L}{2}))$. The density of $\mathcal{S}(L)$ follows at once. ■

The sets $\mathcal{S}_k(L)$ have been numerically computed for $L = \frac{\pi}{2}$ and $k \leq 6$. This choice corresponds to the case of an actuator/sensor which covers half of the length of the beam. The repartition is sketched out in Table 1.

Table 1. $S_k(L)$ for small values of k and for $L = \frac{\pi}{2}$

S_1	0.15				
S_2	0.48				
S_3	0.07	0.62	1.28		
S_4	0.21	0.67	1.1		
S_5	0.04	0.35	0.7	1.05	1.41
S_6	0.13	0.43	0.71	1	1.28

4. CONCLUSION

The paper was devoted to the output stabilization of a clamped-free beam with collocated piezoelectric sensor/actuator. It was proved that for any length of the actuator, the strong stability holds provided that the left endpoint η of the actuator does not belong to a dense countable set $\mathcal{S}(L)$. The determination of the decay rate will be the purpose of further research in a near future.

REFERENCES

Ammari, Kais and Marius Tucsnak (2000). Stabilization of Bernoulli-Euler beams by means of a pointwise feedback force. *SIAM J. Control Optim.* **39**(4), 1160–1181 (electronic).

Cazenave, Thierry and Alain Haraux (1998). *An introduction to semilinear evolution equations*. Vol. 13 of *Oxford Lecture Series in Mathematics and its Applications*. The Clarendon Press Oxford University Press. New York. Translated from the 1990 French original by Yvan Martel and revised by the authors.

Crépeau, Emmanuelle and Christophe Prieur (to appear). Control of a clamped-free beam by a piezoelectric actuator. *ESAIM Control Optim. Calc. Var.*

Destuynder, P. (1999). A mathematical analysis of a smart-beam which is equipped with piezoelectric actuators. *Control Cybern.* **28**(3), 501–530.

Destuynder, P., I. Legrain and L. Castel (1992). Theorical, numerical and experimental discussion of the use of piezoelectric devices for control-structure interaction. *Eur. J. Mech., A/Solids* **11**, 97–106.

Fliess, M., H. Mounier and P. Rouchon (1997). Linear systems over mikusinski operators and control of a flexible beam. *ESAIM: Proc.* **2**, 183–193.

Komornik, V. (1994). *Exact controllability and stabilization*. RAM: Research in Applied Mathematics. Masson. Paris. The multiplier method.

Leleu, Sylvaine (2002). Amortissement actif des vibrations d'une structure flexible de type plaque à l'aide de transducteurs piézoélectriques. PhD thesis. ENS de Cachan. (in french).

Liu, Zhuangyi and Songmu Zheng (1999). *Semigroups associated with dissipative systems.* Vol. 398 of *Chapman & Hall/CRC Research Notes in Mathematics*. Chapman & Hall/CRC, Boca Raton, FL.

Rebarber, R. (1989). Spectral assignability for distribued parameter systems with unbounded scalar control. *SIAM J. Control Optim.* **27**(1), 148–169.

Tucsnak, Marius (1996). Regularity and exact controllability for a beam with piezoelectric actuator. *SIAM J. Control Optim.* **34**(3), 922–930.

OUTPUT FEEDBACK STABILIZATION OF A CLAMPED-FREE BEAM

PIERRE LE GALL, CHRISTOPHE PRIEUR, AND LIONEL ROSIER

Abstract. We consider a Euler-Bernoulli beam, which is clamped at one extremity and free at the other, and to which are attached a piezoelectric actuator and a collocated sensor touching the clamped extremity. We provide an output feedback law and characterize the sensor/actuator lengths for which the strong stabilization holds. Finally, we prove that the energy decreases to zero in a polynomial way for almost all lengths, and in an exponential way for lengths admitting a certain coprime factorization.

1. Introduction

The Euler-Bernoulli equation provides a very commonly used model for the dynamic behavior of a flexible beam, when the cross-sectional dimensions of the beam are small in comparison to its length. In the last decade, a lot of papers were devoted to the pointwise feedback stabilization of a beam (see e.g. [1], [5], [6], [9], [13], [14], [19], [20], [22]), or to the modelling of piezoceramic actuation of beams ([4], [7]) or to the controllability of such systems ([8], [23]). The piezoceramic actuation of beams or plates is investigated numerically and experimentally in [3], [10], and [11].

In this paper, we consider the control problem modelling the vibrations of a Euler-Bernoulli beam which is subject to the action of an attached piezoelectric actuator. If we assume that the beam is clamped at one end and free at the other, and that the actuator is touching the clamped end, then we obtain the system

$$\begin{aligned} &w_{tt}(x,t) + w_{xxxx}(x,t) = -h(t)\frac{d\delta_\xi}{dx}(x),\\ &w(0,t) = w_x(0,t) = w_{xx}(\pi,t) = w_{xxx}(\pi,t) = 0,\\ &w(x,0) = w^0(x),\ \ w_t(x,0) = w^1(x). \end{aligned}$$

In the above equations, $x \in (0,\pi)$ is the spatial coordinate, t is time, w stands for the transverse deflection of the beam, $w_t = \partial w/\partial t$, etc., 0 and ξ are the coordinates of the extremities of the actuator ($0 < \xi \leq \pi$), δ_y is the Dirac mass at the point y, and h stands for the control input (see Figure 1).

We are interested in the stabilization of the above system, the control h being expressed as a function of the *output* $w_x(0,t) - w_x(\xi,t) = -w_x(\xi,t)$. This corresponds to the situation where the output comes from a piezoelectric sensor located on the same interval $(0,\xi)$ as the actuator. Formal computations on the variations of the energy

$$E(w,w_t) = \int_0^\pi (|w_{xx}|^2 + |w_t|^2)\,dx$$

lead to take

$$h(t) := -Kw_{xt}(\xi,t)$$

1991 *Mathematics Subject Classification.* 11K60, 47A10, 74K10, 93D15.

Key words and phrases. Euler-Bernoulli beam equation, collocated piezoelectric sensor/actuator, strong stabilization, exponential decay rate, polynomial decay rate.

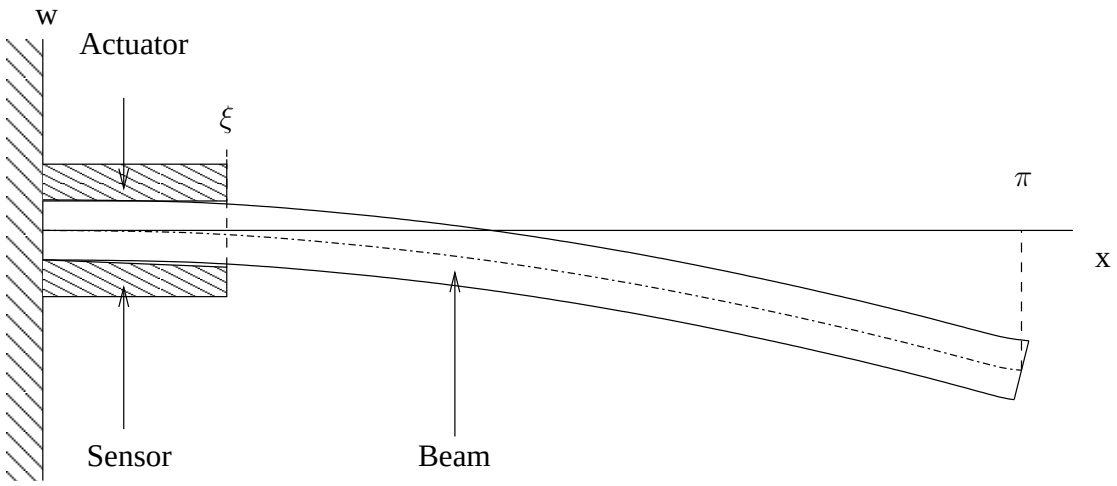

FIGURE 1. Clamped-free beam with collocated sensor/actuator

where K is some number whose range will be specified later. In short, we are interested in the stability properties of the closed-loop system

$$w_{tt}(x,t) + w_{xxxx}(x,t) = K w_{xt}(\xi,t)\frac{d\delta_\xi}{dx}(x), \tag{1.1}$$

$$w(0,t) = w_x(0,t) = w_{xx}(\pi,t) = w_{xxx}(\pi,t) = 0, \tag{1.2}$$

$$w(x,0) = w^0(x),\ w_t(x,0) = w^1(x). \tag{1.3}$$

The main goal of the paper is to characterize the lengths of the sensor/actuator leading to "good" stability properties for (1.1)-(1.3), i.e., with an exponential (or polynomial) energy decay rate.

The study of the controllability properties of a PDE is often considered as the first step towards the control theory of that PDE. The exact controllability of a beam hinged at both ends and subject to the action of a piezoelectric actuator is characterized in function of the location of the actuator in [23]. It is shown in that paper that the space of controllable states is related to Diophantine approximation properties for the extremities of the actuator. A similar study is performed in [8] in the more difficult framework of a clamped-free beam. The stabilization of a beam hinged at both ends and subject to a pointwise force has been deeply studied in [1]. The method of proof consists of deducing the decay estimates from observability inequalities for the associated free problem via sharp trace regularity results.

When we compare our work with [1] we notice that: (i) the boundary conditions considered here are more difficult to handle than the ones in [1] (where e.g. the eigenvectors for the free evolution reduce to sin functions). Here, only an asymptotic expansion of the eigenvalues for the free evolution of (1.1)-(1.3) is known; (ii) the method of proof used in [1] cannot be applied here due to an additional difficulty: the key observed quantity, namely the integral term $\int_0^T |w_{xt}(\xi,t)|^2\,dt$, is of the same order as $||(w^0,w^1)||^2_{H^3\times H^1}$ for the *free evolution* ($K=0$), whereas it is of the same order as $||(w^0,w^1)||^2_{H^2\times H^0}$ for the *controlled system* ($K>0$). Thus, a spectral analysis resting on the free evolution as in [1] cannot be performed here.

To obtain our decay estimates, we follow the frequency-domain approach described in [19] and based on a sharp estimation of a resolvent on the imaginary axis. More precisely,

we combine the multiplier method to a careful computation of the value at $x = \pi$ of the solution to (1.1)-(1.3). Thanks to that calculation, we obtain an explicit polynomial decay estimate valid for almost every value of ξ, and an exponential decay estimate when ξ admits a certain coprime factorization.

The paper is outlined as follows. The well-posedness of (1.1)-(1.3) in the energy space is investigated in Section 2. The lengths ξ of the actuator for which the strong stability holds are characterized in Section 3. The last section contains the main results of the paper, namely Theorem 4.1 (resp. Theorem 4.5) which provides an exponential (resp., polynomial) energy decay rate.

2. Well-posedness of (1.1)-(1.3)

The well-posedness of (1.1)-(1.3) in the energy space is obtained in this section as a direct application of the classical semi-group theory. To specify the operator, we have to see for which function w the r.h.s. of (1.1) belongs to $L^2(0,\pi)$. Let us introduce some notations. If w is any function in $H^1(0,\xi)\cap H^1(\xi,\pi)$, we define $\{w_x\}\in L^2(0,\pi)$ by

$$\{w_x\}(x) := \begin{cases} w_x^{\mathcal{D}'(0,\xi)}(x) & \text{if } x\in(0,\xi),\\ w_x^{\mathcal{D}'(\xi,\pi)}(x) & \text{if } x\in(\xi,\pi),\end{cases}$$

where $w_x^{\mathcal{D}'(0,\xi)}$ (resp. $w_x^{\mathcal{D}'(\xi,\pi)}$) denotes the distributional derivative $\partial w/\partial x$ in $\mathcal{D}'(0,\xi)$ (resp. in $\mathcal{D}'(\xi,\pi)$). We also set $[w]_\xi := w(\xi^+) - w(\xi^-)$. It follows that

$$w_x = \{w_x\} + [w]_\xi\delta_\xi \quad \text{ in } \mathcal{D}'(0,\pi).$$

Assume now that $w, v\in H^2(0,\pi)$, and define $u\in\mathcal{D}'(0,\pi)$ by $u := -w_{xxxx} + Kv_x(\xi)\frac{d}{dx}\delta_\xi$. If $u\in L^2(0,\pi)$, then the restriction of w_{xxxx} to each of the intervals $(0,\xi)$ and (ξ,π) has to be a square-integrable function; hence $w\in H^4(0,\xi)\cap H^4(\xi,\pi)$. Calculating w_{xxx}, w_{xxxx} and u, we obtain

$$\begin{aligned} w_{xxx} &= \{w_{xxx}\} + [w_{xx}]_\xi\delta_\xi,\\ w_{xxxx} &= \{w_{xxxx}\} + [w_{xxx}]_\xi\delta_\xi + [w_{xx}]_\xi\frac{d}{dx}\delta_\xi,\end{aligned}$$

and

$$u = -\{w_{xxxx}\} - [w_{xxx}]_\xi\delta_\xi - [w_{xx}]_\xi\frac{d}{dx}\delta_\xi + Kv_x(\xi)\frac{d}{dx}\delta_\xi. \tag{2.1}$$

Then $u\in L^2(0,\pi)$ provided that all the coefficients in front of the Dirac masses vanish, i.e.,

$$K\,v_x(\xi) = [w_{xx}]_\xi$$

and

$$[w_{xxx}]_\xi = 0.$$

We are now in a position to define the operator associated with (1.1)-(1.3).

Let $V = \{w\in H^2(0,\pi)|\ w(0) = w'(0) = 0\}$ (where $' = d/dx$) $(w_1,w_2)_V = \int_0^\pi w_1''\overline{w_2''}dx$, and $H = L^2(0,\pi)$, $(v_1,v_2)_H = \int_0^\pi v_1\overline{v_2}dx$. Then $\mathcal{H} = V\times H$, endowed with the usual product norm, is a (complex) Hilbert space. If we introduce $v := w_t$ and define the operator $\mathcal{A}$ with domain

$$\begin{aligned}\mathcal{D}(\mathcal{A}) = \{\ & z = (w,v)\,|\ (w,v)\in H^2(0,\pi)^2,\ w\in H^4(0,\xi)\cap H^4(\xi,\pi),\\ & w(0) = w_x(0) = w_{xx}(\pi) = w_{xxx}(\pi) = 0,\ v(0) = v_x(0) = 0,\\ & Kv_x(\xi) = [w_{xx}]_\xi\,,\ [w_{xxx}]_\xi = 0\}\end{aligned}$$

by

$$\mathcal{A}z = \left(v, -w_{xxxx} + Kv_x(\xi)\frac{d}{dx}\delta_\xi \right) = (v, -\{w_{xxxx}\}), \tag{2.2}$$

then we see that the closed-loop system (1.1)-(1.3) may be interpreted as the initial value problem for the abstract first-order evolution equation in $\mathcal{H}$

$$\begin{cases} \dfrac{dz}{dt} = \mathcal{A}z, \ t > 0 \\ \\ z(0) = (w^0, w^1). \end{cases}$$

The first result in this paper is the following one.

Theorem 2.1. *If $K \geq 0$, then $\mathcal{A}$ generates a C_0-semigroup $(e^{t\mathcal{A}})_{t\geq 0}$ of contractions on $\mathcal{H}$.*

Proof: Obviously, $\mathcal{D}(\mathcal{A})$ is dense in $\mathcal{H}$. According to a classical result (see e.g. [19, Thm. 1.2.4]), the theorem is proved if we show that $\mathcal{A}$ is dissipative and that $0 \in \rho(\mathcal{A})$, the resolvent set of $\mathcal{A}$. Let us begin with the dissipativity property.

Lemma 2.2. *For any $z = (w, v) \in \mathcal{D}(\mathcal{A})$ we have that*

$$(\mathcal{A}z, z)_{\mathcal{H}} = 2i \ \mathrm{Im}\Big(\int_0^\pi v_{xx}\overline{w_{xx}}\, dx\Big) - K|v_x(\xi)|^2. \tag{2.3}$$

In particular, $\mathrm{Re}\ (\mathcal{A}z, z)_{\mathcal{H}} = -K|v_x(\xi)|^2 \leq 0$, *i.e., $\mathcal{A}$ is dissipative.*

Proof of Lemma 2.2: Pick any pair of functions $(w, v) \in \mathcal{H}$. Then

$$(\mathcal{A}(w, v), (w, v))_{\mathcal{H}} = \int_0^\pi v_{xx}\overline{w_{xx}}\, dx - \int_0^\pi \{w_{xxxx}\}\overline{v}\, dx.$$

After some integrations by parts on the intervals $(0, \xi)$ and (ξ, π), we obtain that

$$\begin{aligned} -\int_0^\pi \{w_{xxxx}\}\overline{v} &= -\int_0^\xi \{w_{xxxx}\}\overline{v} - \int_\xi^\pi \{w_{xxxx}\}\overline{v} \\ &= -\int_0^\pi w_{xx}\overline{v_{xx}}\, dx + [w_{xx}\overline{v_x}]_{x=0}^{\xi} + [w_{xx}\overline{v_x}]_{x=\xi}^{\pi} \\ &= -\int_0^\pi w_{xx}\overline{v_{xx}}\, dx - [w_{xx}]_\xi \overline{v_x(\xi)}. \end{aligned}$$

Hence

$$\begin{aligned} (\mathcal{A}(w, v), (w, v))_{\mathcal{H}} &= \int_0^\pi (v_{xx}\overline{w_{xx}} - w_{xx}\overline{v_{xx}})\, dx - [w_{xx}]_\xi \overline{v_x(\xi)} \\ &= 2i \ \mathrm{Im}\Big(\int_0^\pi v_{xx}\overline{w_{xx}}\, dx\Big) - K|v_x(\xi)|^2. \end{aligned}$$

■

We now proceed to the study of $\mathcal{A}^{-1}$. The following result holds true.

Proposition 2.3. $0 \in \rho(\mathcal{A})$.

Proof: We have to prove that the operator $\mathcal{A} : \mathcal{D}(\mathcal{A}) \to \mathcal{H}$ is one-to-one and onto, and that its inverse $\mathcal{A}^{-1} : \mathcal{H} \to \mathcal{H}$ is continuous. Let a pair $(f, g) \in \mathcal{H}$ be given, and let us

investigate the equation $\mathcal{A}(w,v)=(f,g)$, where (w,v) has to be found in $\mathcal{D}(\mathcal{A})$. We have to solve the system

$$\left\{\begin{array}{l} v=f \\ -\{w_{xxxx}\}=g \end{array}\right.$$

supplemented by adequate boundary conditions. To eliminate g, we introduce the (unique) solution $\tilde{w}\in H^4(0,\pi)$ of the following elliptic problem

$$\left\{\begin{array}{l} -\tilde{w}_{xxxx}=g \\ \tilde{w}(0)=\tilde{w}_x(0)=\tilde{w}_{xx}(\pi)=\tilde{w}_{xxx}(\pi)=0. \end{array}\right.$$

Setting $w=\tilde{w}+\hat{w}$ and $C:=Kv_x(\xi)=Kf_x(\xi)$, we have to solve

$$\{\hat{w}_{xxxx}\}=0 \tag{2.4}$$

$$\hat{w}(0)=\hat{w}_x(0)=\hat{w}_{xx}(\pi)=\hat{w}_{xxx}(\pi)=0 \tag{2.5}$$

$$[\hat{w}_{xx}]_\xi=C \tag{2.6}$$

$$[\hat{w}_{xxx}]_\xi=0 \tag{2.7}$$

where $\hat{w}$ is to be found in $H^2(0,\pi)\cap H^4(0,\xi)\cap H^4(\xi,\pi)$. In particular,

$$[\hat{w}]_\xi=[\hat{w}_x]_\xi=0. \tag{2.8}$$

We infer from (2.4) and (2.5) that there exist some constants $a_2,\ a_3,\ b_0$, and b_1 such that

$$\hat{w}(x)=\left\{\begin{array}{ll} a_2x^2+a_3x^3 & \text{if } 0<x<\xi, \\ b_0+b_1(x-\pi) & \text{if } \xi<x<\pi. \end{array}\right.$$

It follows from (2.7) that $a_3=0$. Equation (2.6) gives $-2a_2=C$; hence $a_2=-C/2$. Finally, it is easily seen that b_0 and b_1 are uniquely determined by the following system of linear equations (coming from (2.8))

$$\left\{\begin{array}{rl} b_0+b_1(\xi-\pi) & =a_2\xi^2, \\ b_1 & =2a_2\xi. \end{array}\right.$$

This proves the existence and uniqueness of $\hat{w}$, and the existence and uniqueness of a pair $(w,v)\in\mathcal{D}(\mathcal{A})$ such that $\mathcal{A}(w,v)=(f,g)$. To see that $0\in\rho(\mathcal{A})$, it remains to prove that the map $\mathcal{A}^{-1}:\mathcal{H}\to\mathcal{H}$ is continuous. Let $(w,v)=\mathcal{A}^{-1}(f,g)$. Then $||v||_H=||f||_H$, $||\tilde{w}||_{H^4(0,\pi)}\le Const||g||_H$, $||\hat{w}||_V\le Const|C|\le Const||f||_V$. Therefore,

$$||(w,v)||_{\mathcal{H}}\le Const||(f,g)||_{\mathcal{H}}.$$

This completes the proofs of Proposition 2.3 and of Theorem 2.1. ■

Proposition 2.4. *The operator $\mathcal{A}^{-1}:\mathcal{H}\to\mathcal{H}$ is compact.*

Proof: Since

$$||\mathcal{A}^{-1}(f,g)||_{\mathcal{D}(\mathcal{A})}=||\mathcal{A}^{-1}(f,g)||_{\mathcal{H}}+||(f,g)||_{\mathcal{H}},$$

we see that $\mathcal{A}^{-1}$ is continuous from $\mathcal{H}$ into $\mathcal{D}(\mathcal{A})$, therefore it is sufficient to prove that the embedding $\mathcal{D}(\mathcal{A})\to\mathcal{H}$ is compact. Let $\big((w^n,v^n)\big)_{n\ge0}$ be any bounded sequence in $\mathcal{D}(\mathcal{A})$. We have to prove that a subsequence $\big((w^{n'},v^{n'})\big)$ converges (strongly) in $\mathcal{H}$. As $||v^n||_{H^2(0,\pi)}\le Const$, there exist a subsequence $(v^{n'})$ and a function $v\in H=L^2(0,\pi)$ such that $v^{n'}\to v$ in H. On the other hand, $||w^n||_{H^2(0,\pi)}+||\{w^n_{xxxx}\}||_{L^2(0,\pi)}\le Const$, so

$$||w^n||_{H^4(0,\xi)}+||w^n||_{H^4(\xi,\pi)}\le Const.$$

Extracting if needed a subsequence again denoted by $\big((w^{n'},v^{n'})\big)$, we infer that there exists a function $w\in V$ such that $w^{n'}\rightharpoonup w$ in $H^2(0,\pi)$, and $w^{n'}\rightharpoonup w$ in $H^4(0,\xi)$ and in

$H^4(\xi,\pi)$. It follows that $w^{n'} \to w$ in $H^2(0,\xi)$ and in $H^2(\xi,\pi)$. We conclude that $w^{n'} \to w$ in V. ∎

3. Strong stability

3.1. **Free evolution.**

In this section we recall some useful facts about the *free* evolution of (1.1)-(1.3); i.e., when $K = 0$. Thus we consider the homogeneous Cauchy problem

$$\phi_{tt} + \phi_{xxxx} = 0, \tag{3.1}$$

$$\phi(0,t) = \phi_x(0,t) = \phi_{xx}(\pi,t) = \phi_{xxx}(\pi,t) = 0, \tag{3.2}$$

$$\phi(.,0) = \phi^0,\ \phi_t(.,0) = \phi^1. \tag{3.3}$$

Let $A : \mathcal{D}(A) \to L^2(0,\pi)$ be the operator with domain

$$\mathcal{D}(A) := \{\phi \in H^4(0,\pi);\ \phi(0) = \phi_x(0) = \phi_{xx}(\pi) = \phi_{xxx}(\pi) = 0\}$$

and defined by $A\phi = \phi_{xxxx}$. Obviously, A^{-1} is a compact symmetric operator on $L^2(0,\pi)$, hence there exists a countable orthonormal basis of $L^2(0,\pi)$ constituted of eigenvectors of A^{-1} (and of A). The following result [8, Lemma 2.1] provides useful results about the eigenvectors of A.

Proposition 3.1. *The $L^2(0,\pi)$-normalized eigenfunctions of A are the functions $(\psi_k)_{k\geq 1}$ defined by*

$$\psi_k(x) = \frac{1}{\sqrt{\pi}}\big\{\cos(\alpha_k x) - \cosh(\alpha_k x) + \mu_k\big(\sinh(\alpha_k x) - \sin(\alpha_k x)\big)\big\}, \tag{3.4}$$

where α_k is the k-th positive root of

$$1 + \cos(\alpha_k\pi)\cosh(\alpha_k\pi) = 0, \tag{3.5}$$

and

$$\mu_k = \frac{\cos(\alpha_k\pi) + \cosh(\alpha_k\pi)}{\sin(\alpha_k\pi) + \sinh(\alpha_k\pi)},$$

and the eigenvalue associated with ψ_k is $\lambda_k = |\alpha_k|^4$. Moreover, we have as $k \to +\infty$

$$\alpha_k = k - \frac{1}{2} + (-1)^{k+1}\frac{2e^{\frac{\pi}{2}}}{\pi}e^{-\pi k} + o(e^{-\pi k}), \tag{3.6}$$

$$\mu_k = 1 + 2(-1)^k e^{-\alpha_k\pi} + o(e^{-\alpha_k\pi}), \tag{3.7}$$

and

$$-\sinh(\alpha_k\rho) + \mu_k\cosh(\alpha_k\rho) = \begin{cases} e^{-\alpha_k\rho} + o(e^{-\alpha_k\rho}) & \text{if } 0 < \rho < \frac{\pi}{2}, \\ (-1)^k e^{-\alpha_k(\pi-\rho)} + o(e^{-\alpha_k(\pi-\rho)}) & \text{if } \frac{\pi}{2} < \rho < \pi. \end{cases} \tag{3.8}$$

It is easily seen that if $\phi^0 = \sum_{k\geq 1}\phi^0_k\psi_k$, and $\phi^1 = \sum_{k\geq 1}\phi^1_k\psi_k$, then the solution $\phi = \phi(x,t)$ of (3.1)-(3.3) reads

$$\phi(x,t) = \sum_{k=1}^{+\infty}\left(\phi^0_k\cos(|\alpha_k|^2 t) + \frac{\phi^1_k}{|\alpha_k|^2}\sin(|\alpha_k|^2 t)\right)\psi_k(x). \tag{3.9}$$

3.2. **Statement of the Strong Stability result.**

For any $k \geq 1$ let

$$\mathcal{S}_k := \{\xi \in (0,\pi] \mid \psi_k'(\xi) = 0\}, \tag{3.10}$$

and set

$$\mathcal{S} := \cup_{k\geq 1}\mathcal{S}_k.$$

Definition 3.2. We say that (1.1)-(1.3) is *strongly stable* in $\mathcal{H}$, if for any $(w^0, w^1) \in \mathcal{H}$ we have that

$$E(w(t), w_t(t)) = ||(w(t), w_t(t))||^2_{\mathcal{H}} \to 0$$

as $t \to +\infty$.

The following theorem provides a characterization of the length of the sensor/actuator for which the strong stability holds.

Theorem 3.3. *The system* (1.1)-(1.3) *is strongly stable in* $\mathcal{H}$ *if and only if* $K > 0$ *and* $\xi \notin \mathcal{S}$.

Proof: First, it follows from Lemma 2.2 that for any $(w^0, w^1) \in \mathcal{D}(A)$ and for any $t \geq 0$,

$$E(w(T), v(T)) - E(w^0, w^1) = -2K \int_0^T |v_x(\xi, t)|^2 \, dt. \tag{3.11}$$

Thus, the condition $K > 0$ is needed for the energy to decrease. On the other hand, if $\xi \in \mathcal{S}_k$ for some $k \geq 1$, then any state of the form $(\phi^0, \phi^1) = (\phi^0_k \psi_k, \phi^1_k \psi_k)$ gives rise to a solution of (1.1)-(1.3) whose energy does not tend to 0. Thus $K > 0$ together with $\xi \notin \mathcal{S}$ constitutes a *necessary* condition for (1.1)-(1.3) to be strongly stable. Let us now check that this condition is also *sufficient*. We need the following result, which extends Proposition 2.3.

Proposition 3.4. $i\mathbb{R} \subset \rho(\mathcal{A})$.

Proof of Proposition 3.4. Since $\mathcal{A}^{-1}$ is compact, the spectrum of $\mathcal{A}$ is constituted only of eigenvalues, so to prove the claim it is sufficient to check that for any $\beta \in \mathbb{R}^*$ the equation

$$(i\beta - \mathcal{A})(w, v) = (0, 0), \quad (w, v) \in \mathcal{D}(\mathcal{A}) \tag{3.12}$$

admits only the trivial solution $(w, v) = (0, 0)$. Using (3.12) and (2.3), we obtain that

$$0 = ((i\beta - \mathcal{A})(w, v), (w, v))_{\mathcal{H}} = i\left(\beta||(w, v)||^2_{\mathcal{H}} - 2\,\mathrm{Im}\int_0^\pi v_{xx}\overline{w_{xx}}\, dx\right) + K|v_x(\xi)|^2,$$

hence

$$[w_{xx}]_\xi = K v_x(\xi) = 0$$

and $w \in H^4(0, \pi)$. On the other hand, (3.12) yields

$$\begin{cases} -\beta^2 w + w^{(4)} = 0 \\ w(0) = w'(0) = w(\pi) = w'(\pi) = 0, \end{cases}$$

so if $w \neq 0$, then $\beta^2 = \lambda_k$ and $w = C\psi_k$ for some $k \geq 1$, $C \in \mathbb{C}$. It follows that $0 = Kv'(\xi) = i\beta K C \psi_k'(\xi)$; hence $C = 0$ (since $K \neq 0$ and $\xi \notin \mathcal{S}$), contradicting the assumption $w \neq 0$. Therefore $w = v = 0$. ■

Applying a classical stability theorem due to Arendt-Batty (see [2]), we infer from Proposition 3.4 that the system (1.1)-(1.3) is strongly stable in $\mathcal{H}$. ■

Remark 3.5. (1) Proceeding as in [16], one may write a more elementary proof of Theorem 3.3 by using LaSalle principle (see [1] for strong stability results obtained this way).

(2) If $\xi \in \mathcal{S}_k$ and $\xi \notin \mathcal{S}_{k'}$ for $k' \neq k$, then a strong stability result also holds true in the subspace $\mathcal{H}' := \mathrm{Span}\{(\psi_k, 0),\, (0, \psi_k)\}^\perp$ of codimension 2.

3.3. **Properties of the set $\mathcal{S}$ of critical lengths.**

As the set $\mathcal{S}$ plays a crucial role in all the stability results, we collect some of its properties in the following proposition.

Proposition 3.6. *The set $\mathcal{S}$ is countable and dense in $(0, \pi]$.*

To prove that $\mathcal{S}$ is countable, it is sufficient to prove that each set $\mathcal{S}_k$ is finite. But $\mathcal{S}_k = (\psi_k')^{-1}(0) \cap (0, \pi]$, and the function ψ_k', which is analytic, has only a finite number of zeros in the interval $(0, \pi]$ if it is not identically null. To check the last property, we need first to establish the following

Claim 1. $\mu_k \neq 1 \quad \forall k \geq 1$.
Argue by contradiction. If the claim is false, then there exists some $k \geq 1$ with

$$\mu_k = \frac{\cos(\alpha_k \pi) + \cosh(\alpha_k \pi)}{\sin(\alpha_k \pi) + \sinh(\alpha_k \pi)} = 1. \tag{3.13}$$

Let $x = \cos(\alpha_k \pi)$. Using (3.5) and (3.13), we arrive to the equation

$$x - x^{-1} = \pm\sqrt{1 - x^2} + \sqrt{x^{-2} - 1}$$

whose solutions are easily found to be ± 1. Now, (3.5) has no solution if $\cos(\alpha_k \pi) = \pm 1$. The claim is proved. □

Derivating in (3.4) we obtain

$$\begin{aligned} \psi_k'(x) &= \pi^{-\frac{1}{2}}\big(-\alpha_k \sin(\alpha_k x) - \alpha_k \sinh(\alpha_k x) \\ &\qquad + \mu_k(\alpha_k \cosh(\alpha_k x) - \alpha_k \cos(\alpha_k x))\big) \\ &\sim \pi^{-\frac{1}{2}} \alpha_k (\mu_k \cosh(\alpha_k x) - \sinh(\alpha_k x)) \\ &\sim \pi^{-\frac{1}{2}} \alpha_k (\mu_k - 1) e^{\alpha_k x}/2 \end{aligned}$$

as $x \to +\infty$, hence $\psi_k' \not\equiv 0$. The proof that $\mathcal{S}$ is countable is achieved.

Let us now check that $\mathcal{S}$ is dense in $(0, \pi]$. Applying Proposition 3.1, we obtain that

$$\psi_k'(x) = -\sqrt{2}\pi^{-\frac{1}{2}} \alpha_k \left(\sin(\alpha_k x + \frac{\pi}{4}) + O(e^{-\delta \alpha_k}) \right)$$

on each of the intervals $[0, \pi/2 - \varepsilon]$ and $[\pi/2 + \varepsilon, \pi]$ ($\varepsilon > 0$ being arbitrarily small), $\delta = \delta(\varepsilon) \in (0, \pi/2)$ denoting some appropriate constant. Applying the intermediate values theorem, we conclude that the function ψ_k' vanishes between any pair of successive extrema of the function $\sin(\alpha_k x + \frac{\pi}{4})$ on each of the above intervals. The density of $\mathcal{S}$ follows at once. ■

4. Energy decay rates

In this section we provide explicit energy decay rates in function of the length ξ of the sensor/actuator.

4.1. **Exponential decay rate.**

An exponential decay rate is first derived when ξ/π is rational with

$$\frac{\xi}{\pi} \neq \frac{4k'+3}{4k+2}, \qquad \forall k, k' \in \mathbb{Z}. \tag{4.1}$$

Theorem 4.1. *Let $\xi \notin \mathcal{S}$ be such that $\xi/\pi \in \mathbb{Q}$ and (4.1) holds true. Then*

$$\sup_{|\beta|\geq 1} ||(i\beta - \mathcal{A})^{-1}|| < \infty. \tag{4.2}$$

It follows that the semigroup $(e^{t\mathcal{A}})_{t\geq 0}$ is exponentially stable*; i.e., there exist two constants $C > 0$ and $\delta > 0$ such that*

$$||e^{t\mathcal{A}} z_0||_{\mathcal{H}} \leq Ce^{-\delta t}||z_0||_{\mathcal{H}}$$

for any $z_0 = (w_0, v_0) \in \mathcal{H}$ and any $t \geq 0$.

Proof of Theorem 4.1. The exponential stability of the semigroup $(e^{t\mathcal{A}})_{t\geq 0}$ is in fact equivalent to the resolvent estimate (4.2) by virtue of a well-known result due to Huang and Prüss (see [12],[21]). Therefore, we shall focus on the proof of (4.2). As the usefulness of the condition (4.1) will appear quite far in the proof, we assume at the beginning of the proof that ξ is any number in $(0, \pi]$. Let us argue by contradiction. If (4.2) is false, then there exist $\beta_n \in \mathbb{R}$, $(w_n, v_n) \in \mathcal{D}(\mathcal{A})$ for $n = 1, 2, ...$ such that

$$||(w_n, v_n)||_{\mathcal{H}} = 1, \quad |\beta_n| \to +\infty \tag{4.3}$$

and if we set $(f_n, g_n) := (i\beta_n - \mathcal{A})(w_n, v_n)$,

$$(f_n, g_n) \to (0, 0) \quad \text{ in } \mathcal{H}, \tag{4.4}$$

i.e.

$$i\beta_n w_n - v_n = f_n \to 0 \quad \text{ in } V, \tag{4.5}$$

$$i\beta_n v_n + \{w_n^{(4)}\} = g_n \to 0 \quad \text{ in } H. \tag{4.6}$$

Replacing if necessary β_n, w_n and v_n by $-\beta_n$, $\overline{w}_n$ and $\overline{v}_n$, respectively, we may assume that $\beta_n > 0$ for all n. Our goal is to obtain a contradiction to (4.3). This will be done in four steps. In the first step, using the multiplier method we establish some estimates which show that we are done if $\beta_n w_n(\pi) \to 0$ as $n \to +\infty$. In the second step, we show that the couple $(w_n(\pi), w_n'(\pi))$ may be obtained as the solution of a 2×2 linear system by performing a direct integration of (4.5)-(4.6). In the two remaining steps we estimate the determinants involved in the resolution of that linear system. In what follows, the letters $C, C', C'', ...$ will denote positive constants which may vary from line to line.

Step 1. Basic Estimates by the Multiplier Method.
We infer from (2.3) that

$$K|v_n'(\xi)|^2 = \text{Re } ((i\beta_n - \mathcal{A})(w_n, v_n), (w_n, v_n))_{\mathcal{H}} = \text{Re } ((f_n, g_n), (w_n, v_n))_{\mathcal{H}}, \tag{4.7}$$

hence, using (4.3) and (4.4),

$$|v_n'(\xi)|^2 \to 0 \quad \text{ as } n \to +\infty. \tag{4.8}$$

On the other hand, (4.5) and (4.6) give as $n \to \infty$

$$i\beta_n ||w_n||_V^2 - (v_n, w_n)_V \to 0, \tag{4.9}$$

$$i\beta_n ||v_n||_H^2 + (\{w_n^{(4)}\}, v_n)_H \to 0. \tag{4.10}$$

Taking the difference of (4.9) and (4.10) we obtain

$$i\beta_n(||w_n||_V^2 - ||v_n||_H^2) - \int_0^\pi v_n''\overline{w_n''}\,dx - \int_0^\pi \{w_n^{(4)}\}\overline{v_n}\,dx \to 0.$$

But

$$\mathrm{Im}\left(\int_0^\pi v_n''\overline{w_n''}\,dx + \int_0^\pi \{w_n^{(4)}\}\overline{v_n}\,dx\right) = 0$$

by (2.3), hence

$$\beta_n(||w_n||_V^2 - ||v_n||_H^2) \to 0. \tag{4.11}$$

Therefore, using (4.3) and (4.5) we conclude that

$$\lim_{n\to+\infty} ||w_n||_V^2 = \lim_{n\to+\infty} ||v_n||_H^2 = \lim_{n\to+\infty} ||\beta_n w_n||_H^2 = \frac{1}{2}\cdot \tag{4.12}$$

Eliminating v_n in (4.6) by using (4.5), we obtain

$$-\beta_n^2 w_n + \{w_n^{(4)}\} = g_n + i\beta_n f_n, \tag{4.13}$$

hence

$$(-\beta_n^2 w_n + \{w_n^{(4)}\}, qw_n')_H = (g_n + i\beta_n f_n, qw_n')_H \tag{4.14}$$

for any real function $q \in C^3([0,\pi])$.

It follows from (4.12) and a classical interpolation inequality (see e.g. [17]) that for any $s \in [0,2)$

$$w_n \to 0 \quad \text{in } H^s(0,\pi). \tag{4.15}$$

In particular,

$$(g_n, qw_n')_H \to 0. \tag{4.16}$$

On the other hand,

$$\int_0^\pi f_n q\overline{w_n'}\,dx = -\int_0^\pi (f_n q)'\overline{w_n}\,dx + f_n(\pi)q(\pi)\overline{w_n(\pi)}. \tag{4.17}$$

But, using (4.5) and (4.12), we obtain

$$\beta_n \left|\int_0^\pi (f_n q)'\overline{w_n}\,dx\right| \le C||f_n||_{H^1(0,\pi)}||\beta_n w_n||_H \to 0, \tag{4.18}$$

and

$$\beta_n f_n(\pi)q(\pi)\overline{w_n(\pi)} = o(\beta_n w_n(\pi)). \tag{4.19}$$

It follows that

$$(i\beta_n f_n, qw_n')_H = o(\beta_n w_n(\pi)) + o(1). \tag{4.20}$$

Let us now turn to the left hand side of (4.14). We have

$$2\mathrm{Re}\ (-\beta_n^2 w_n, qw_n')_H = \beta_n^2 \int_0^\pi q'|w_n|^2\,dx - \beta_n^2|w_n(\pi)|^2 q(\pi). \tag{4.21}$$

Integrating by parts in

$$(\{w_n^{(4)}\}, qw_n')_H = \int_0^\xi w_n^{(4)} q\overline{w_n'}\,dx + \int_\xi^\pi w_n^{(4)} q\overline{w_n'}\,dx,$$

we arrive to

$$\begin{aligned} 2\mathrm{Re}\ (\{w_n^{(4)}\}, qw_n')_H &= 3\int_0^\pi |w_n''|^2 q'dx + |w_n''(0)|^2 q(0) - \int_0^\pi |w_n'|^2 q'''\,dx \\ &\quad + q(\xi)\left[\,|w_n''|^2\right]_\xi + 2\mathrm{Re}(q'(\xi)\overline{w_n'(\xi)}\left[w_n''\right]_\xi) + |w_n'(\pi)|^2 q''(\pi) \\ &= 3\int_0^\pi |w_n''|^2 q'\,dx + 2Kq(\xi)\mathrm{Re}\big(v_n'(\xi)\overline{w_n''(\xi^+)}\big) + o(1) \end{aligned} \tag{4.22}$$

by (4.15) and (4.8), provided that $q(0) = 0$. Gathering together (4.16), (4.20), (4.21) and (4.22) with $q(x) = x$, we obtain

(4.23)

$$3\int_0^\pi |w_n''|^2\,dx + \beta_n^2\int_0^\pi |w_n|^2\,dx = (\pi\beta_n\overline{w_n(\pi)} + o(1))\beta_n w_n(\pi) - 2K\xi\mathrm{Re}\big(v_n'(\xi)\overline{w_n''(\xi^+)}\big) + o(1).$$

The above equality may be simplified thanks to the next result.

Proposition 4.2.

$$|w_n''(\xi^+)|^2 = O(|\beta_n w_n(\pi)|^2) + o(1). \tag{4.24}$$

Proof. Multiplying each term in (4.13) by $q\overline{w_n'}$ where $q \in C^3([\xi,\pi])$, and integrating over (ξ,π), we arrive to

$$-\beta_n^2\int_\xi^\pi qw_n\overline{w_n'}\,dx + \int_\xi^\pi qw_n^{(4)}\overline{w_n'}\,dx = \int_\xi^\pi (g_n + i\beta_n f_n)q\overline{w_n'}\,dx.$$

Clearly

$$\left|\int_\xi^\pi g_n q\overline{w_n'}\,dx\right| \le C||g_n||_H||w_n'||_H \to 0$$

and

$$\int_\xi^\pi i\beta_n f_n q\overline{w_n'}\,dx = -i\int_\xi^\pi (f_n q)'\beta_n\overline{w_n}\,dx + \left[if_n q\beta_n\overline{w_n}\right]_\xi^\pi,$$

so using again (4.5) and (4.12),

$$\left|\int_\xi^\pi (g_n + i\beta_n f_n)q\overline{w_n'}\,dx\right| \le \frac{\xi}{4}\left(|\beta_n w_n(\xi)|^2 + |\beta_n w_n(\pi)|^2\right) + o(1).$$

On the other hand, we obtain after some integrations by parts that

$$2\mathrm{Re}\int_\xi^\pi (-\beta_n^2)qw_n\overline{w_n'}dx = \beta_n^2\left\{\int_\xi^\pi q'|w_n|^2\,dx - \left[q|w_n|^2\right]_\xi^\pi\right\}$$

and that

$$\begin{aligned} 2\mathrm{Re}\int_\xi^\pi w_n^{(4)}q\overline{w_n'}\,dx &= 3\int_\xi^\pi q'|w_n''|^2\,dx - \left[|w_n''|^2 q\right]_\xi^\pi - \int_\xi^\pi q'''|w_n'|^2\,dx + \left[q''|w_n'|^2\right]_\xi^\pi \\ &\quad -2\mathrm{Re}\left[w_n''q'\overline{w_n'}\right]_\xi^\pi + 2\mathrm{Re}\left[w_n'''q\overline{w_n'}\right]_\xi^\pi. \end{aligned}$$

Taking $q(x) = x$ and using the fact that $w_n''(\pi) = w_n'''(\pi) = 0$, we arrive to

$$\begin{aligned} &3\int_\xi^\pi |w_n''|^2\,dx + \beta_n^2\int_\xi^\pi |w_n|^2\,dx + \xi(|w_n''(\xi^+)|^2 + \frac{1}{2}|\beta_n w_n(\xi)|^2) \\ &\quad +2\mathrm{Re}\left((w_n''(\xi^+) - \xi w_n'''(\xi))\overline{w_n'(\xi)}\right) = O(|\beta_n w_n(\pi)|^2) + o(1). \end{aligned} \tag{4.25}$$

The following claims are needed.

Claim 2. $\beta_n w_n'(\xi) \to 0$ as $n \to \infty$.
Indeed, derivating once in (4.5) and evaluating at $x = \xi$, we infer that $i\beta_n w_n'(\xi) = v_n'(\xi) + f_n'(\xi) \to 0$, by (4.4) and (4.8). ■

Claim 3. $||w_n||_{H^4(\xi,\pi)} \leq C\beta_n$.
Indeed, it follows from (4.6) and (4.12) that

$$||\beta_n^{-1} w_n^{(4)}||_{L^2(\xi,\pi)} \leq \beta_n^{-1}||g_n||_{L^2(\xi,\pi)} + ||v_n||_{L^2(\xi,\pi)} \leq C.$$

Since $||w_n||_V$ is bounded, the claim follows. ■
We infer from Claim 3 that $|w_n''(\xi^+)| + |w_n'''(\xi)| \leq C\beta_n$ which, combined to Claim 2, yields

$$\mathrm{Re}\big((w_n''(\xi^+) - \xi w_n'''(\xi))\overline{w_n'(\xi)}\big) \to 0 \text{ as } n \to \infty.$$

Therefore, (4.25) yields

$$3\int_\xi^\pi |w_n''|^2\,dx + \beta_n^2 \int_\xi^\pi |w_n|^2\,dx + \xi\left(|w_n''(\xi^+)|^2 + \frac{1}{2}|\beta_n w_n(\xi)|^2\right) = O(|\beta_n w_n(\xi)|^2) + o(1),$$

hence (4.24) follows. The proof of Proposition 4.2 is complete. ■

Using (4.8), (4.23) and (4.24), we arrive to

$$3\int_0^\pi |w_n''|^2\,dx + \beta_n^2 \int_0^\pi |w_n|^2\,dx = O(|\beta_n w_n(\pi)|^2) + o(1). \tag{4.26}$$

Therefore, we obtain a contradiction with (4.12) if $\beta_n w_n(\pi) \to 0$. In the next steps, we show that $\beta_n w_n(\pi) \to 0$.

Step 2. Computation of $w_n(\pi)$.
To compute $w_n(\pi)$ we integrate (4.13) on $(0,\pi)$. More precisely, setting $F_n := g_n + i\beta_n f_n$, we solve the system

$$\begin{cases} -\beta_n^2 w_n + \{w_n^{(4)}\} = F_n \qquad \text{on } (0,\pi), \\ w_n(0) = w_n'(0) = w_n''(\pi) = w_n'''(\pi) = 0, \\ [w_n]_\xi = [w_n']_\xi = [w_n''']_\xi = 0, \\ [w_n'']_\xi = K v_n'(\xi) = K(i\beta_n w_n'(\xi) - f_n'(\xi)). \end{cases}$$

To simplify the notations we drop the subscript n in what follows. Let λ and μ be given numbers. We first solve the following (backwards) Cauchy Problem on (ξ,π)

$$(S_1) \quad \begin{cases} w^{(4)} - \beta^2 w = F \quad \text{in } (\xi,\pi), \\ w(\pi) = \lambda,\ w'(\pi) = \mu,\ w''(\pi) = w'''(\pi) = 0, \end{cases}$$

and next the following (backwards) Cauchy Problem on $(0,\xi)$

$$(S_2) \quad \begin{cases} w^{(4)} - \beta^2 w = F \quad \text{in } (0,\xi), \\ w(\xi^-) = w(\xi^+),\ w'(\xi^-) = w'(\xi^+),\ w'''(\xi^-) = w'''(\xi^+), \\ w''(\xi^-) = w''(\xi^+) - K\left(i\beta w'(\xi^+) - f'(\xi)\right). \end{cases}$$

Then λ and μ have to be chosen so that $w(0) = w'(0) = 0$.

The ODE $w^{(4)} - \beta^2 w = F$ may be written as

$$\begin{pmatrix} w \\ w' \\ w'' \\ w''' \end{pmatrix}' = M \begin{pmatrix} w \\ w' \\ w'' \\ w''' \end{pmatrix} + \begin{pmatrix} 0 \\ 0 \\ 0 \\ F \end{pmatrix}, \text{ with } \quad M = \begin{pmatrix} 0 & 1 & 0 & 0 \\ 0 & 0 & 1 & 0 \\ 0 & 0 & 0 & 1 \\ \beta^2 & 0 & 0 & 0 \end{pmatrix}.$$

Easy computations show that

$$e^{xM} = \begin{pmatrix} a & \beta^{-2}a''' & \beta^{-2}a'' & \beta^{-2}a' \\ a' & a & \beta^{-2}a''' & \beta^{-2}a'' \\ a'' & a' & a & \beta^{-2}a''' \\ a''' & a'' & a' & a \end{pmatrix}, \tag{4.27}$$

where $a(x) := \frac{1}{2}(\cos(bx) + \cosh(bx))$ and $b = \sqrt{\beta}$. An integration of (S_1) yields

$$\begin{pmatrix} w \\ w' \\ w'' \\ w''' \end{pmatrix}(x) = e^{(x-\pi)M} \begin{pmatrix} \lambda \\ \mu \\ 0 \\ 0 \end{pmatrix} + \int_\pi^x e^{(x-y)M} \begin{pmatrix} 0 \\ 0 \\ 0 \\ F(y) \end{pmatrix} dy, \quad x \in (\xi, \pi),$$

hence

$$\begin{pmatrix} w \\ w' \\ w'' \\ w''' \end{pmatrix}(\xi^+) = e^{(\xi-\pi)M} \begin{pmatrix} \lambda \\ \mu \\ 0 \\ 0 \end{pmatrix} + \int_\pi^\xi e^{(\xi-y)M} \begin{pmatrix} 0 \\ 0 \\ 0 \\ F(y) \end{pmatrix} dy. \tag{4.28}$$

On the other hand, an integration of (S_2) leads to

$$\begin{pmatrix} w \\ w' \\ w'' \\ w''' \end{pmatrix}(x) = e^{(x-\xi)M} \begin{pmatrix} w \\ w' \\ w'' \\ w''' \end{pmatrix}(\xi^-) + \int_\xi^x e^{(x-y)M} \begin{pmatrix} 0 \\ 0 \\ 0 \\ F(y) \end{pmatrix} dy. \tag{4.29}$$

Gathering (4.28) and (4.29), we obtain

$$\begin{aligned} \begin{pmatrix} w \\ w' \\ w'' \\ w''' \end{pmatrix}(0) &= e^{-\xi M}\Big(\begin{pmatrix} w \\ w' \\ w'' \\ w''' \end{pmatrix}(\xi^+) + \begin{pmatrix} 0 \\ 0 \\ -[w'']_\xi \\ 0 \end{pmatrix}\Big) + \int_\xi^0 e^{-yM} \begin{pmatrix} 0 \\ 0 \\ 0 \\ F(y) \end{pmatrix} dy \\ &= e^{-\pi M} \begin{pmatrix} \lambda \\ \mu \\ 0 \\ 0 \end{pmatrix} + \int_\pi^0 e^{-yM} \begin{pmatrix} 0 \\ 0 \\ 0 \\ F(y) \end{pmatrix} dy + e^{-\xi M} \begin{pmatrix} 0 \\ 0 \\ -K\big(i\beta w'(\xi^+) - f'(\xi)\big) \\ 0 \end{pmatrix} \end{aligned} \tag{4.30}$$

By (4.27) and (4.28),

$$w'(\xi^+) = a'(\xi-\pi)\lambda + a(\xi-\pi)\mu + \int_\pi^\xi \beta^{-2}a''(\xi-y)F(y)\,dy,$$

hence, keeping only the two first equations in (4.30), we arrive to

$$\begin{aligned} \begin{pmatrix} w(0) \\ w'(0) \end{pmatrix} &= \begin{pmatrix} a(-\pi) & \beta^{-2}a'''(-\pi) \\ a'(-\pi) & a(-\pi) \end{pmatrix} \begin{pmatrix} \lambda \\ \mu \end{pmatrix} + \int_\pi^0 \begin{pmatrix} \beta^{-2}a'(-y) \\ \beta^{-2}a''(-y) \end{pmatrix} F(y)\,dy + \begin{pmatrix} \beta^{-2}a''(-\xi) \\ \beta^{-2}a'''(-\xi) \end{pmatrix} \\ &\quad \times \left(Kf'(\xi) - iK\beta\big(a'(\xi-\pi)\lambda + a(\xi-\pi)\mu + \int_\pi^\xi \beta^{-2}a''(\xi-y)F(y)\,dy\big)\right). \end{aligned}$$

Therefore, $w(0) = w'(0) = 0$ if and only if

$$\begin{pmatrix} m_{11} & m_{12} \\ m_{21} & m_{22} \end{pmatrix} \begin{pmatrix} \lambda \\ \mu \end{pmatrix} = \begin{pmatrix} c_1 \\ c_2 \end{pmatrix},$$

where

$$\begin{aligned}
m_{11} &= a(-\pi) - iK\beta^{-1}a''(-\xi)a'(\xi-\pi)\\
m_{12} &= \beta^{-2}a'''(-\pi) - iK\beta^{-1}a''(-\xi)a(\xi-\pi)\\
m_{21} &= a'(-\pi) - iK\beta^{-1}a'''(-\xi)a'(\xi-\pi)\\
m_{22} &= a(-\pi) - iK\beta^{-1}a'''(-\xi)a(\xi-\pi)\\
c_1 &= -\int_\pi^0 \beta^{-2}a'(-y)F(y)\,dy + K\beta^{-2}a''(-\xi)\left(-f'(\xi) + i\beta\int_\pi^\xi \beta^{-2}a''(\xi-y)F(y)\,dy\right)\\
c_2 &= -\int_\pi^0 \beta^{-2}a''(-y)F(y)\,dy + K\beta^{-2}a'''(-\xi)\left(-f'(\xi) + i\beta\int_\pi^\xi \beta^{-2}a''(\xi-y)F(y)\,dy\right).
\end{aligned}$$

Letting

$$\begin{aligned}
N &= c_1m_{22} - c_2m_{12}\\
D &= m_{11}m_{22} - m_{12}m_{21}
\end{aligned}$$

we obtain by Cramer rule $\lambda = N/D$. In the next step we show that $|D| \geq Ce^{b\pi}$ if the number ξ/π is rational and fulfills (4.1).

Step 3. Estimation of D.
Substituting the expressions of m_{11}, m_{12}, m_{21} and m_{22} into D we obtain

$$\begin{aligned}
D &= (a(-\pi) - iK\beta^{-1}a''(-\xi)a'(\xi-\pi))(a(-\pi) - iK\beta^{-1}a'''(-\xi)a(\xi-\pi))\\
&\quad -(\beta^{-2}a'''(-\pi) - iK\beta^{-1}a''(-\xi)a(\xi-\pi))(a'(-\pi) - iK\beta^{-1}a'''(-\xi)a'(\xi-\pi))\\
&= a(-\pi)^2 - \beta^{-2}a'''(-\pi)a'(-\pi) - iK\beta^{-1}\left\{a''(-\xi)a'(\xi-\pi)a(-\pi) + a(-\pi)a'''(-\xi)a(\xi-\pi)\right.\\
&\quad \left. -a''(-\xi)a(\xi-\pi)a'(-\pi) - \beta^{-2}a'''(-\pi)a'''(-\xi)a'(\xi-\pi)\right\}\\
&=: D_1 + iD_2.
\end{aligned}$$

Substituting the values of a and of its derivatives in D_1 we obtain

$$\begin{aligned}
D_1 &= \left(\frac{1}{2}(\cos b\pi + \cosh b\pi)\right)^2 - \beta^{-2}\frac{b^3}{2}(-\sin b\pi - \sinh b\pi)\frac{b}{2}(\sin b\pi - \sinh b\pi)\\
&= \frac{1}{4}\left(\cos^2 b\pi + \cosh^2 b\pi + 2\cos b\pi\cosh b\pi + \sin^2 b\pi - \sinh^2 b\pi\right)\\
&= \frac{1}{2}(1 + \cos b\pi\cosh b\pi). \qquad (4.31)
\end{aligned}$$

Let us now turn to the estimation of D_2.

$$\begin{aligned}
D_2 &= -K\beta^{-1}\left\{a'(\xi-\pi)\left(a''(-\xi)a(-\pi) - \beta^{-2}a'''(-\pi)a'''(-\xi)\right)\right.\\
&\quad \left. +a(\xi-\pi)\left(a(-\pi)a'''(-\xi) - a''(-\xi)a'(-\pi)\right)\right\}.
\end{aligned}$$

To estimate D_2 we introduce the functions $G, H : [0,\pi] \to \mathbb{R}$ defined by

$$\begin{aligned}
G(y) &= a''(-\xi)a(-y) - \beta^{-2}a'''(-y)a'''(-\xi)\\
H(y) &= a(-y)a'''(-\xi) - a''(-\xi)a'(-y).
\end{aligned}$$

Then the following result holds.

Lemma 4.3.

$$\begin{aligned}
G(y) &= \frac{b^2}{4}\left(\cosh b(y-\xi) + \frac{e^{b\xi}}{2}(\cos by - \sin by) - \frac{e^{by}}{2}(\cos b\xi + \sin b\xi) + O(1)\right), \qquad (4.32)\\
H(y) &= \frac{b^3}{4}\left(\sinh b(y-\xi) - \frac{e^{b\xi}}{2}(\cos by + \sin by) - \frac{e^{by}}{2}(\cos b\xi + \sin b\xi) + O(b)\right), \qquad (4.33)
\end{aligned}$$

where $O(1)$ denotes a term which is bounded in y, ξ, and b.

Proof of Lemma 4.3. Expanding a in the expression of G, we obtain

$$\begin{aligned} G(y) &= \frac{b^2}{4}\left\{(-\cos b\xi+\cosh b\xi)(\cos by+\cosh by)-(\sin by+\sinh by)(\sin b\xi+\sinh b\xi)\right\} \\ &= \frac{b^2}{4}\left\{\cosh by\cosh b\xi-\sinh by\sinh b\xi+\frac{1}{2}(e^{b\xi}+e^{-b\xi})\cos by-\frac{1}{2}(e^{by}+e^{-by})\cos b\xi\right. \\ &\qquad \left.-\frac{1}{2}(e^{by}-e^{-by})\sin b\xi-\frac{1}{2}(e^{b\xi}-e^{-b\xi})\sin by-\cos b\xi\cos by-\sin by\sin b\xi\right\} \\ &= \frac{b^2}{4}\left\{\cosh b(y-\xi)+\frac{e^{b\xi}}{2}(\cos by-\sin by)-\frac{e^{by}}{2}(\cos b\xi+\sin b\xi)+O(1)\right\}. \end{aligned}$$

Thus (4.32) is proved. (4.33) may be obtained by noticing that $H(y)=G'(y)$. ∎

Applying Lemma 4.3 with $y=\pi$, we obtain

$$\begin{aligned} D_2 &= -K\beta^{-1}\left(a'(\xi-\pi)G(\pi)+a(\xi-\pi)H(\pi)\right) \\ &= -K\beta^{-1}\left\{\frac{b}{2}\left(-\sin b(\xi-\pi)+\frac{e^{b(\xi-\pi)}-e^{b(\pi-\xi)}}{2}\right)\right. \\ &\qquad \times\frac{b^2}{4}\left(\frac{e^{b(\pi-\xi)}}{2}+\frac{e^{b\xi}}{2}(\cos b\pi-\sin b\pi)-\frac{e^{b\pi}}{2}(\cos b\xi+\sin b\xi)+O(1)\right) \\ &\qquad +\frac{1}{2}\left(\cos b(\xi-\pi)+\frac{e^{b(\xi-\pi)}+e^{b(\pi-\xi)}}{2}\right) \\ &\qquad \left.\times\frac{b^3}{4}\left(\frac{e^{b(\pi-\xi)}}{2}-\frac{e^{b\xi}}{2}(\cos b\pi+\sin b\pi)-\frac{e^{b\pi}}{2}(\cos b\xi+\sin b\xi)+O(1)\right)\right\}. \end{aligned}$$

Expanding D_2, we notice that the coefficients in front of the exponential terms $e^{b(2\pi-\xi)}$ and $e^{2b(\pi-\xi)}$ vanish, so that the leading exponential term is $e^{b\pi}$, and the remaining exponential terms read $e^{b(\pi-\xi)}$, $e^{b(2\xi-\pi)}$, $e^{b\xi}$, e^0, and $e^{b(\xi-\pi)}$. We conclude that if $\xi<\pi$, then

$$D_2=\frac{Kb}{16}\left(\cos b\pi+(\cos b\xi+\sin b\xi)(\cos b(\xi-\pi)-\sin b(\xi-\pi))\right)e^{b\pi}+O(e^{b(\pi-\delta)}) \tag{4.34}$$

for some $\delta>0$, and if $\xi=\pi$, then

$$D_2=\frac{Kb}{4}\Big((\cos b\pi+\sin b\pi)e^{b\pi}+O(b)\Big). \tag{4.35}$$

It is clear that $|D_1+iD_2|\geq Ce^{b\pi}$ for b large enough if $\xi=\pi$, for $(\cos b\pi)^2+(\cos b\pi+\sin b\pi)^2\geq C>0$ for all $b\in\mathbb{R}$.

Let us assume from now on that $\xi<\pi$, and that the number ξ/π is rational and admits a coprime factorization $\xi/\pi=p/q$, with $p,q\in\mathbb{N}^*$, $0<p<q$, and let us introduce the functions

$$c(b) := \cos b\pi+(\cos b\xi+\sin b\xi)(\cos b(\xi-\pi)-\sin b(\xi-\pi)), \tag{4.36}$$

$$h(b) := (\cos b\pi)^2+(c(b))^2. \tag{4.37}$$

Lemma 4.4. *$\inf_{b\in\mathbb{R}}|h(b)|>0$ if and only if p/q is not of the form $(4k'+3)/(4k+2)$, $k,k'\in\mathbb{Z}$.*

Proof. Since h is $2q-$periodic, we only have to characterize the rational numbers p/q for which $h(b) > 0$ for all $b \in \mathbb{R}$. As h is the sum of two squared terms, we may restrict to the b's for which $\cos b\pi = 0$, namely $b = (1/2) + k$, $k \in \mathbb{Z}$. Then $h(b) = 4\cos^2((\frac{1}{2}+k)\xi - \frac{\pi}{4})\cos^2((\frac{1}{2}+k)(\xi-\pi)+\frac{\pi}{4})$, and a straightforward calculation shows that $h(b) = 0$ if and only if p/q is of the form $\frac{4k'+3}{4k+2}$, $k, k' \in \mathbb{Z}$. ∎
Applying Lemma 4.4, we infer that as $b \to +\infty$

$$\begin{aligned} |D|^2 &= D_1^2 + D_2^2 \\ &\geq Ch(b)e^{2b\pi} + O(e^{b(2\pi-\delta)}) \\ &\geq C'e^{2b\pi} \end{aligned}$$

provided that the condition (4.1) is fulfilled.

Step 4. Estimation of N.
We have to bound the quantity $N = c_1 m_{22} - c_2 m_{12}$. Letting

$$\begin{aligned} Z_1 &:= -\int_\pi^0 \beta^{-2} a'(-y)F(y)\,dy \\ Z_2 &:= -\int_\pi^0 \beta^{-2} a''(-y)F(y)\,dy \\ \text{and} \quad Z_3 &:= i\beta^{-1}\int_\pi^\xi a''(\xi-y)F(y)\,dy - f'(\xi), \end{aligned}$$

we obtain that

$$c_1 = Z_1 + K\beta^{-2}a''(-\xi)Z_3, \quad c_2 = Z_2 + K\beta^{-2}a'''(-\xi)Z_3,$$

hence

$$\begin{aligned} N &= (Z_1 + K\beta^{-2}a''(-\xi)Z_3)(a(-\pi) - iK\beta^{-1}a'''(-\xi)a(\xi-\pi)) \\ &\quad -(Z_2 + K\beta^{-2}a'''(-\xi)Z_3)(\beta^{-2}a'''(-\pi) - iK\beta^{-1}a''(-\xi)a(\xi-\pi)) \\ &= K\beta^{-2}\left(a''(-\xi)a(-\pi) - \beta^{-2}a'''(-\xi)a'''(-\pi)\right)Z_3 + Z_1\left(a(-\pi) - iK\beta^{-1}a'''(-\xi)a(\xi-\pi)\right) \\ &\quad -Z_2\left(\beta^{-2}a'''(-\pi) - iK\beta^{-1}a''(-\xi)a(\xi-\pi)\right) \\ &= -K\beta^{-2}G(\pi)f'(\xi) + iK\beta^{-3}G(\pi)\int_\pi^\xi a''(\xi-y)F(y)\,dy \\ &\quad -\beta^{-2}\int_\pi^0 \left\{a'(-y)(a(-\pi) - iK\beta^{-1}a'''(-\xi)a(\xi-\pi)) \right. \\ &\quad \left. -a''(-y)(\beta^{-2}a'''(-\pi) - iK\beta^{-1}a''(-\xi)a(\xi-\pi))\right\}F(y)\,dy \\ &= -K\beta^{-2}G(\pi)f'(\xi) - \beta^{-2}\int_\pi^0 (a'(-y)a(-\pi) - a''(-y)\beta^{-2}a'''(-\pi))F(y)\,dy \\ &\quad +iK\beta^{-3}\int_\xi^0 (a'(-y)a'''(-\xi) - a''(-y)a''(-\xi))a(\xi-\pi)F(y)\,dy \\ &\quad \left. +iK\beta^{-3}\int_\pi^\xi \left\{G(\pi)a''(\xi-y) + \left(a'(-y)a'''(-\xi) - a''(-y)a''(-\xi)\right)a(\xi-\pi)\right\}F(y)\,dy.\right\} \\ &=: I_1 + I_2 + I_3 + I_4. \end{aligned}$$

By virtue of Lemma 4.3,

$$\begin{aligned} |G(\pi)| &= \frac{b^2}{4}\left|\cosh b(\pi-\xi)+\frac{e^{b\xi}}{2}(\cos b\pi-\sin b\pi)-\frac{e^{b\pi}}{2}(\cos b\xi+\sin b\xi)+O(1)\right| \\ &\le Cb^2e^{b\pi}, \end{aligned}$$

hence

$$|I_1|\le Cb^{-2}e^{b\pi}||f||_V.$$

Let $K(y):=a'(-y)a(-\pi)-a''(-y)\beta^{-2}a'''(-\pi)$ for $y\in[0,\pi]$. Then

$$I_2=\beta^{-2}\int_0^\pi K(y)g(y)\,dy+i\beta^{-1}\int_0^\pi K(y)f(y)\,dy=:I_2^1+I_2^2.$$

Since

$$\begin{aligned} K(y) &= \frac{b}{4}\left\{(\sin by-\sinh by)(\cos b\pi+\cosh b\pi)-(-\cos by+\cosh by)(-\sin b\pi-\sinh b\pi)\right\} \\ &= \frac{b}{4}\left\{\cosh by\sinh b\pi-\sinh by\cosh b\pi-\frac{e^{by}-e^{-by}}{2}\cos b\pi+\frac{e^{b\pi}+e^{-b\pi}}{2}\sin by\right. \\ &\qquad \left.-\frac{e^{b\pi}-e^{-b\pi}}{2}\cos by+\frac{e^{by}+e^{-by}}{2}\sin b\pi+\sin by\cos b\pi-\cos by\sin b\pi\right\} \\ &= \frac{b}{4}\left\{\sinh b(\pi-y)+\frac{e^{b\pi}}{2}(\sin by-\cos by)+\frac{e^{by}}{2}(-\cos b\pi+\sin b\pi)+O(1)\right\} \end{aligned}$$

we see that

$$\begin{aligned} |I_2^1| &\le \beta^{-2}||K(y)||_H\,||g||_H \\ &\le Cb^{-3}\left(||\sinh b(\pi-y)||_H+e^{b\pi}||\sin by-\cos by||_H+||e^{by}||_H+O(1)\right)||g||_H \\ &\le Cb^{-3}e^{b\pi}||g||_H. \end{aligned}$$

On the other hand, integrating by parts in I_2^2 yields

$$I_2^2=i\beta^{-1}\left(-\int_0^\pi \tilde K(y)f'(y)\,dy+\left[\tilde K(y)f(y)\right]_0^\pi\right)$$

with

$$\begin{aligned} \tilde K(y) &= \int_0^y K(z)\,dz \\ &= \frac{1}{4}\left\{-\cosh b(\pi-y)-\frac{e^{b\pi}}{2}(\cos by+\sin by)+\frac{e^{by}}{2}(-\cos b\pi+\sin b\pi)+O(1)\right\}. \end{aligned}$$

Thus

$$|I_2^2|\le C\beta^{-1}e^{b\pi}\left(||f'||_H+|f(\pi)|\right)\le C\beta^{-1}e^{b\pi}||f||_V.$$

We now turn to the next term I_3. We notice that

$$\begin{aligned} I_3 &= iK\beta^{-3}a(\xi-\pi)\int_\xi^0(-H'(y))(g(y)+i\beta f(y))\,dy \\ &= iK\beta^{-3}a(\xi-\pi)\int_0^\xi H'(y)g(y)\,dy-K\beta^{-2}a(\xi-\pi)\int_0^\xi H'(y)f(y)\,dy \\ &=: I_3^1+I_3^2. \end{aligned}$$

Since

$$H'(y)=\frac{b^4}{4}\left\{\cosh b(y-\xi)+\frac{e^{b\xi}}{2}(\sin by-\cos by)-\frac{e^{by}}{2}(\cos b\xi+\sin b\xi)+O(b^2)\right\}.$$

we have that

$$\begin{aligned} |I_3^1| &\leq Cb^{-2}e^{b(\pi-\xi)}\Big(||\cosh b(y-\xi)||_{L^2(0,\xi)} + e^{b\xi}||\sin by - \cos by||_{L^2(0,\xi)} \\ &\qquad + ||e^{by}||_{L^2(0,\xi)} + O(b^2)\Big)\,||g||_H \\ &\leq Cb^{-2}e^{b\pi}||g||_H. \end{aligned}$$

Integrating twice by parts in I_3^2 yields

$$I_3^2 = -K\beta^{-2}a(\xi-\pi)\left(\int_0^\xi G(y)f''(y)\,dy + \big[H(y)f(y) - G(y)f'(y)\big]_0^\xi\right)$$

(since $G' = H$). Using (4.32) and the fact that $f(0) = f'(0) = 0$, we obtain that

$$\begin{aligned} |I_3^2 + K\beta^{-2}a(\xi-\pi)H(\xi)f(\xi)| &\leq C\beta^{-2}e^{b(\pi-\xi)}\Big(b^2e^{b\xi}||f''||_H + b^2e^{b\xi}|f'(\xi)|\Big) \\ &\leq C\beta^{-1}e^{b\pi}||f||_V. \end{aligned}$$

Using (4.33) to estimate $H(\xi)$, we conclude that

$$I_3^2 = \frac{K}{16}b^{-1}e^{b\pi}(\cos b\xi + \sin b\xi)f(\xi) + O\big(\beta^{-1}e^{b\pi}||f||_V\big).$$

It remains to bound

$$\begin{aligned} I_4 &= iK\beta^{-3}\int_\pi^\xi L(y)\big(g(y) + i\beta f(y)\big)\,dy \\ &= iK\beta^{-3}\int_\pi^\xi L(y)g(y)\,dy - K\beta^{-2}\int_\pi^\xi L(y)f(y)\,dy \\ &=: I_4^1 + I_4^2 \end{aligned}$$

where we have set

$$L(y) := G(\pi)a''(\xi-y) - H'(y)a(\xi-\pi).$$

We first estimate the function L.

$$\begin{aligned} L(y) &= \frac{b^4}{8}\Big\{\big(\cosh b(\pi-\xi) + \frac{e^{b\xi}}{2}(\cos b\pi - \sin b\pi) - \frac{e^{b\pi}}{2}(\cos b\xi + \sin b\xi) + O(1)\big) \\ &\qquad \times(-\cos b(\xi-y) + \cosh b(\xi-y)) - \big(\cosh b(y-\xi) + \frac{e^{b\xi}}{2}(\sin by - \cos by) \\ &\qquad -\frac{e^{by}}{2}(\cos b\xi + \sin b\xi) + O(b^2)\big)(\cos b(\xi-\pi) + \cosh b(\xi-\pi))\Big\} \\ &= \frac{b^4}{8}\Big\{e^{b\pi}(\frac{1}{2}(\cos b\xi + \sin b\xi)\cos b(\xi-y) + \frac{1}{4}(\cos by - \sin by) \\ &\qquad +e^{by}(\frac{1}{2}(\cos b\xi + \sin b\xi)\cos b(\xi-\pi) + \frac{1}{4}(\cos b\pi - \sin b\pi)) \\ &\qquad +e^{b(\pi+\xi-y)}(-\frac{1}{4})(\cos b\xi + \sin b\xi) + O(e^{b(\pi-\delta)})\Big\} \end{aligned}$$

for every $y \in [\xi,\pi]$ and some $\delta > 0$. Thus

$$\begin{aligned} |I_4^1| &\leq Cb^{-2}||g||_H\Big(e^{b\pi}(||\cos b(\xi-y)||_{L^2(\xi,\pi)} + ||\cos by - \sin by||_{L^2(\xi,\pi)}) \\ &\qquad + ||e^{by}||_{L^2(\xi,\pi)} + ||e^{b(\pi+\xi-y)}||_{L^2(\xi,\pi)} + O(e^{b(\pi-\delta)})\Big) \\ &\leq Cb^{-2}e^{b\pi}||g||_H. \end{aligned}$$

Next we introduce the function $\tilde{L}(y) := G(\pi)a(\xi - y) - G(y)a(\xi - \pi)$ which fulfills $\tilde{L}'' = L$. Easy calculations show that

$$\begin{aligned}\tilde{L}(y) &= \frac{b^2}{8}\Big\{-e^{b\pi}(\frac{1}{2}(\cos b\xi + \sin b\xi)\cos b(\xi - y) + \frac{1}{4}(\cos by - \sin by)\\ &\quad +e^{by}(\frac{1}{2}(\cos b\xi + \sin b\xi)\cos b(\xi - \pi) + \frac{1}{4}(\cos b\pi - \sin b\pi))\\ &\quad +e^{b(\pi+\xi-y)}(-\frac{1}{4})(\cos b\xi + \sin b\xi) + O(e^{b(\pi-\delta)})\Big\}\end{aligned}$$

and that

$$\begin{aligned}\tilde{L}'(y) &= \frac{b^3}{8}\Big\{e^{b\pi}(\frac{1}{2}(\cos b\xi + \sin b\xi)\sin b(y - \xi) + \frac{1}{4}(\cos by + \sin by)\\ &\quad +e^{by}(\frac{1}{2}(\cos b\xi + \sin b\xi)\cos b(\xi - \pi) + \frac{1}{4}(\cos b\pi - \sin b\pi))\\ &\quad -e^{b(\pi+\xi-y)}(-\frac{1}{4})(\cos b\xi + \sin b\xi) + O(e^{b(\pi-\delta)})\Big\},\end{aligned}$$

hence for all $y \in [\xi, \pi]$

$$|\tilde{L}(y)| \le Cb^2e^{b\pi} \text{ and } |\tilde{L}'(y)| \le Cb^3e^{b\pi}.$$

Integrating twice by parts in I_4^2, we obtain

$$I_4^2 = K\beta^{-2}\left(\int_\xi^\pi \tilde{L}(y)f''(y)\,dy + \Big[\tilde{L}'(y)f(y) - \tilde{L}(y)f'(y)\Big]_\xi^\pi\right),$$

hence

$$\begin{aligned}\left|I_4^2 - K\beta^{-2}\Big[\tilde{L}'(y)f(y)\Big]_\xi^\pi\right| &\le C\beta^{-2}\left(b^2e^{b\pi}||f''||_H + b^2e^{b\pi}(|f'(\pi)| + |f'(\xi)|)\right)\\ &\le C\beta^{-1}e^{b\pi}||f||_V.\end{aligned}$$

On the other hand

$$K\beta^{-2}\Big[\tilde{L}'(y)f(y)\Big]_\xi^\pi = \frac{K}{16}b^{-1}e^{b\pi}\Big\{-(\cos b\xi + \sin b\xi)f(\xi) + c(b)f(\pi) + O(e^{-b\delta})||f||_V\Big\},$$

where the function $c(b)$ is defined in (4.36) and $\delta > 0$ is small enough. It follows that

$$I_3^2 + I_4^2 = \frac{K}{16}b^{-1}e^{b\pi}c(b)f(\pi) + O(\beta^{-1}e^{b\pi}||f||_V).$$

We conclude that

$$N = \frac{K}{16}b^{-1}e^{b\pi}c(b)f(\pi) + O(\beta^{-1}e^{b\pi}(||f||_V + ||g||_H)) \tag{4.38}$$

and that (writing again the subscript n)

$$\begin{aligned}|\beta_n w_n(\pi)| &= |\beta_n\frac{N}{D}|\\ &\le \left|\frac{(K/16)b_ne^{b_n\pi}c(b_n)f_n(\pi)}{D_1 + iD_2}\right| + C(||f_n||_V + ||g_n||_H)\\ &\le C(||f_n||_V + ||g_n||_H)\\ &\to 0 \quad \text{as } n \to \infty\end{aligned}$$

by (4.4) and (4.34). Using (4.26), we obtain the promised contradiction to (4.12). The proof of Theorem 4.1 is achieved. ■

4.2. **Polynomial decay rate.**

The next result asserts that a polynomial decay rate still holds true for almost every value of ξ.

Theorem 4.5. *For almost every $\xi \in (0,\pi)$ we have for every $l > 1$*

$$\sup_{|\beta|\geq 1} |\beta|^{-l} ||(i\beta - \mathcal{A})^{-1}|| < \infty. \tag{4.39}$$

This implies by [18] *that for every positive integer k there exists a constant $C_k > 0$ such that*

$$||e^{t\mathcal{A}} z_0||_{\mathcal{H}} \leq C_k \left(\frac{\ln t}{t}\right)^{\frac{k}{l}} (\ln t) ||z_0||_{\mathcal{D}(\mathcal{A}^k)} \qquad \forall z_0 \in \mathcal{D}(\mathcal{A}^k).$$

Proof of Theorem 4.5. Notice first that it is sufficient to prove (4.39) for all numbers $l \in (1,+\infty) \cap \mathbb{Q}$ and for a.e. $\xi \in (0,\pi)$. Pick any $l \in (1,+\infty) \cap \mathbb{Q}$, any $\xi \in (0,\pi)$ (to be specified later) and argue by contradiction as in the proof of Theorem 4.1. If (4.39) is false, then there exist $\beta_n \in (0,+\infty)$, $(w_n, v_n) \in \mathcal{D}(\mathcal{A})$ for $n = 1, 2, ...$ such that

$$||(w_n, v_n)||_{\mathcal{H}} = 1, \qquad \beta_n \to +\infty, \tag{4.40}$$

and such that, setting $(f_n, g_n) := (i\beta_n - \mathcal{A})(w_n, v_n)$,

$$\beta_n^l (f_n, g_n) \to (0,0) \text{ in } \mathcal{H}. \tag{4.41}$$

Then (4.12) and (4.26) hold true, and to obtain a contradiction to (4.12) it is sufficient to prove that $\beta_n w_n(\pi) \to 0$. The same calculations as in the proof of Theorem 4.1 lead to $w(\pi) = N/D$ (the subscript n being again omitted), where N fulfills (4.38), and $D = D_1 + iD_2$ with D_1 and D_2 given by (4.31) and (4.34), respectively. We aim to prove that $|D| \geq Ce^{b\pi}/b^{2+2\varepsilon}$ for any $\varepsilon > 0$, a.e. $\xi \in (0,\pi)$, and every $b > 0$ large enough. To this end, we notice first that

$$(\cos b\xi + \sin b\xi)(\cos b(\xi - \pi) - \sin b(\xi - \pi)) = 2\sin \pi(b\frac{\xi}{\pi} + \frac{1}{4}) \sin \pi(b(1 - \frac{\xi}{\pi}) + \frac{1}{4}).$$

Let $|||x||| = \inf_{k\in\mathbb{Z}} |x - k|$. We need the following result, which is a variant of a classical result in Diophantine approximations (compare [15, Theorem 4]). Its proof may be found in [8].

Lemma 4.6. *Pick any $\varepsilon > 0$. Then for almost every $\alpha \in (0,1)$, there is only a finite number of solutions $q \in \mathbb{N}^*$ to the inequality*

$$|||(q + \frac{1}{2})\alpha + \frac{1}{4}||| < \frac{1}{q^{1+\varepsilon}}.$$

In particular, for a.e. $\alpha \in (0,1)$ one may find a positive constant C such that for all $q \in \mathbb{N}^*$

$$|||(q + \frac{1}{2})\alpha + \frac{1}{4}||| \geq \frac{C}{q^{1+\varepsilon}}.$$

Applying that property to $\frac{\xi}{\pi}$ and to $1 - \frac{\xi}{\pi}$, we conclude that for a.e. $\xi \in (0,\pi)$, we have for some constant $C > 0$ and for all numbers $b = q + \frac{1}{2}$, $q \in \mathbb{N}^*$,

$$\left|\sin \pi(b\frac{\xi}{\pi} + \frac{1}{4})\right| \geq \frac{C}{b^{1+\varepsilon}} \text{ and } \left|\sin \pi(b(1 - \frac{\xi}{\pi}) + \frac{1}{4})\right| \geq \frac{C}{b^{1+\varepsilon}},$$

hence $|c(b)| \geq Cb^{-2-2\varepsilon}$ and

$$|D_2(b)| \geq C\frac{e^{b\pi}}{b^{1+2\varepsilon}}$$

if b is large enough. Since the function $c(b)$ is uniformly Lipschitz continuous on $\mathbb{R}$, the same inequalities hold (with different constants) for b (large enough) in

$$\bigcup_{q\in\mathbb{N}^*}(q+\frac{1}{2}-\frac{C'}{q^{2+2\varepsilon}},q+\frac{1}{2}+\frac{C'}{q^{2+2\varepsilon}}),$$

if the constant $C'>0$ is small enough. On the other hand, one may associate with that constant $C'>0$ a constant $C''>0$ such that

$$|D_1(b)|\geq C''\frac{e^{b\pi}}{b^{2+2\varepsilon}}$$

for b large enough fulfilling $|b-(q+\frac{1}{2})|\geq C'/q^{2+2\varepsilon}$ for each $q\in\mathbb{N}^*$. It follows that for a.e. $\xi\in(0,\pi)$, we have

$$|D(b)|\geq C\frac{e^{b\pi}}{b^{2+2\varepsilon}} \tag{4.42}$$

for b large enough. Gathering together (4.38) and (4.42), we arrive to

$$|\beta_n w_n(\pi)|\leq Cb_n^{2+2\varepsilon}\big(||g_n||_H+||f_n||_V\big)\to 0$$

as $n\to+\infty$ by (4.41), if we pick $\varepsilon:=l-1$. Thus we have obtained the desired contradiction to (4.12). The proof of Theorem 4.5 is complete. ∎

5. Conclusion

The paper was devoted to the output stabilization of a clamped-free beam with collocated piezoelectric sensor/actuator. Under the assumption that the actuator is touching the clamped extremity of the beam, it has been proved that the strong stability holds provided that the length ξ of the actuator does not belong to a certain dense countable set of $(0,\pi)$. Under this assumption it has been shown that the energy decreases exponentially if the ratio ξ/π belongs to a certain set of rational numbers. The question whether this last assumption may be dropped will be the purpose of further research in a near future.

References

[1] Kais Ammari and Marius Tucsnak. Stabilization of Bernoulli-Euler beams by means of a pointwise feedback force. *SIAM J. Control Optim.*, 39(4):1160–1181 (electronic), 2000.

[2] W. Arendt and C. J. K. Batty. Tauberian theorems and stability of one-parameter semigroups. *Trans. Amer. Math. Soc.*, 306(2):837–852, 1988.

[3] H. T. Banks, W. Fang, R. J. Silcox, and R. C. Smith. Approximation methods for control of tye acoustic/structure interaction with piezoceramic actuator. *Journal of Intelligent Material Systems and Structures*, 4:98–116, 1993.

[4] H. T. Banks and R. C. Smith. The modelling of piezoceramic patch interactions with shells, plates and beams. *Tech. Report no. 92-66, Institute for Computer Applications in Science and Engineering, Hampton, VA*, 1992.

[5] G. Chen, S. G. Krantz, D. W. Ma, C. E. Wayne, and H. H. West. The Euler-Bernoulli beam equation with boundary energy dissipation. In *Operator methods for optimal control problems (New Orleans, La., 1986)*, volume 108 of *Lecture Notes in Pure and Appl. Math.*, pages 67–96. Dekker, New York, 1987.

[6] F. Conrad. Stabilization of beams by pointwise feedback control. *SIAM J. Control Optim.*, 28(2):423–437, 1990.

[7] E. F. Crawley and E. H. Anderson. Detailed models for piezoceramics actuation of beams. *Journal of Intelligent Material Systems and Structures*, 1:79–83, 1990.

[8] Emmanuelle Crépeau and Christophe Prieur. Control of a clamped-free beam by a piezoelectric actuator. *ESAIM Control Optim. Calc. Var.*, to appear.

[9] Marcio S. de Queiroz, Darren M. Dawson, Siddharth P. Nagarkatti, and Fumin Zhang. *Lyapunov-based control of mechanical systems*. Control Engineering. Birkhäuser Boston Inc., Boston, MA, 2000.

[10] Ph. Destuynder, I. Legrain, L. Castel, and N. Richard. Theoretical, numerical and experimental discussion on the use of piezoelectric devices for control-structure interaction. *European J. Mech. A Solids*, 11(2):181–213, 1992.

[11] Philippe Destuynder. A mathematical analysis of a smart-beam which is equipped with piezoelectric actuators. *Control Cybernet.*, 28(3):503–530, 1999. Recent advances in control of PDEs.

[12] Fa Lun Huang. Characteristic conditions for exponential stability of linear dynamical systems in Hilbert spaces. *Ann. Differential Equations*, 1(1):43–56, 1985.

[13] J. Lagnese and G. Leugering. Uniform energy decay of a class of cantilevered nonlinear beams with nonlinear dissipation at the free end. In *Differential equations with applications in biology, physics, and engineering (Leibnitz, 1989)*, volume 133 of *Lecture Notes in Pure and Appl. Math.*, pages 227–239. Dekker, New York, 1991.

[14] J. E. Lagnese and G. Leugering. Uniform stabilization of a nonlinear beam by nonlinear boundary feedback. *J. Differential Equations*, 91(2):355–388, 1991.

[15] Serge Lang. *Introduction to Diophantine approximations*. Springer-Verlag, New York, second edition, 1995.

[16] P. Le Gall, C. Prieur, and L. Rosier. Stabilization of a clamped-free beam with collocated piezoelectric sensor/actuator. *CAO'06, to appear*.

[17] J.-L. Lions and E. Magenes. *Non-homogeneous boundary value problems and applications. Vol. I*. Springer-Verlag, New York, 1972. Translated from the French by P. Kenneth, Die Grundlehren der mathematischen Wissenschaften, Band 181.

[18] Zhuangyi Liu and Bopeng Rao. Characterization of polynomial decay rate for the solution of linear evolution equation. *Z. Angew. Math. Phys.*, 56(4):630–644, 2005.

[19] Zhuangyi Liu and Songmu Zheng. *Semigroups associated with dissipative systems*, volume 398 of *Chapman & Hall/CRC Research Notes in Mathematics*. Chapman & Hall/CRC, Boca Raton, FL, 1999.

[20] Ömer Morgül. Dynamic boundary control of an Euler-Bernoulli beam. *IEEE Trans. Automat. Control*, 37(5):639–642, 1992.

[21] Jan Prüss. On the spectrum of C_0-semigroups. *Trans. Amer. Math. Soc.*, 284(2):847–857, 1984.

[22] Richard Rebarber. Exponential stability of coupled beams with dissipative joints: a frequency domain approach. *SIAM J. Control Optim.*, 33(1):1–28, 1995.

[23] Marius Tucsnak. Regularity and exact controllability for a beam with piezoelectric actuator. *SIAM J. Control Optim.*, 34(3):922–930, 1996.

Current address: Institut Élie Cartan, UMR 7502 UHP/CNRS/INRIA, B.P. 239, F-54506 Vandœuvre-lès-Nancy Cedex, France.

E-mail address: `legall@iecn.u-nancy.fr`

Current address: LAAS-CNRS, 7 avenue du colonel Roche, 31077 Toulouse, France

E-mail address: `Christophe.Prieur@laas.fr`

Current address: Institut Élie Cartan, UMR 7502 UHP/CNRS/INRIA, B.P. 239, F-54506 Vandœuvre-lès-Nancy Cedex, France.

E-mail address: `rosier@iecn.u-nancy.fr`

Conclusion

Les différents problèmes que nous avons tenté de résoudre ont tous deux points en commun : les problématiques soulevées apparaissent naturellement dans le champ d'étude de l'optique adaptative, et un grand nombre de questions restent ouvertes.

Dans le cas de la reconstruction du front d'onde à partir des mesures de l'analyseur de Shack-Hartmann, les deux approches zônales et modales offrent chacune des avantages et des inconvénients : les méthodes zônales ne font pas disparaître les oscillations rapides du front d'onde, et les méthodes modales permettent d'obtenir naturellement une fonction définie sur l'ensemble du domaine, avec en plus une approximation directe du gradient. En astronomie, où les premiers ordres sont les plus importants, l'utilisation de méthodes modales se révèle donc efficace. En revanche, en ophtalmologie[4], les reconstructions locales seront privilégiées.

Une question ouverte demeure quant à la correction parfaite du front d'onde incident : comment caractériser l'ensemble des fronts d'onde pouvant être vraiment corrigés, i.e. pour lesquels le miroir n'admet pas de points multiples. Il serait également intéressant de confronter les différentes méthodes au niveau d'un télescope, et voir comment la forme corrigeant *parfaitement* le front d'onde améliore les systèmes d'optique adaptative. Le souci de travailler en temps réel correspond à une incitation à travailler avec une boîte noire, et réduire le nombre de reconstructions du front d'onde. Un tel système permettrait-il de garder les avantages liés à la méthode proposée ici ?

Dans les deux parties concernant la stabilisation de miroir bimorphe et de poutre, l'étape naturelle suivante consiste à étudier les propriétés de contrôle robuste des deux systèmes. Dans le cas de la poutre avec piezoélectriques colocalisés, une étude intéressante, mais avec des calculs plus compliqués, consisterait à étudier les mêmes questions, mais cette fois-ci sans placer les cellules au bord, c'est-à-dire en conservant les deux paramètres ξ et η. Egalement, il conviendrait de chercher quelle position assure la meilleure stabilité exponentielle.

Enfin, le problème de la poutre pourrait être élargi au contrôle et à la stabilisation d'une plaque encastrée à l'un de ses bords, les trois autres bords restant libres.

[4] référence à retrouver

Bibliographie

[Rog96] M. C. Roggemann and B. Welsh *Imaging through turbulence* CRC Press, 1996

[Rod99] F. Roddier *Adaptive Optics in Astronomy* Cambridge University Press, 1999

[Tys98] R. K. Tyson *Principles of Adaptive Optics* Academic Press, 1998

[Har98] J. W. Hardy *Adaptive Optics for Astronomical Telescopes* Oxford University Press, 1998

[Kad00] M. Kader *Contributions à la modélisation et au contrôle des systèmes intelligents distribués : Application au contrôle de vibrations d'une poutre* Université de Franche-Comté

[Tli05] S. Tliba and H. Abou-Kandil and C. Prieur *Active vibration damping of a smart flexible structure using piezoelectric transducers : H-infinity design and experimental results* Proceedings of the 16th IFAC WORLD CONGRESS, Prague, Czech Republic, July 4-8, 2005

[Can95] .C. Cannon *Global wave-front reconstruction using Shack-Hartmann sensors* Journal of the Optical Society of America A : Optics, Image Science, and Vision, Volume 12, Issue 9, September 1995, pp.2031-2039

[Pri06] . Lenczner and C. Prieur *Asymptotic model of an active mirror* 13th IFAC Workshop on Control applications of Optimization, Cachan, France, 2006.

[Bab48] .W. Babcock *The possibility of compensating astronomical seeing* Pub. Astr. Soc. Pac. 65. 229-236

Résumé

L'optique adaptative est une technique qui permet de corriger en temps réel les déformations évolutives et non prédictibles d'un front d'onde grâce à un miroir déformable. Les perturbations apparaissent typiquement lors de la traversée par les rayons lumineux de l'atmosphère. Ce travail s'articule autour de quatre problèmes liés à la plupart des systèmes d'optique adaptative actuels : - la reconstruction du front d'onde incident, à partir ici de l'analyseur de Shack-Hartmann. - la mise en place d'équations décrivant la forme à donner à un miroir pour assurer la correction parfaite du front d'onde. - le contrôle et la stabilisation d'un premier modèle de miroir, appelé miroir bimorphe, issu des travaux de Lenczner et Prieur, sont étudiés. Composé de trois couches, correspondant au miroir lui-même (couche flexible), et de deux couches équipées de piézoélectriques servant respectivement de capteurs et d'actionneurs. Le couplage de deux EDPs de natures très différentes rend l'étude du problème extrêmement intéressante. - plusieurs théorèmes portant sur la stabilisation, forte, exponentielle et polynômiale, d'un deuxième modèle, constitué d'une poutre encastrée à une extrêmité et libre à l'autre, et de deux cellules piézoélectriques, sont mis en place.

Mots-clés: Optique adaptative, Equation des poutres de Bernoulli-Euler, Stabilisation forte, Contrôle de poutre avec actionneur/senseur colocalisés, Stabilisation par retour de sortie, Correction de front d'onde, Reconstruction de front d'onde.

Abstract

Study of some mathematical Problems appearing in Adaptive Optics

Adaptive Optics is a technics allowing for the correction in real-time of the evoluting and non-predictive of a wavefront, thanks to a deformable mirror.. Perturbations usually appear when optical rays cross the Earth's atmosphere. This work is constituted of the study of four main problems arising in most actual adaptive optics systems : - the reconstruction of the incoming wavefront, from measures here of a Shack-Hartmann sensor. - setting the equations describing the shape of the deformable mirror achieving a perfect correction of the incoming wavefront. - the control and the stabilization of a first mirror model, called bimorph mirror, built by Lenczner and Prieur, are studied. Constituted of three layers, the mirror itself (flexible layer), and two layers equipped with respectively piezelectric sensors and piezoelectric actuators. The coupling of two PDEs, very different in nature, leads to a really interesting problem. - Several theorems about strong, exponential and polynomial stabilization of a second model, a beam clamped at an extremity and free at the other, and two piezoelectric cells, are proved.

Keywords: Adaptive Optics, Bernoulli-Euler beam equation,Strong stabilization, Collocated piezoelectric sensor/actuator, Bimorph mirror, Output feedback stabilization, Exact wavefront correction, Wavefront reconstruction

Institut Elie Cartan Nancy
Laboratoire de mathématiques
BP 239 54506 Vandoeuvre-lès-Nancy Cedex